8-3-2002

Distribution and Morphology of Bacteria and their Byproducts in Microbial Enhanced Oil Recovery Operations

Sarah Elizabeth Fratesi

DISTRIBUTION AND MORPHOLOGY OF BACTERIA AND THEIR BYPRODUCTS IN MICROBIAL ENHANCED OIL RECOVERY OPERATIONS

By

Sarah Elizabeth Fratesi

A Thesis
Submitted to the Faculty of
Mississippi State University
in Partial Fulfillment of the Requirements
for the Degree of Master of Science
in Geosciences
in the Department of Geosciences

Mississippi State, Mississippi

August 2002

DISTRIBUTION AND MORPHOLOGY OF BACTERIA AND THEIR

BYPRODUCTS IN MICROBIAL ENHANCED

OIL RECOVERY OPERATIONS

By

Sarah Elizabeth Fratesi

Approved:

_____	_____
F. Leo Lynch Assistant Professor of Geosciences (Director of Thesis)	John E. Mylroie Professor of Geosciences Graduate Coordinator of the Department of Geosciences (Committee Member)
_____	_____
Lewis R. Brown Professor of Microbiology (Committee Member)	Brenda L. Kirkland Adjunct Professor of Geosciences (Committee Member)

_____

Philip B. Oldham
Dean of the College of Arts and Sciences

Name: Sarah Elizabeth Fratesi

Date of Degree: August 3, 2002

Institution: Mississippi State University

Major Field: Geosciences

Major Professor: Dr. F. Leo Lynch

Title of Study: DISTRIBUTION AND MORPHOLOGY OF BACTERIA AND THEIR BYPRODUCTS IN MICROBIAL ENHANCED OIL RECOVERY OPERATIONS

Pages in Study: 79

Candidate for Degree of Master of Science

This study uses scanning electron microscopy (SEM) to examine the occurrence of bacteria and their exopolysaccharide slime layer in microbial enhanced oil recovery experiments. A test of SEM preservation techniques showed that air drying and 10% glutaraldehyde fixation preserved the slime layer but distorted and flattened bacteria. Techniques with ethanol dehydration preserved the bacterial textures but fragmented the slime layer. In sandstones that had been plugged during microbial enhanced oil recovery experiments, bacteria are sparsely distributed. An irregular, confluent slime sheet covers grains and coats pore spaces and is responsible for permeability modification in microbial enhanced oil recovery. The development of the slime layer over time involves several steps: growth of ultramicrobacteria into full-sized bacteria; creation of a slime capsule; growth of globular masses, ropy masses, webs, thin sheets; and growth of a thicker, pore-filling mass of slime associated with large balls of slime.

DEDICATION

To my dad, gentleman farmer and armchair scientist,

and to my mom, the greatest lady I know.

ACKNOWLEDGEMENTS

For helping with the thesis work: Richard Kuklinski, Bill Monroe, and Kay Nevels Milam in the SEM lab; John Ed and Ali at Buckner Lane; and especially Lew Brown.

For funding the thesis work: the Department of Energy and the Department of Geosciences at Mississippi State University

For helping me manage Leo: Brenda Kirkland (who knows so much more than Leo does and always takes my side), and his three girls: Maggie George, Billiejean Kirkland, and Fang Lynch.

For managing me: Laura Barnhart and John Mylroie.

For being the coolest: big sister Sydney Dean, big brother Brian Dean, and especially little brother Patrick Fratesi.

For just about everything else: Thanks, Leo. It's been real.

TABLE OF CONTENTS

Page

DEDICATION ii

ACKNOWLEDGMENTS iii

LIST OF FIGURES vi

CHAPTER

I. INTRODUCTION 1

II. REVIEW OF LITERATURE 4

Microbial Enhanced Oil Recovery 4
The Role of Polysaccharides in Enhanced Oil Recovery 5
Preservation Techniques for Scanning Electron Microscopy 7

III. MATERIALS AND METHODS 9

Development of Preservation Protocols and Preliminary Characterization of Bacteria 9
Investigation of Growth of *in situ* Bacteria in Sandstone Reservoir Rocks 11

IV. RESULTS 13

Preservation of Rod-Shaped Bacteria and Associated Slime Layer 13
Preservation of Reservoir Bacteria and Associated Slime Layer 28
Experiment I: Occurrence of Bacteria and Slime in Fully Plugged Cores 37
Experiment II: Growth of Bacteria and Slime Layer in Timed Feeding Experiments 37
Week 1 37
Week 2 45
Week 3 45
Week 4 54

CHAPTER Page

V. DISCUSSION AND CONCLUSIONS 60

Preservation of Bacteria and Slime Layer 60
Sheets 61
Plates 62
Strands and Balls 62
Preservation of Different Slime Layers 66
Slime Layer as Plugging Agent 66
Nannobacteria and Ultramicrobacteria 68
Development of Slime Layer Over Time 69
Early Exopolysaccharides 69
Early Slime Forms 69
Hexagonal Outline 70
Large Balls 70

VI. SUMMARY 72

REFERENCES CITED 75

LIST OF FIGURES

FIGURE Page

1 A quartz overgrowth covered with air-dried, rod-shaped bacteria and slime 14

2 Air-dried, rod-shaped bacteria on the surface of the quartz overgrowth in Fig. 1. . . . 14

3 Air-dried bacteria (B) and slime (S) on the surface of a limestone piece. 15

4 Air-dried, stretched bacteria (B) and slime (S) on the surface of a limestone piece. 15

5 Two glutaraldehyde-preserved bacteria covered by a thin layer of slime 16

6 Colony of glutaraldehyde-preserved bacteria. 16

7 10% Glutaraldehyde-preserved bacteria (B) and slime (S) on the surface of a limestone piece. 17

8 Thick, glutaraldehyde-preserved slime layer 17

9 Ethanol/hexamethyldisilazane-preserved bacteria and slime sheet 19

10 Colony of bacteria preserved with ethanol/hexamethyldisilazane on a quartz overgrowth 19

11 Platy texture of slime preserved with ethanol/ hexamethyldisilazane 20

12 Grape clusters (GC) and platy slime texture (P) in ethanol/ hexamethyldisilazane preserved sample 20

13 High-magnification photo of grape cluster (GC) and underlying platy slime texture in ethanol/hexamethyldisilazane-preserved sample 21

14 High-magnification photo of nanno-scale balls that make up grape clusters 21

FIGURE Page

15 Colony of bacteria preserved with ethanol/critical point drying 22

16 High-magnification photo of bacteria preserved with ethanol/critical point drying . . 22

17 Cluster of free-standing, critical-point-dried bacteria 23

18 Pair of ethanol/critical point dried bacteria exhibiting cylindrical forms with flattened ends and irregular surfaces 23

19 Platy slime texture preserved with ethanol/critical point drying. Plates have fingers of slime along their edges 24

20 Bacterium and platy slime preserved with ethanol/critical point drying 24

21 Bacteria and cracked slime sheet (S) preserved with ethanol/acetone/ critical point drying. 25

22 Rod-shaped bacteria preserved with ethanol/acetone/critical point drying. 25

23 High-magnification photo of rod-shaped bacterium from Fig. 22. 26

24 Platy slime texture in ethanol/acetone/critical point dried sample. 26

25 High-magnification photo of platy slime and grape cluster from Fig. 24. 27

26 High-magnification photo of nanno-scale balls that make up the grape clusters in ethanol/acetone/critical point dried sample. 27

27 Two types of slime in air-dried reservoir sandstone sample: globular slime (G) and sheet-like hexagonal slime (H). 29

28 Air-dried reservoir bacteria (B) and two types of slime: globular (G) and hexagonal (H). 29

29 High-magnification photo of two types of slime in reservoir sandstones. 30

30 A rare colony of slightly flattened reservoir bacteria and an irregular layer of slime (S) preserved by air drying. 30

FIGURE Page

31 Thick, irregular layer of slime in reservoir sandstone preserved in 10% glutaraldehyde. 31

32 A meniscus of slime in reservoir sandstone preserved in 10% glutaraldehyde. 31

33 A meniscus of slime in reservoir sandstone preserved with 10% glutaraldehyde. 32

34 Glutaraldehyde-preserved slime layer and menisci of slime (M) on kaolinite crystallites in a reservoir sandstone. 32

35 Flattened bacteria (B) and irregular slime layer covering a quartz overgrowth in a 10% glutaraldehyde sample. 33

36 Flattened reservoir bacteria and slime layer preserved with 10% glutaraldehyde fixation. 33

37 Reservoir bacterium and slime preserved with ethanol/hexamethyldisilazane. 34

38 Slime on the surface of a quartz overgrowth in a reservoir sandstone preserved with ethanol/hexamethyldisilazane. 34

39 Mats of slime in reservoir sandstone preserved with ethanol/critical point drying. . . . 35

40 High-magnification photo of reservoir bacteria and slime web from Fig. 39. 35

41 Web of slime over kaolinite crystallites in a reservoir sandstone. 36

42 High-magnification photo of slime web in reservoir sandstone preserved with ethanol/critical point drying. 36

43 Thick slime layer coating the surface of quartz overgrowths in a fully plugged North Blowhorn Creek sandstone. 38

44 Thick meniscus of slime spanning pore throat in a fully plugged North Blowhorn Creek sandstone. 38

45 Meniscus and layer of slime within a pore space of a fully plugged North Blowhorn Creek sandstone. 39

46 Pore-lining slime layer in a fully plugged North Blowhorn Creek sandstone. 39

FIGURE Page

47 Web of slime in pore space of fully plugged North Blowhorn Creek sandstone. 40

48 Strand of slime in fully plugged North Blowhorn Creek sandstone. 40

49 Strand of slime in fully plugged North Blowhorn Creek sandstone. 41

50 Rare colony of bacteria in fully plugged North Blowhorn Creek sandstone. 41

51 Two distinct sizes of bacteria during first week of growth experiment. 42

52 Full-sized, rod-shaped bacterium and smaller bacteria in both rod-shaped (R) and spheroid (S) shapes. 42

53 Small bacteria-like forms in first week of timed experiments. 43

54 Small bacterium with holdfast (arrow) during first week of timed experiments. 43

55 Full-sized, rod-shaped bacteria with holdfasts on quartz overgrowths during first week of timed experiments. 44

56 High magnification photo of full-sized, rod-shaped bacteria with exopolysaccharide holdfasts. 44

57 A bacterium in the first week of timed experiments covered with a thin exopolysaccharide sheath 46

58 A flattened bacterium on the surface of a quartz overgrowth during the first week of the timed experiments. 46

59 Ropy slime masses (R) and small globular masses (G) of slime in the first week of timed experiments. 47

60 Ropy slime mass in first week of timed experiments. 47

61 Thin slime sheet draped over the edge of a quartz overgrowth in first week of timed experiments. 48

62 Thin slime sheet draped across the surface of a quartz overgrowth. 48

FIGURE Page

63 Ropy masses of slime on the surface of a quartz overgrowth during the second week of the timed experiments. 49

64 Ropy masses of slime on the surface of a quartz overgrowth during the second week of the timed experiments. 49

65 Globular masses of slime scattered over the surface of a quartz overgrowth during the second week of the timed growth experiment. 50

66 High-magnification photo of a globular mass of slime during the second week of the timed experiments. 50

67 Thin slime layer stretching between two quartz overgrowths in the second week of the timed experiments. 51

68 Curled slime sheet in a reservoir sandstone during the second week of timed growth experiments. 51

69 Full-sized bacteria in the third week of the timed experiments. 52

70 Full-sized, rod-shaped bacterium in the third week of the timed experiments. 52

71 Small forms of rod-shaped and spheroid-shaped bacteria during the third week of the timed experiments. 53

72 Thick, continuous slime sheet in the third week of timed experiment. 53

73 Pore-filling mass of slime in the third week of the timed experiments. 55

74 Pore-filling mass of slime in the third week of the timed experiments. 55

75 Large (10µm) balls of slime in the fourth week of the timed experiments. 56

76 Higher magnification photo of a large ball of slime from Fig. 71. 56

77 Large ball of slime and colony of rod-shaped bacteria during fourth week of growth. 57

78 Large ball of slime from Fig. 73. 57

FIGURE Page

79 Higher magnification photo of colony of bacteria at the base of the ball of slime from Figs. 73 & 74. 58

80 Large ball of slime during the fourth week of timed experiments. 58

81 Thin sheet of slime on the surface of a quartz overgrowth during the fourth week of the timed experiments. 59

82 High-magnification photo of a ropy mass of slime during the fourth week of the timed experiments. 59

83 Comparison of nanno-scale spheroidal structures in slime layer with different preservation techniques and interpretation of the effects of dehydration on slime texture. 63

84 Platy slime with fingers along the edges of the plates. Preserved with ethanol/critical point drying. 64

85 Clays from subsurface oil reservoir in Texas. 64

86 Two alternative explanations for the formation of balls and strands from dehydration of the slime layer. 65

87 Possible genesis of ropy masses and globular masses. 65

88 “Grape cluster” slime texture composed of nanno-scale spheroids in preservation experiments on rod-shaped bacteria. 67

89 “Grape cluster” texture in filtrate from Austin city drinking water. 67

CHAPTER I

INTRODUCTION

The purpose of this study was to investigate the spatial relationships between microbes, their exopolysaccharides (external bacterial secretions), and the pore spaces within sandstone cores used in microbial enhanced oil recovery experiments. Techniques were developed to preserve the exopolysaccharides for scanning electron microscopy in order to study their morphology and occurrence within the sandstone cores, and plugging experiments were run to examine the morphology and development of the bacteria and exopolysaccharides.

Typically, only about one-third of the oil in U. S. reservoirs can be economically produced with current technology. Approximately 37% of that oil is produced during primary recovery. Secondary recovery, most often waterflooding, is responsible for another 51% of the economically recoverable oil in the U. S. The remainder (about 12%) of the recoverable oil is produced using tertiary methods, including thermal, chemical, and microbial methods (Department of Energy, 2002). There is opportunity and impetus for development of more effective tertiary methods of oil recovery. Of these methods, one of the most promising and cost-effective is the microbial method, referred to as microbial enhanced oil recovery.

Microbial enhanced oil recovery is a general term that refers to the use of bacteria and their byproducts to increase recovery of oil from depleted reservoirs. This term actually

incorporates a variety of processes, the most effective and widely used of which is the bacterial plugging of high-permeability zones within the reservoir (*e. g.* Jenneman and others, 1984; Lappin-Scott and others, 1988, Brown and Vadie, 2000).

Porosity-blocking microbial enhanced oil recovery is valuable primarily as an adjunct to waterflooding operations, in which water is pumped into injection wells in the reservoir in order to force the oil ahead of it towards the production well. The major weakness in the waterflooding process is the tendency of the water to travel along narrow zones of high permeability, leaving the oil in the rest of the reservoir stagnant. If the water reaches the production well, it will be pulled from the high permeability zone and the well will produce no more oil. Unless the high permeability zones can be plugged and flow diverted to other parts of the reservoir, the oil within it is economically unrecoverable.

Bacterial plugging usually involves the feeding of injected or *in situ* bacteria within the reservoir. Bacteria and/or nutrients will preferentially enter the reservoir along high-permeability pathways. The growth of the biomass in those laminae plugs the pore throats, thereby decreasing the permeability in what had once been the high-permeability zones. This tends to equalize the permeability across the reservoir and restore the sweep efficiency of waterflooding operations (Crawford, 1961; Raiders and others, 1986).

Microbial permeability profile modification refers specifically to the use of *in situ* bacteria (Brown and Vadie, 2000). The feeding of *in situ* microbes with nitrate- and phosphate-containing nutrients has been demonstrated to be effective in plugging sandstone cores under laboratory conditions (Jenneman and others, 1984; Brown, 1982). The application of these

processes in field trials has shown the feeding program to be effective in slowing the deterioration of hydrocarbon production in wells undergoing waterflooding operations by diverting the flow of water from high-permeability zones to other areas of the reservoir (Jenneman and others, 1996; Brown and Vadie, 2000). Since microbial activity within sandstones is governed by relationships at the microenvironmental level, an understanding of the interaction between microbes, their exopolysaccharide secretions, and the mineral substrate is key to predicting the efficacy of microbial enhanced oil recovery operations in the field.

Current studies by Brown and others (2002) involve the feeding of *in situ* microbes in combination with polymer flooding in oil-bearing sandstones taken from the North Blowhorn Creek Oil Unit, Lamar County, Alabama, under simulated reservoir conditions. The North Blowhorn Field is the largest producer of oil in the Black Warrior Basin. Production is from the Carter Sandstone, a Mississippian reservoir at 700 m depth which has undergone waterflooding since 1983 (Brown and Vadie, 2000). Feeding of these microbes in laboratory experiments has resulted in complete plugging of both low- and high-permeability cores; application of this technique in the field has resulted in an increase in reserves of 400,000 to 600,000 barrels and extended the economic life of the North Blowhorn Creek reservoir by 5-11 years (Brown and Vadie, 2000).

CHAPTER II

REVIEW OF LITERATURE

MICROBIAL ENHANCED OIL RECOVERY

Early microbial enhanced oil recovery research focused on the sulfate-reducing bacteria (especially *Desulfovibrio* species) and their byproducts (Zobell, 1947). Important processes were thought to include the production of acids that dissolve limestone reservoir rocks, the production of gaseous byproducts that reduce the viscosity of oil, production of detergents, displacement of oil by bacteria, and direct chemical action upon oil (Updegraff and Wren, 1954). Although most of these processes were shown to occur within the reservoir environment, the growth of sulfate-reducing bacteria did not consistently liberate oil from sands under laboratory conditions (Updegraff and Wren, 1954).

Focus has shifted to the use of bacteria to plug high-permeability zones during waterflooding operations. It was assumed initially that any bacteria present in the oil reservoir were introduced in drilling muds (Davis and Updegraff, 1954). Consequently, initial microbial enhanced oil recovery efforts involved the injection of cultured bacteria, which resulted in shallow plugging of the inlet face and inadequate penetration of the bacteria into the sandstone (Jenneman and others, 1984; Shaw and others, 1985; Cusack and others, 1987). Some researchers used dwarf or starved cells, which penetrated further into the sandstones and were

fed once in place (Lappin-Scott and others, 1988; MacLeod and others, 1988). However, once the presence of indigenous bacteria within subsurface reservoirs was demonstrated (Clark and others, 1981; Azadpour and others, 1996), experiments were designed which involved feeding of *in situ* bacteria. Nutrient sources, including maltodextrins and phosphates (Jenneman and others, 1996; Davey and others, 1998) as well as sodium citrate growth medium (Lappin-Scott and others, 1988) were injected directly into the reservoir rocks. Feeding bacteria with nitrogen- and phosphorus-rich nutrients resulted in plugging of sandstone cores (Brown and others, 2002). Field trials involving injected nutrients resulted in increased production from treated reservoirs (Jenneman and others, 1996; Brown and Vadie, 2000).

THE ROLE OF EXOPOLYSACCHARIDES IN ENHANCED OIL RECOVERY

Selective plugging was initially thought to have occurred primarily due to sieving action (bacteria clogging the pore throats), an effect best achieved when the average pore throat radius is less than 2 times the diameter of the bacteria (Davis and Updegraff, 1954). However, plugging also occurs in reservoir rock with microorganisms much smaller than the pore throat radius. This led researchers to speculate that another mechanism, such as the production of exopolysaccharides, is in operation (Mitchell and Nevo, 1964). Dead bacteria or non-slime-producing bacteria either do not plug porous media (Jack and others, 1989; Lappan and Fogler, 1995), or plug the media to a lesser extent than do similar strains that produce an exopolysaccharide layer (Kalish and others, 1964; Mitchell and Nevo, 1964; Vandevivere and Bayeve, 1992).

The polysaccharides secreted by many strains of bacteria serve mainly to protect the bacteria against desiccation and predation, as well as to assist in adhesion to surfaces. These exopolysaccharides generally occur in two forms: a "capsule", which is bound to the surface of the bacterium and is often sheathlike in form, and "slime", which is only loosely attached to the bacterium (Whitfield, 1988). The polysaccharide capsule surrounding a bacterium may occupy 20 times more space than the bacterium itself (Bayer and others, 1985). As a plugging agent, therefore, exopolysaccharides are perhaps more important than the bacterial bodies themselves. Exopolysaccharides are involved in irreversible adhesion of bacteria to surfaces, and especially with the formation of bacterial colonies (Fletcher and Floodgate, 1973; Allison and Sutherland, 1987). "Biofilms" are heterogenous systems of bacteria, their exopolysaccharides, and water channels (Costerton and others, 1994). Lawrence and others (1991) used confocal laser microscopy to study the biofilms produced by *Pseudomonas* and *Vibrio* species and found them to be composed of less than 27% bacterial bodies. The remainder (73%-98%) was assumed to be composed of extracellular products (probably exopolysaccharides) and void space.

Exopolysaccharides may occur in several different morphologies within porous media. At the inlet face, a continuous, amorphous sheet is often present (Shaw and others, 1985). Within the pore spaces, however, the morphology at some stages of growth may incorporate a weblike structure, which Paulsen and others (1997) termed a "bioweb". Paulsen suggested that this morphology facilitates quicker plugging of pore throats by trapping floating biofilm fragments and other detritus. Growth of bacteria and the accompanying exopolysaccharides

are governed by such parameters as water chemistry, pH , surface charge, physiology, nutrients, and fluid flow (Bennett and others, 2000; Fletcher and Floodgate, 1973; Lappan and Fogler, 1995).

PRESERVATION TECHNIQUES FOR SCANNING ELECTRON MICROSCOPY

Scanning electron microscopy was used for this study in order to characterize the spatial relationships between the bacteria and the exopolysaccharides within the pore spaces of the sandstone. This technique has been demonstrated to be effective in studying surficial and spatial relationships of minerals and organics within soils and sediments (Ransom and others, 1997).

Samples observed using this method must be preserved and dehydrated before insertion into the microscope. Preservation and dehydration techniques used in scanning electron microscopy may create artifacts caused by shrinkage, dessication, cracking, and distortion (Postek and others, 1980). The preservation of the exopolysaccharide poses extra problems during dehydration of samples. Biofilm water content ranges from 87% to 99% (Christensen and Characklis, 1990). Removal of this water is likely to greatly distort or deflate the slime layer. In addition, some polysaccharides are soluble in ethanol, which is often used in the dehydration process.

Preservation techniques are traditionally geared towards maintaining the living textures of the bacteria, often at the expense of the slime layer. Carr and others (1996) reported that critical point drying increased the apparent number of bacteria in a sample as compared to

chemical dehydration. Ravenscroft and others (1991) reported that cryofixation and freeze-substitution methods revealed fibrous networks of exopolysaccharides not seen in glutaraldehyde-fixed samples. This implies that these preservation procedures effect the morphology of the slime. It was necessary, therefore, to begin this study with a test of preservation techniques on the organic materials used in these experiments.

CHAPTER III

MATERIALS AND METHODS

DEVELOPMENT OF PRESERVATION PROTOCOLS AND PRELIMINARY CHARACTERIZATION OF BACTERIA

A test of scanning electron microscope preservation techniques was carried out and also served as an initial characterization of the bacteria and the slime indigenous to the North Blowhorn Creek Unit. Pieces of the Edwards Limestone and Berea Sandstone pieces were inoculated with (1) a single, aerobic species of rod-shaped bacteria, and (2) a culture of anaerobic bacteria from the North Blowhorn Creek reservoir. The bacteria were grown on the surface of rock pieces by placing the rock pieces in bottles of inoculum and nutrient broth for two weeks. This experiment was performed to determine which preservation technique best preserved the texture of both the slime and the bacteria. All subsequent work was done using only the most effective preservation techniques as determined by this experiment.

Five preservation techniques were tested on the samples used in this study:

Air Drying. Samples were air dried by sitting under a fume hood for 6 hours, then in a desiccation chamber overnight.

10% Glutaraldehyde Fixation. Samples were fixed in 10% glutaraldehyde in a phosphate buffer for two hours and then dried in a desiccation chamber overnight.

Ethanol Dehydration with Hexamethyldisilizane. Samples were fixed in 2.5% glutaraldehyde for two hours and then dehydrated by immersing for ten-minute intervals in 30%, 50%, 70%, and 95% ethanol. Residual water was removed by making changes of 100% ethanol every ten minutes for an hour. The samples were then transferred to 100% hexamethyldisilazane, a chemical dehydrant and substitute for critical point drying (Oshel, 1997), through a single 50% gradational step, followed by three changes of 100% hexamethyldisilazane, all of ten minutes duration.

Ethanol Dehydration with Critical Point Drying. Samples were fixed in 2.5% glutaraldehyde for two hours and then dehydrated by immersing for ten-minute intervals in 30%, 50%, 70%, and 95% ethanol as in the previous technique. Residual water was removed by making changes of 100% ethanol every ten minutes for an hour. The samples were critical point dried in ethanol in a Polaron E3000 critical point dryer, which uses CO_2 as a transitional fluid. Five flushes of CO_2 were made before taking samples to critical point.

Ethanol/Acetone Dehydration with Critical Point Drying. Samples were fixed in 2.5% glutaraldehyde for two hours and dehydrated in ten-minute steps of 30%, 50%, 70%, and 95% ethanol and four changes of 100% ethanol. The samples were then transferred to 100%

acetone through four gradational steps of 30%, 50%, 70%, 90%, and 100%. The samples were critical point dried in acetone with five flushes of CO_2.

Samples were mounted on aluminum stubs with hot glue or carbon tape and coated with a gold/palladium alloy using a Polaron E5100 sputter coater. This step is necessary to render the surface of the samples conductive. A gold coating process of about 30 seconds was used, which our tests show does not produce nm-scale artifacts (Folk and Lynch, 1997). The samples were imaged using a Leo Stereoscan 360 scanning electron microscope. The voltage was kept at 15 kV and the samples imaged at an average distance from the electron gun of about 12mm, depending on the size of the samples.

INVESTIGATION OF GROWTH OF *IN SITU* BACTERIA IN SANDSTONE RESERVOIR ROCKS

Experiment I. The first experiment was conducted to investigate the occurrence and morphology of the slime within sandstones which had been fed and plugged in a microbial enhanced oil recovery experiment. The sandstone cores from these experiments are 1.5 in (3.81cm) in diameter and had been fed with alternating courses of nitrate- and phosphate- rich nutrients until fluid no longer penetrated the cores. Pieces for this experiment were cut off of the ends of these cores with a dry rock saw and broken into smaller chunks. At least two chunks were taken from each sandstone core.

Experiment II. A test of the development of the biofilm was conducted over a period of 20 days. Small pieces (approximately 1 cm) of live cores were fed by immersion in nitrate- and phosphate- rich nutrient broth for five, ten, fifteen, and twenty days. Pieces were cut from the cores and chunks broken off of these. Interior surfaces were preserved and examined using scanning electron microscopy. This experiment allowed us to explore the spatial and textural changes in the exopolysaccharides likely to occur in reservoir sandstones undergoing microbial enhanced oil recovery.

CHAPTER IV

RESULTS

PRESERVATION OF ROD-SHAPED BACTERIA AND ASSOCIATED SLIME LAYER

Air Drying. Rod-shaped bacteria in air-dried samples are visible as deflated, flattened, or stretched rods (Figs. 1-4). Bacterial bodies are indistinct, with partially collapsed cell walls, almost merging into the slime layer in some areas (Fig. 4). A discontinuous, sometimes cracked slime layer is present in some areas (Figs. 1,3,4).

10% Glutaraldehyde Fixation. Glutaraldehyde-preserved bacteria may retain some volume but are uneven in diameter (Figs. 5 and 6). In some places, bacteria are so severely distorted that they are virtually indistinguishable from the slime layer (Fig. 6). Slime preserved with this method occurs as a discontinuous sheet over the substrate and the bacteria and is generally thicker than in air-dried samples (Figs. 5 and 7). An especially thick sheet of slime forms a slightly cracked meniscus, stretching from one grain to another (Fig. 8).

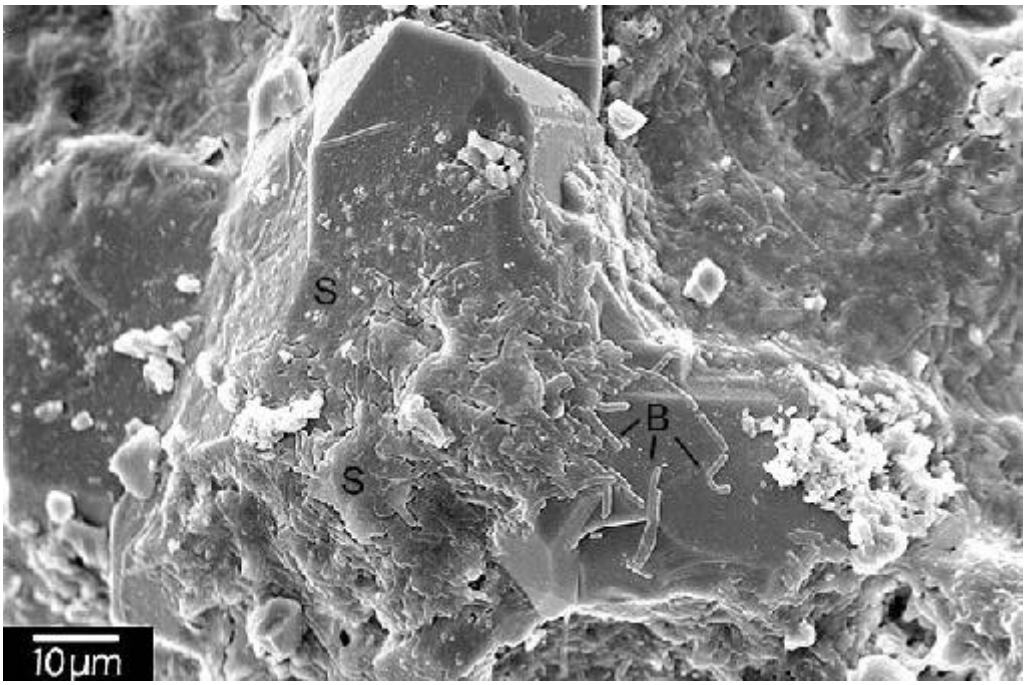

Figure 1: A quartz overgrowth covered with air-dried, rod-shaped bacteria (B) and slime (S). The slime has begun to crack in some places.

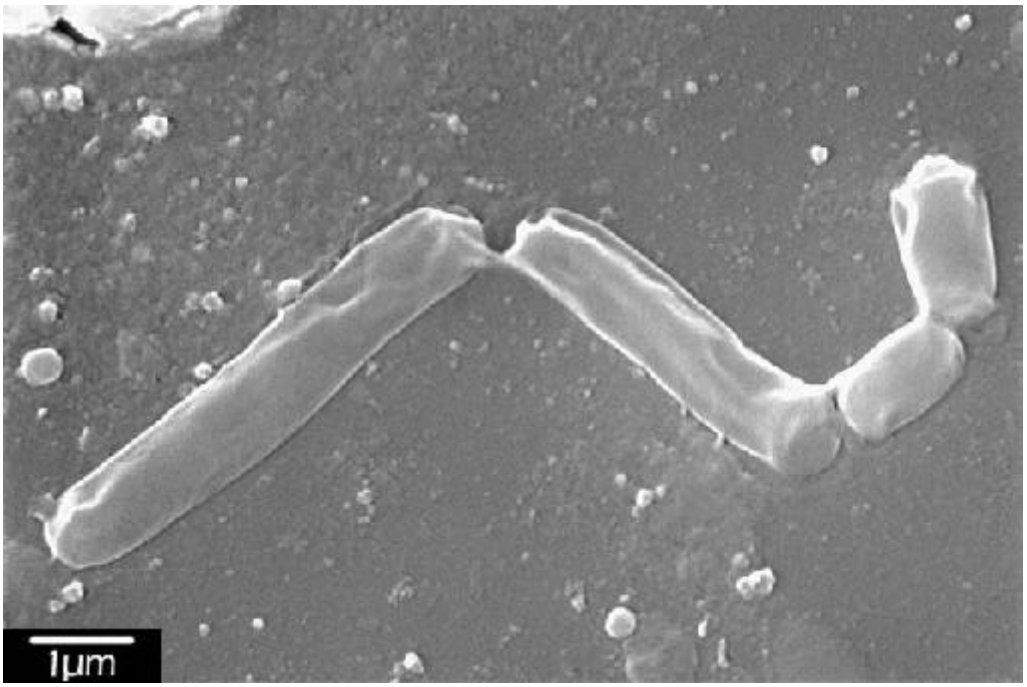

Figure 2: Air-dried, rod-shaped bacteria on the surface of the quartz overgrowth in Fig. 1. Walls of the bacteria have partially collapsed, creating a deflated texture.

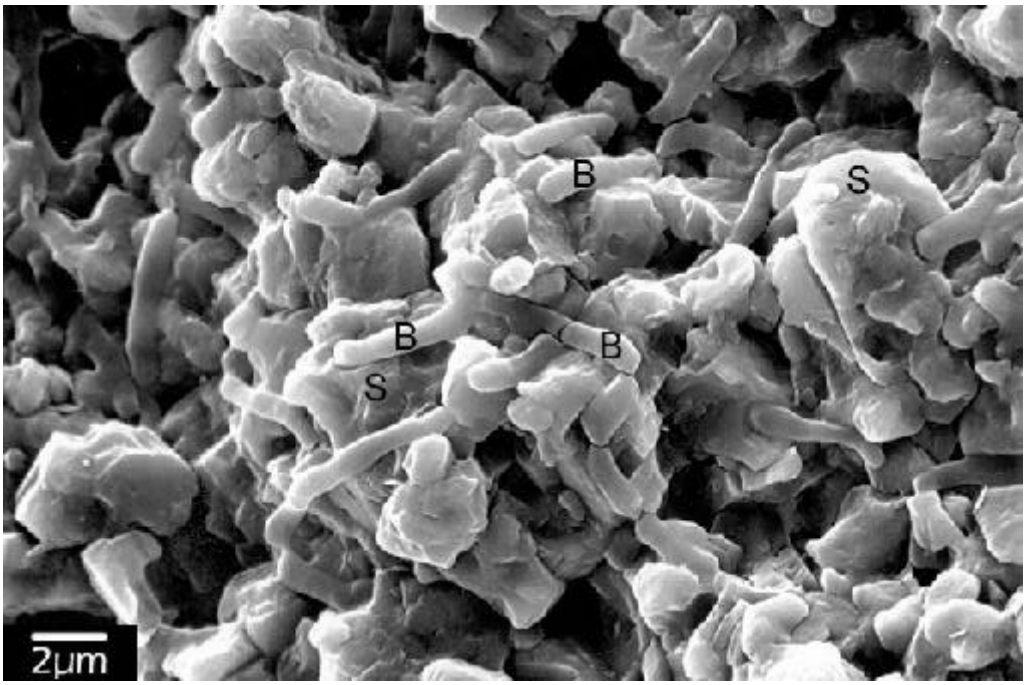

Figure 3: Air-dried bacteria (B) and slime (S) on the surface of a limestone piece.

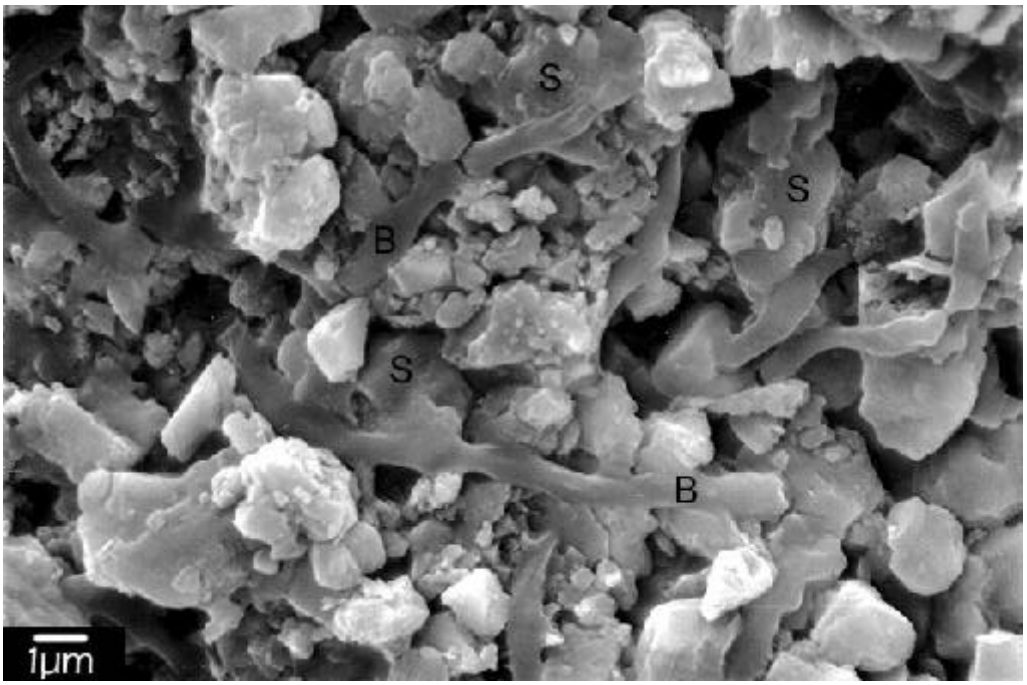

Figure 4: Air-dried, stretched bacteria (B) and slime (S) on the surface of a limestone piece. More severely distorted bacteria tend to merge into the slime layer.

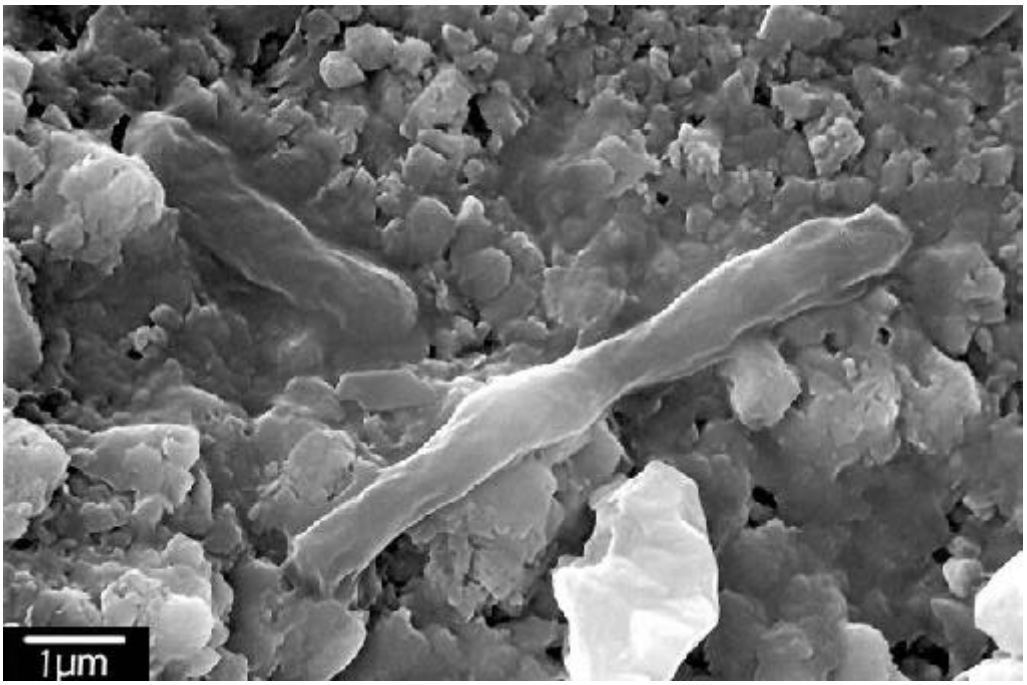

Figure 5: Two glutaraldehyde-preserved bacteria covered by a thin layer of slime. The surface of the bacteria are irregular and the cylindrical shape distorted.

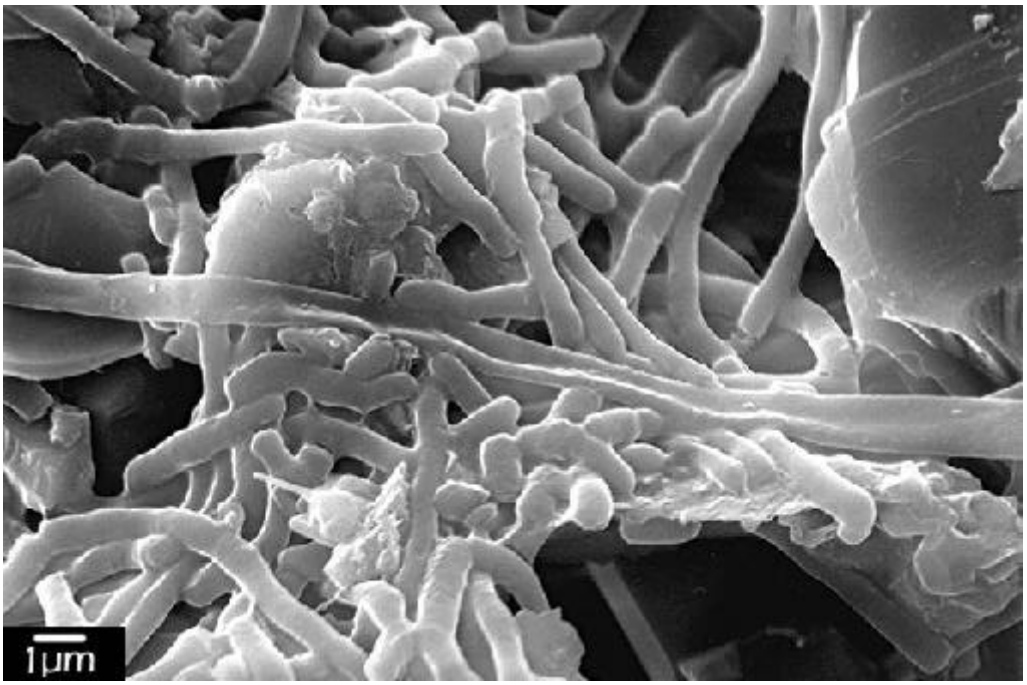

Figure 6: Colony of glutaraldehyde-preserved bacteria. The long bacterium in the center of the photo has cell walls that have completely collapsed. Other bacteria are slightly more intact.

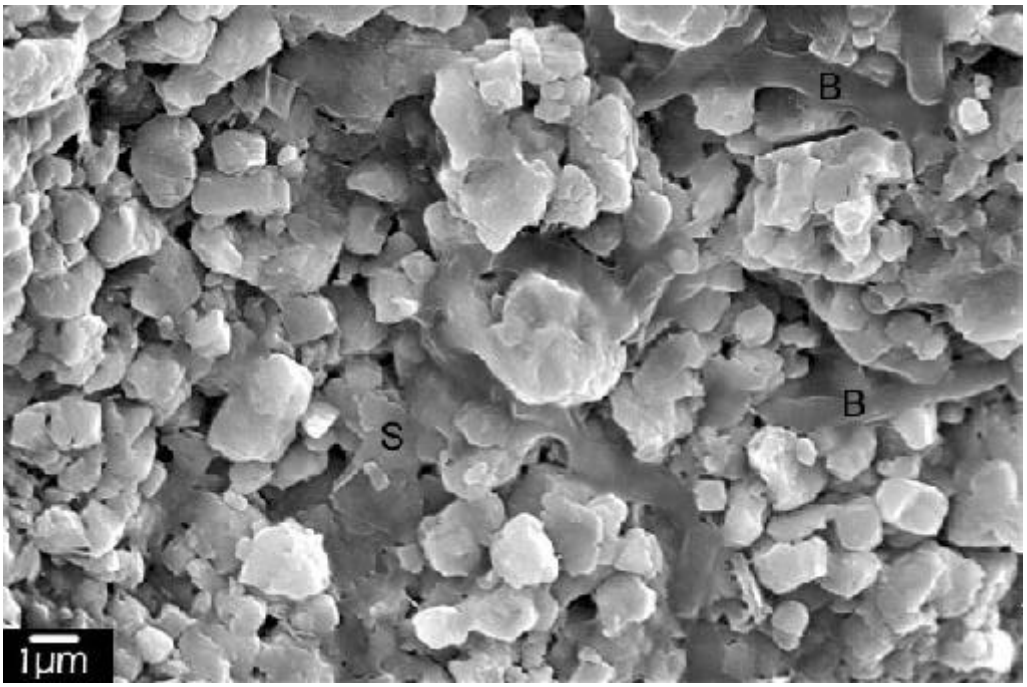

Figure 7: 10% Glutaraldehyde-preserved bacteria (B) and slime (S) on the surface of a limestone piece. Some of the bacteria are so distorted that they are difficult to distinguish from the slime layer.

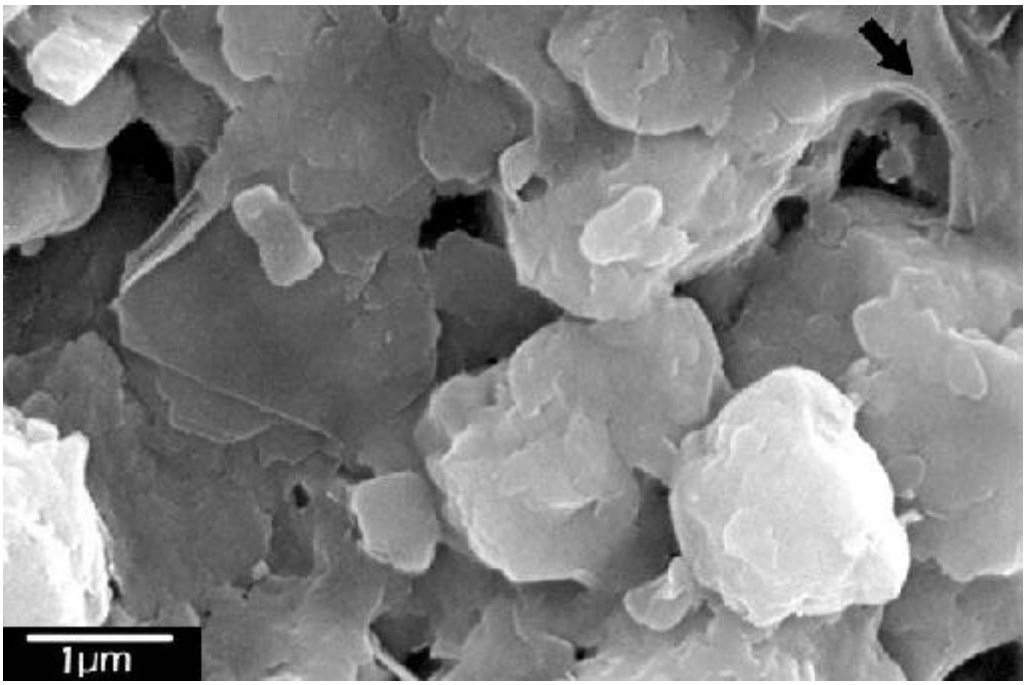

Figure 8: Thick, glutaraldehyde-preserved slime layer. A meniscus (arrow) has been preserved, and shows signs of cracking.

Ethanol Dehydration with Hexamethyldisilazane. Bacteria preserved with ethanol dehydration are generally three-dimensional, with their volume better preserved than either air-dried or glutaraldehyde-preserved bacteria (Figs. 9 and 10). In places where the slime sheet is intact, it is pulled away from the bacteria (Fig. 9). Much of the slime preserved by this method occurs in fragmented sheets or plates that have peeled free from the substrate (Figs. 11-13), as well as in "grape clusters" of 200 nm balls associated with the platy texture (Figs. 12-14). These balls are spherical in shape and are not seen in air-dried or glutaraldehyde-fixed samples.

Ethanol Dehydration with Critical Point Drying. Bacteria preserved with critical point drying are modified cylinders of roughly consistent diameter with flattened ends and some irregular surfaces (Figs. 15-18 and 20). They tend to be free-standing and occur in clusters. The slime sheet is absent in most areas, but rarely occurs as plates with balls or fingers of slime along the edges (Figs. 19 and 20).

Ethanol and Acetone Dehydration with Critical Point Drying. Bacteria preserved with ethanol/acetone dehydration and critical point drying have even thicknesses along their lengths and rounded ends (Figs. 21-23). They stand away from the substrate and have strands and pieces of slime attached to their bodies (Figs. 22 and 23). The slime sheet occurs in plates (Figs. 24 and 25) or very rarely as a cracked sheet covering the surface (Fig. 21). Clusters of 200 nm balls are associated with the platy slime in acetone/critical point dried samples (Figs. 24-26), as with ethanol/hexamethyldisalazane (Figs. 12-14).

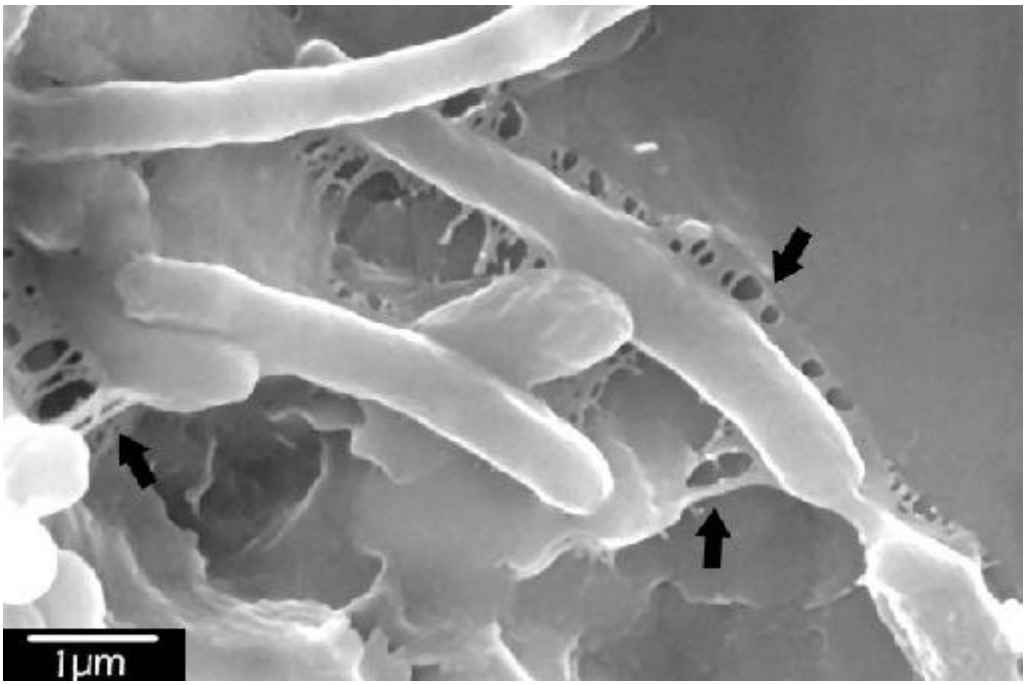

Figure 9: Ethanol/Hexamethyldisilazane-preserved bacteria and slime sheet. The shape and volume of the bacteria is well-preserved, but the edge of the slime sheet is pulling away from the bacterial bodies, forming a tattered fringe (arrows).

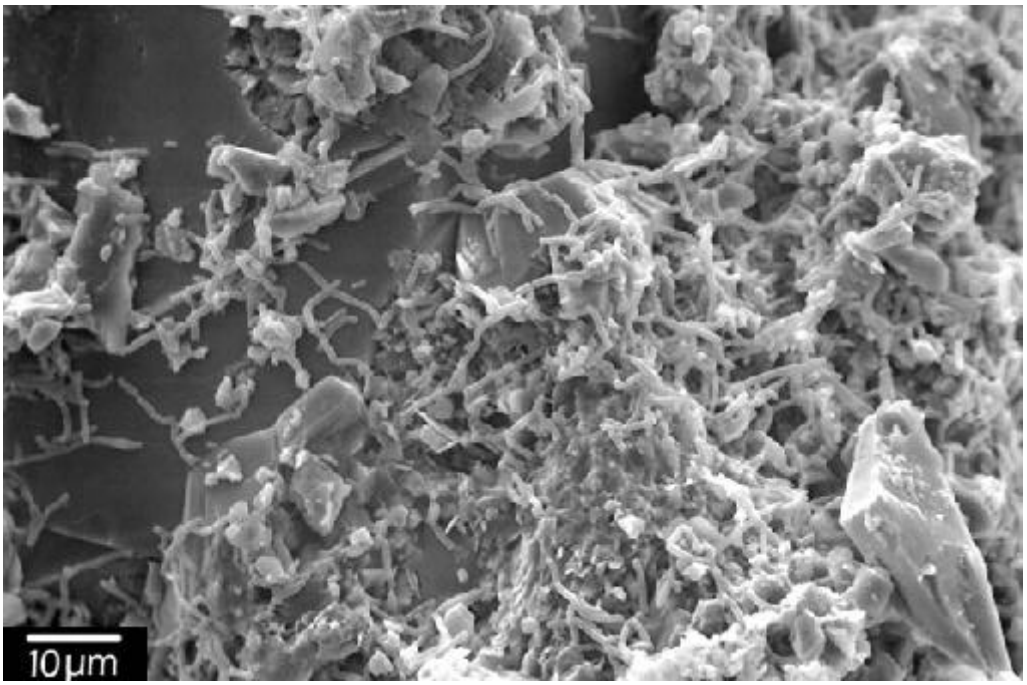

Figure 10: Colony of bacteria preserved with ethanol/hexamethyldisilazane on a quartz overgrowth.

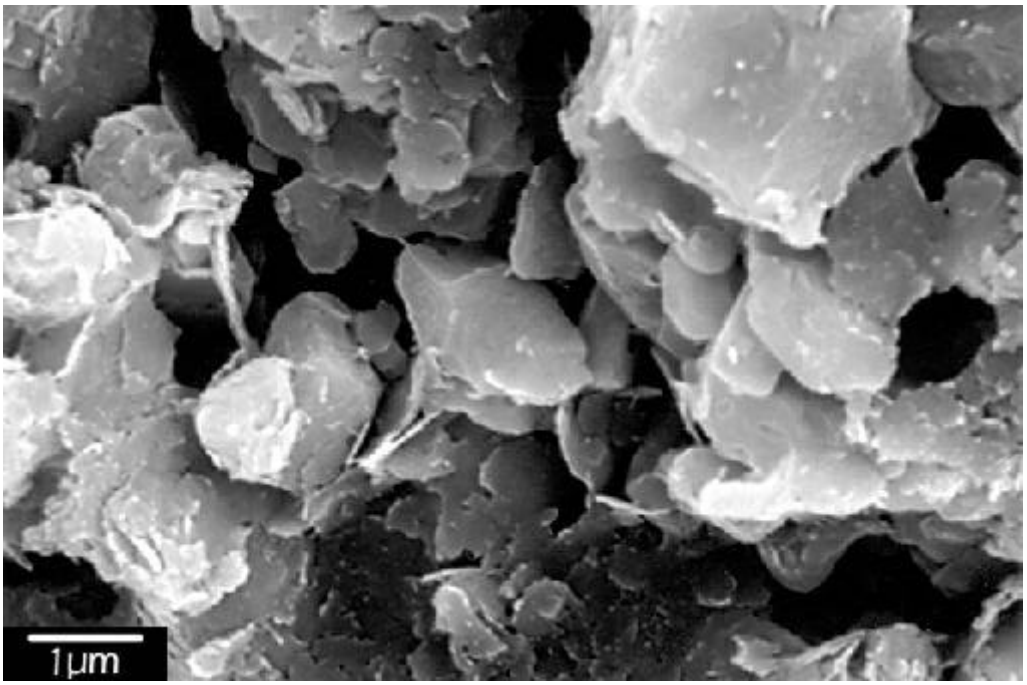

Figure 11: Platy texture of slime preserved with ethanol/ hexamethyldisilazane.

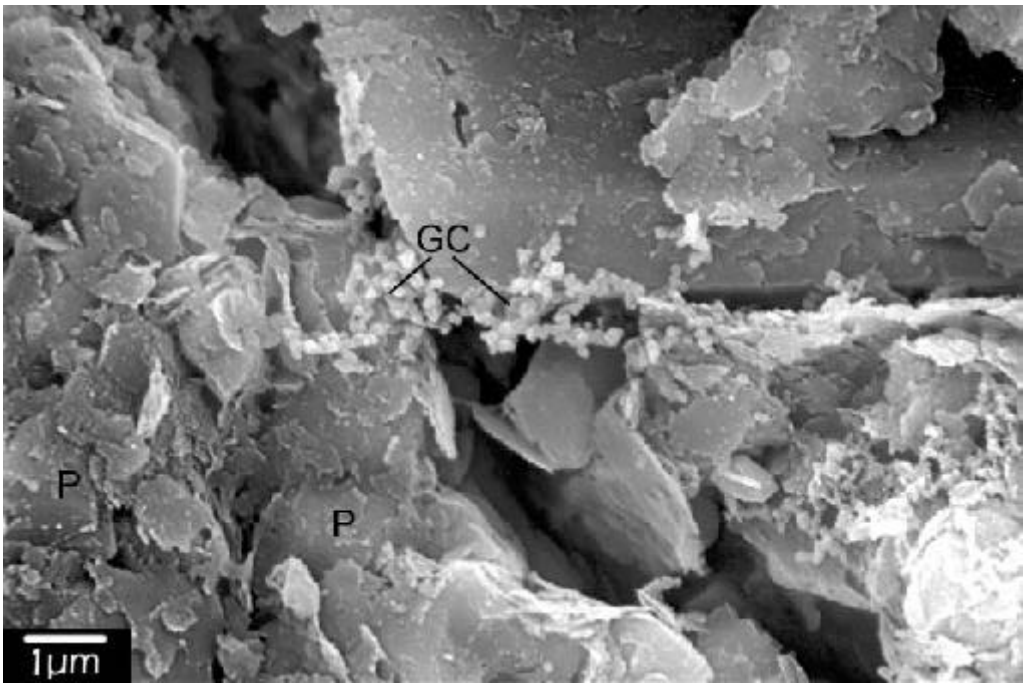

Figure 12: Grape clusters (GC) and platy slime texture (P) in ethanol/ hexamethyldisilazane preserved sample. Grape clusters are made of individual balls about 100-200 nm in diameter.

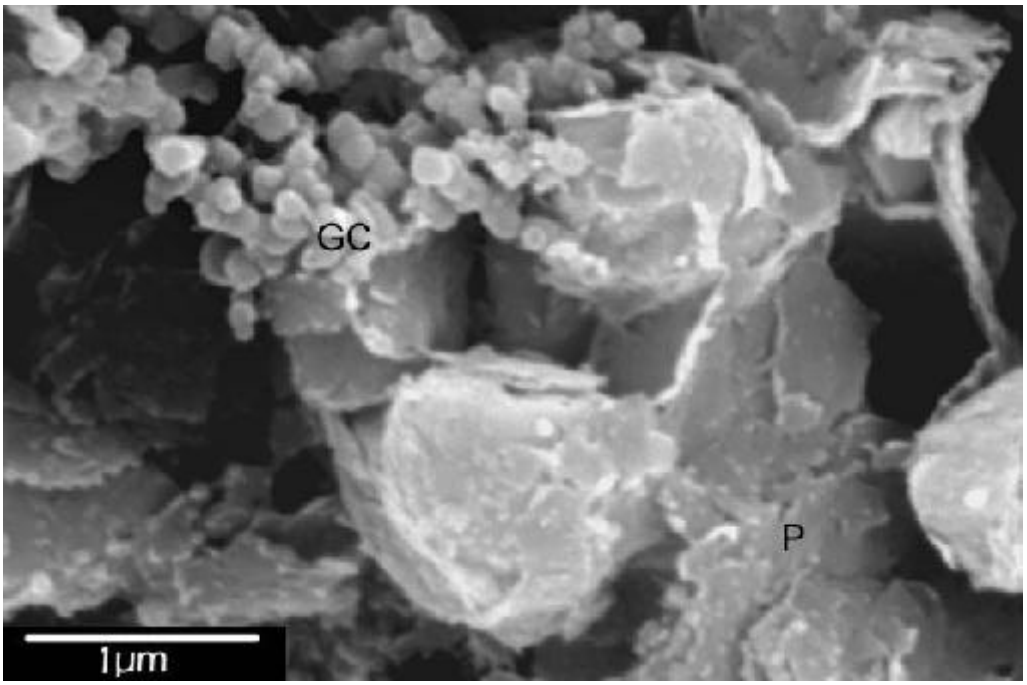

Figure 13: High-magnification photo of grape cluster (GC) and underlying platy slime texture in ethanol/hexamethyldisilazane-preserved sample.

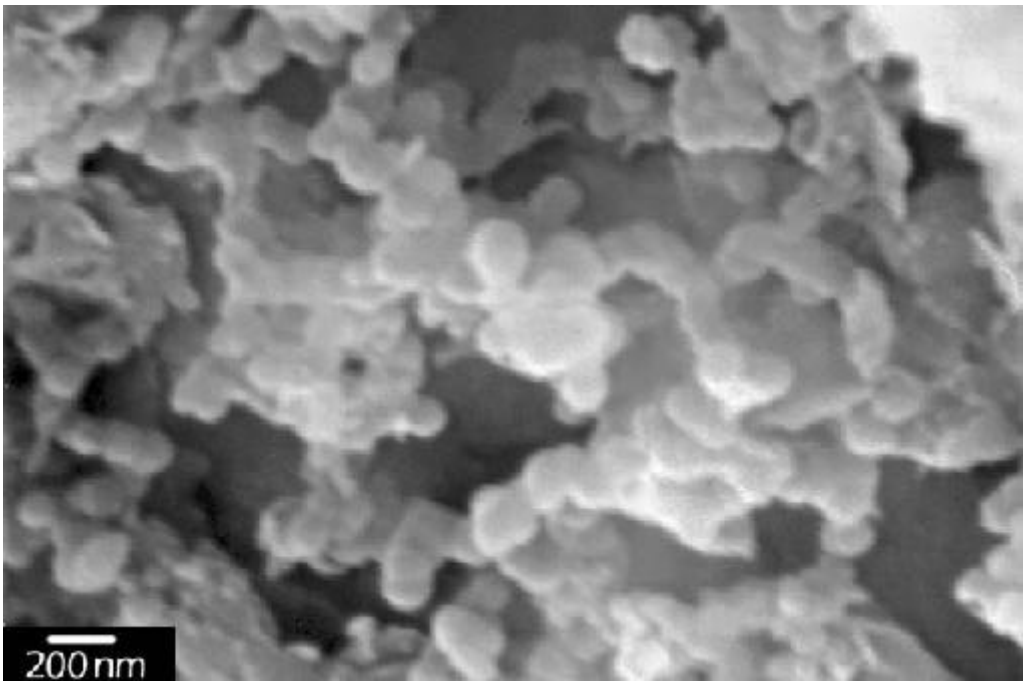

Figure 14: High-magnification photo of nanno-scale balls that make up grape clusters.

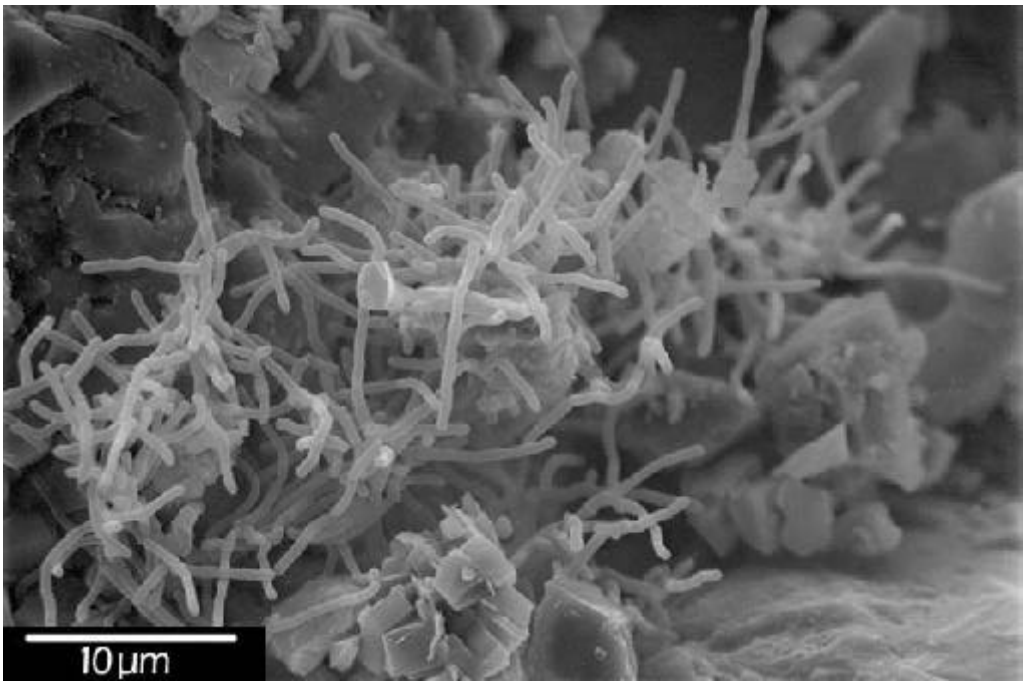

Figure 15: Colony of bacteria preserved with ethanol/critical point drying. These bacteria are free-standing, compared to air-dried and glutaraldehyde-preserved bacteria, which lie flat against the grains.

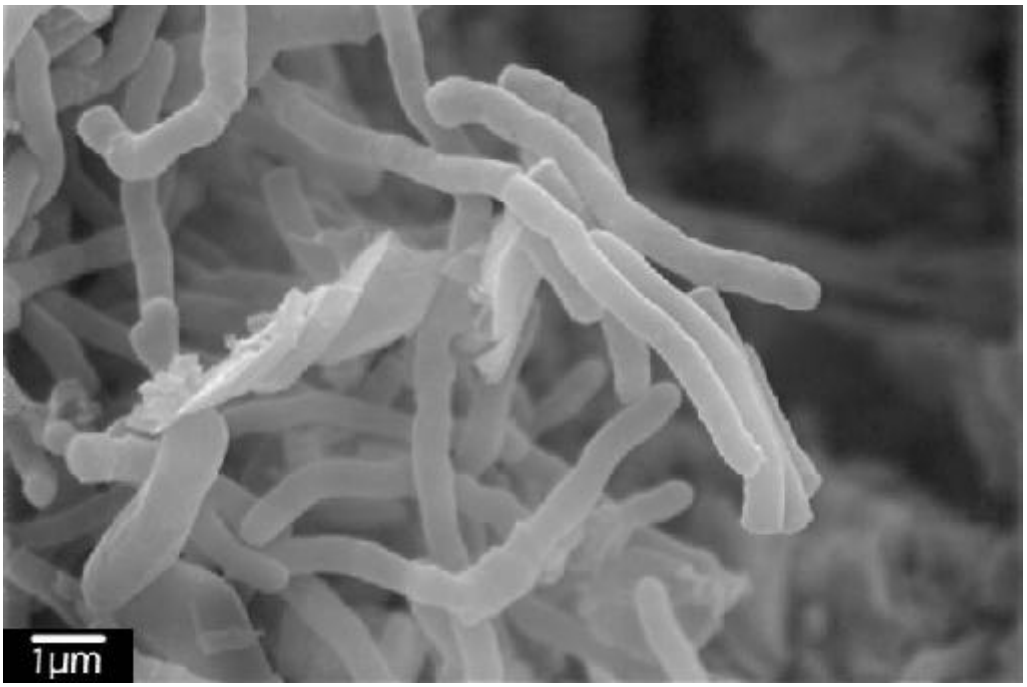

Figure 16: High-magnification photo of bacteria preserved with ethanol/critical point drying. Bacteria have irregular surfaces but exhibit less distortion than air-dried or glutaraldehyde-preserved bacteria.

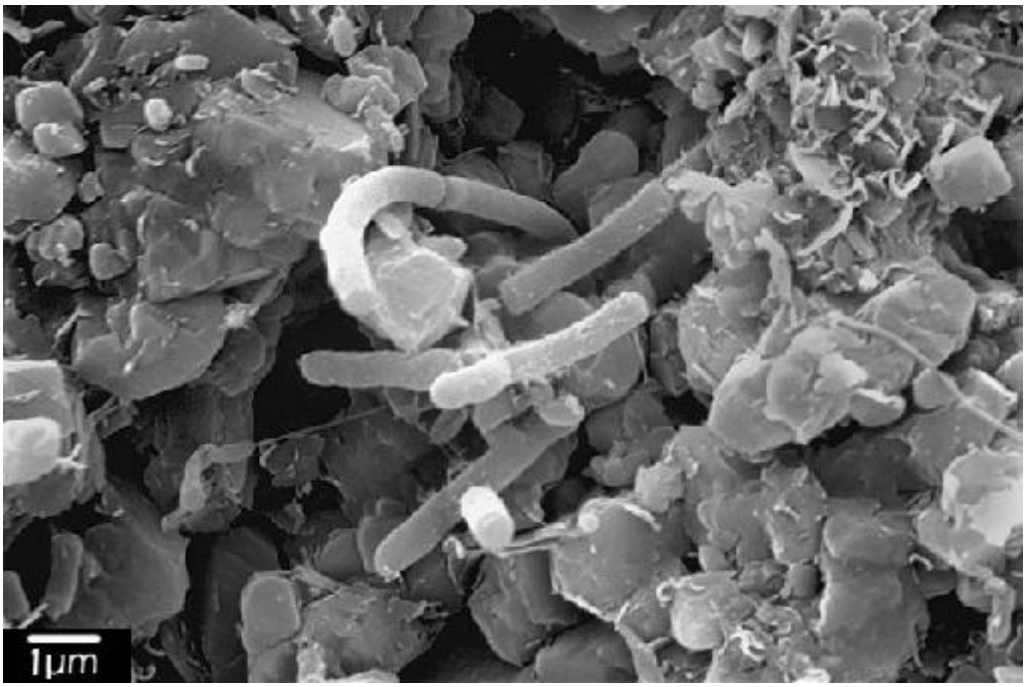

Figure 17: Cluster of free-standing, critical-point-dried bacteria.

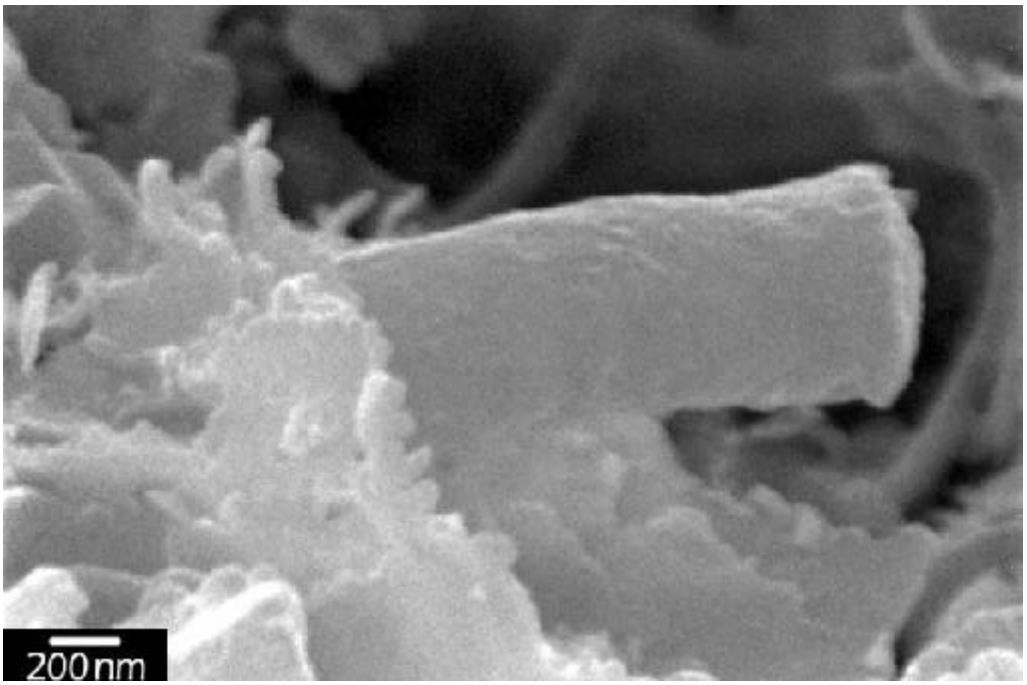

Figure 18: Ethanol/critical point dried bacterium exhibiting a cylindrical form with flattened ends. Fingers on the edges of slime plates are visible.

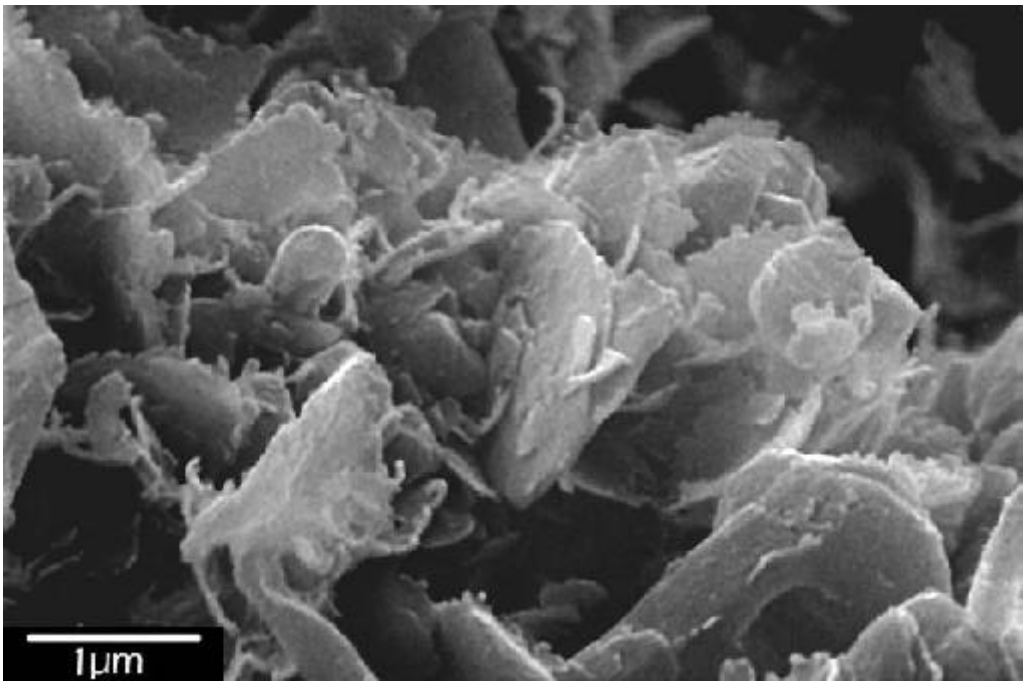

Figure 19: Platy slime texture preserved with ethanol/critical point drying. Plates have fingers of slime along their edges.

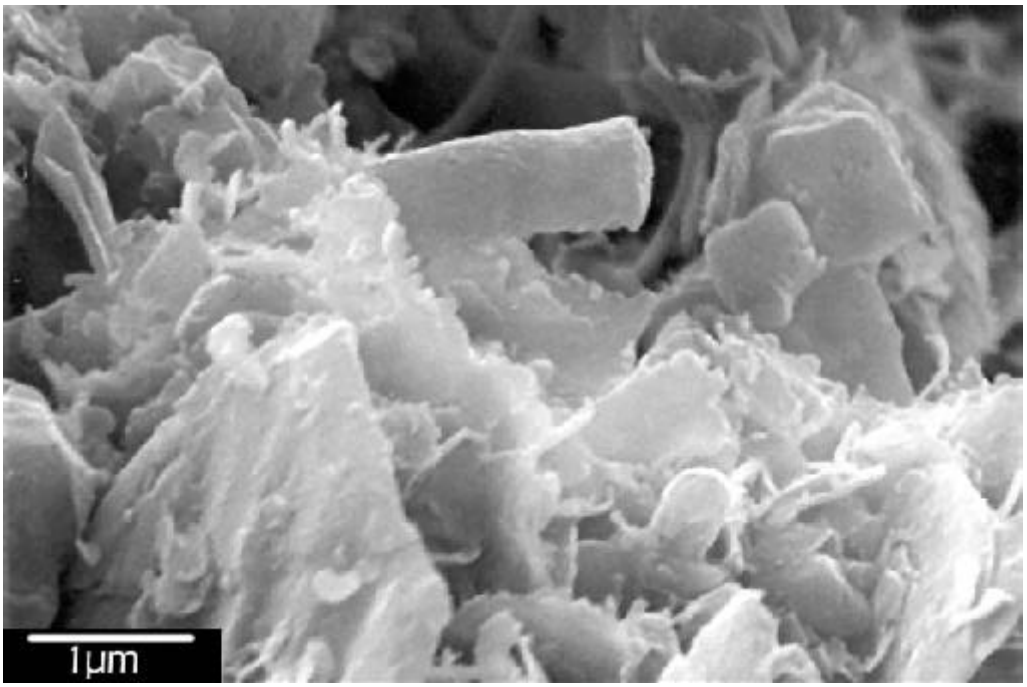

Figure 20: Bacterium and platy slime preserved with ethanol/critical point drying.

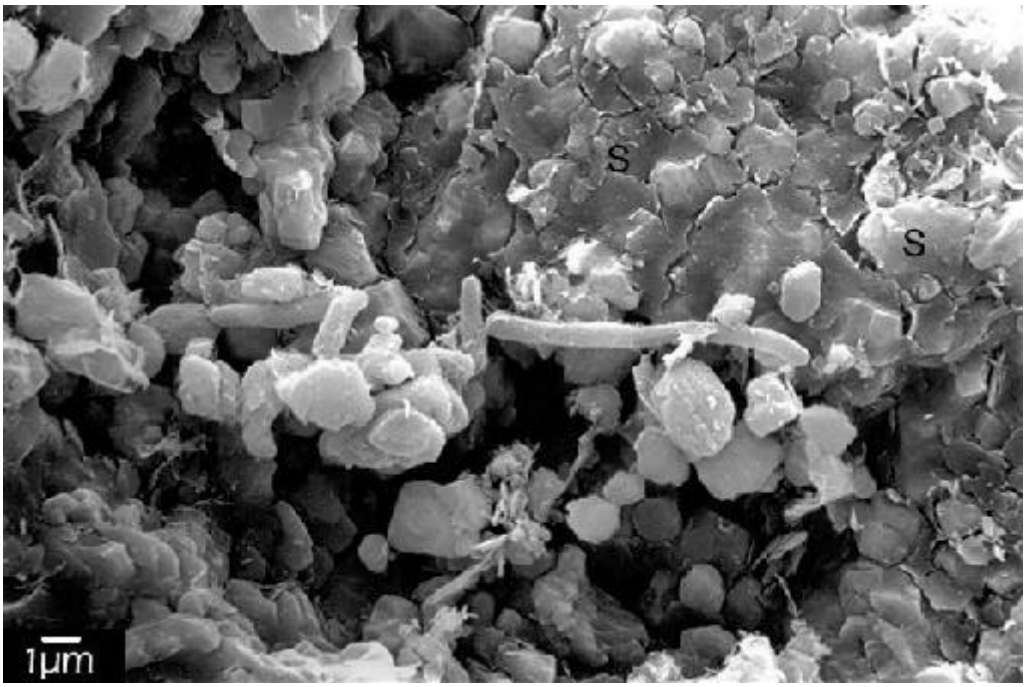

Figure 21: Bacteria and cracked slime sheet (S) preserved with ethanol/acetone/ critical point drying.

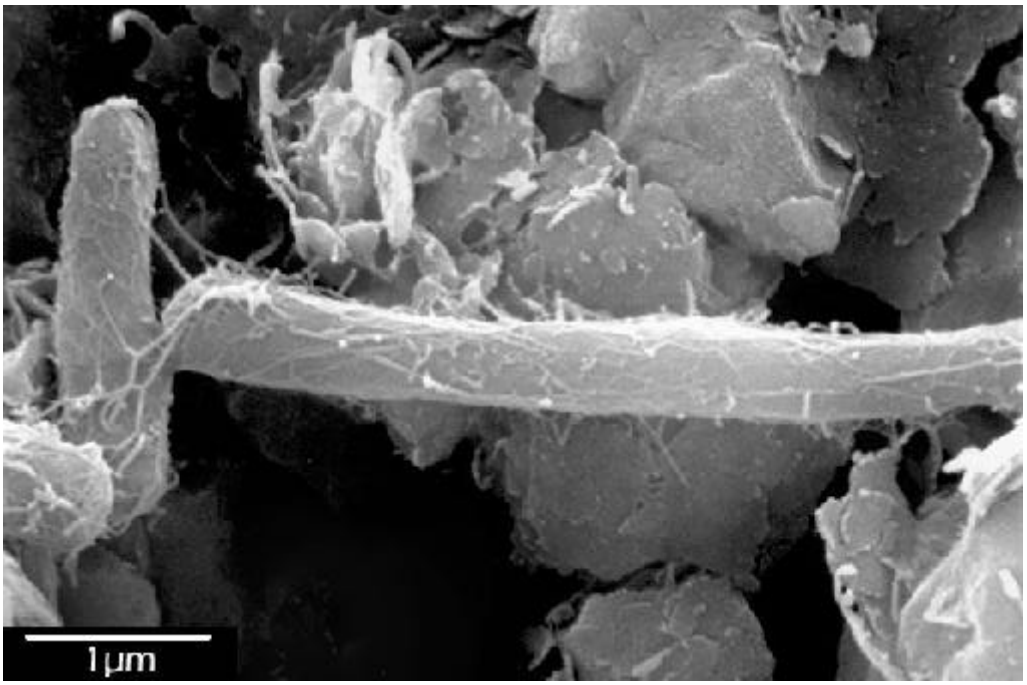

Figure 22: Rod-shaped bacteria preserved with ethanol/acetone/critical point drying. The bacterial bodies are covered with slime strands that stretch between the bacteria and surface of the grains.

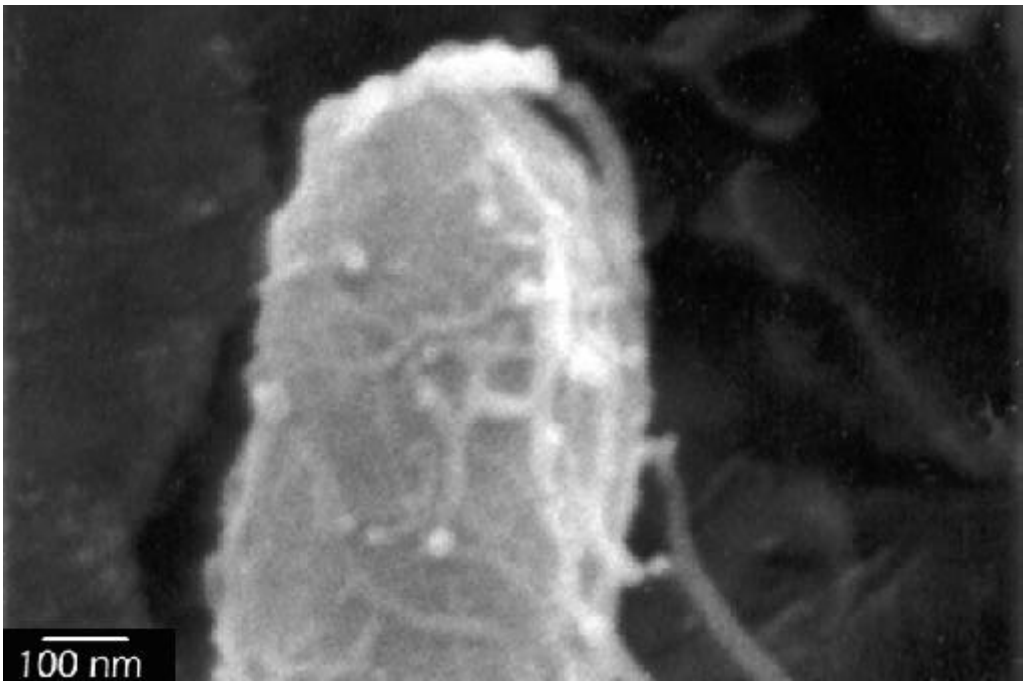

Figure 23: High-magnification photo of rod-shaped bacterium from Fig. 22. The bacterium was preserved with ethanol/acetone/critical point drying and has rounded ends with strands of slime covering its body.

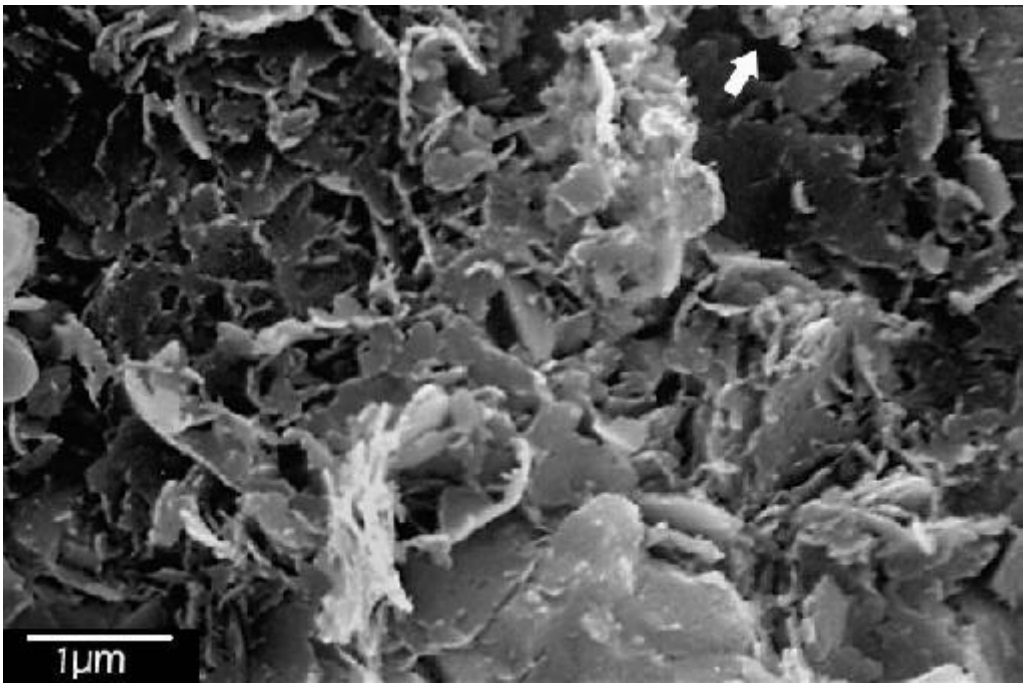

Figure 24: Platy slime texture in ethanol/acetone/critical point dried sample. A grape cluster is visible in the upper right corner of the photo (arrow).

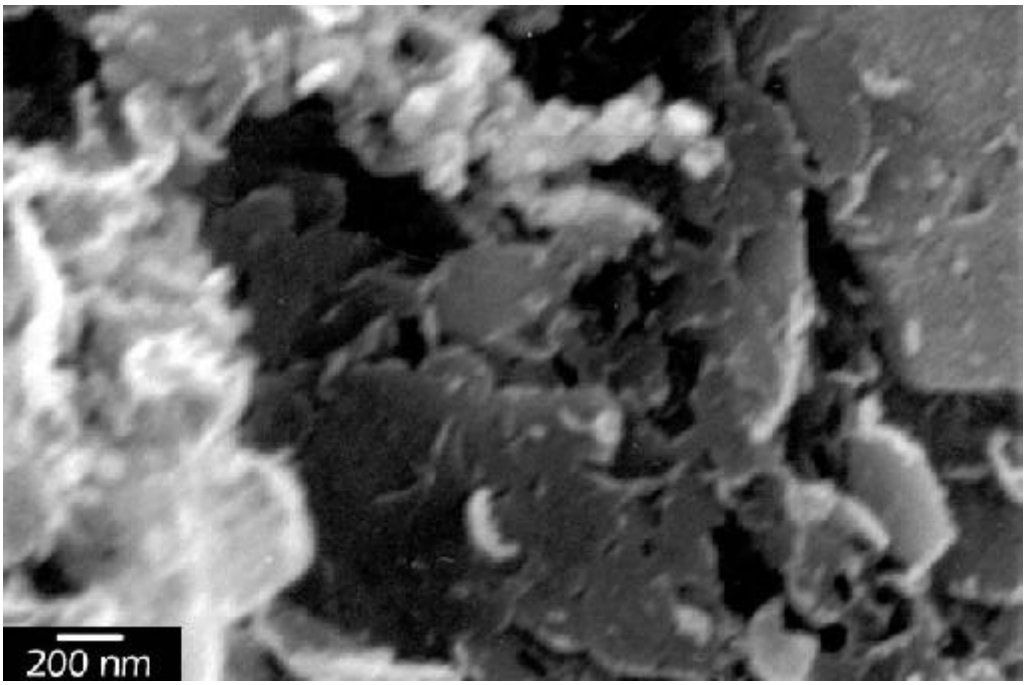

Figure 25: High-magnification photo of platy slime and grape cluster from Fig. 24. This sample was preserved with ethanol/acetone/critical point drying.

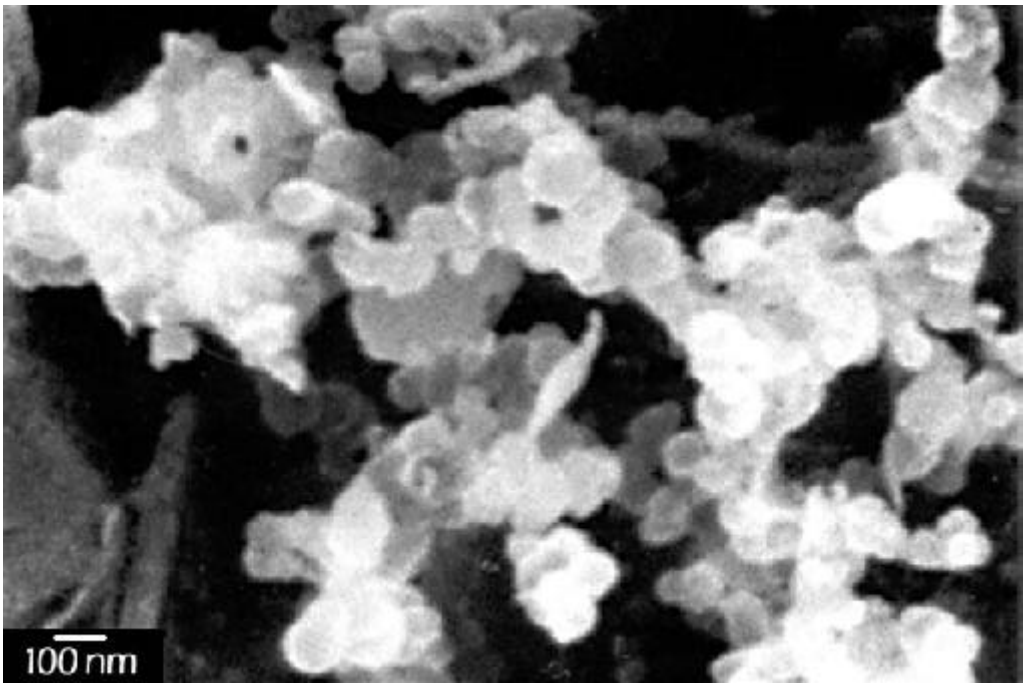

Figure 26: High-magnification photo of nanno-scale balls that make up the grape clusters in ethanol/acetone/critical point dried sample.

PRESERVATION OF RESERVOIR BACTERIA AND ASSOCIATED SLIME LAYER

Air Drying. In air-dried samples inoculated with bacteria from the North Blowhorn Creek Unit, exopolysaccharide slime has two morphologies: a globular, beaded texture and a sheet-like form with hexagonal outlines (Figs. 27-29). The minute balls within the first layer of slime are 100-150 nm in diameter. Few bacteria were observed in air dried samples (Figs. 28-30).

10% Glutaraldehyde Fixation. Samples fixed in 10% glutaraldehyde include a globular, but slightly more coherent, slime sheet than in air-dried samples that coats the entire surface of the rock (Figs. 31-36). The slime stretches across pore spaces and over clay crystallites (Figs. 32, 33 and 34). Reservoir bacteria fixed in 10% glutaraldehyde are completely flat and only visible where the slime layer is thin (Figs. 35 and 36).

Ethanol Dehydration with Hexamethyldisilazane. The volume of bacteria preserved with ethanol dehydration is greater than that of bacteria fixed with 10% glutaraldehyde (Fig. 37). The exopolysaccharide slime occurs as a ubiquitous residuum of small fragments coating all grains and occasionally as accumulated chunky patches (Fig. 38).

Ethanol Dehydration and Critical Point Drying. North Blowhorn Creek reservoir bacteria in critical point dried samples have uneven surfaces, but their volume is preserved (Fig. 40). The exopolysaccharide slime layer is present in mats of a weblike network of slime strands with small spheroids about 100 nm in diameter (Figs. 39-42).

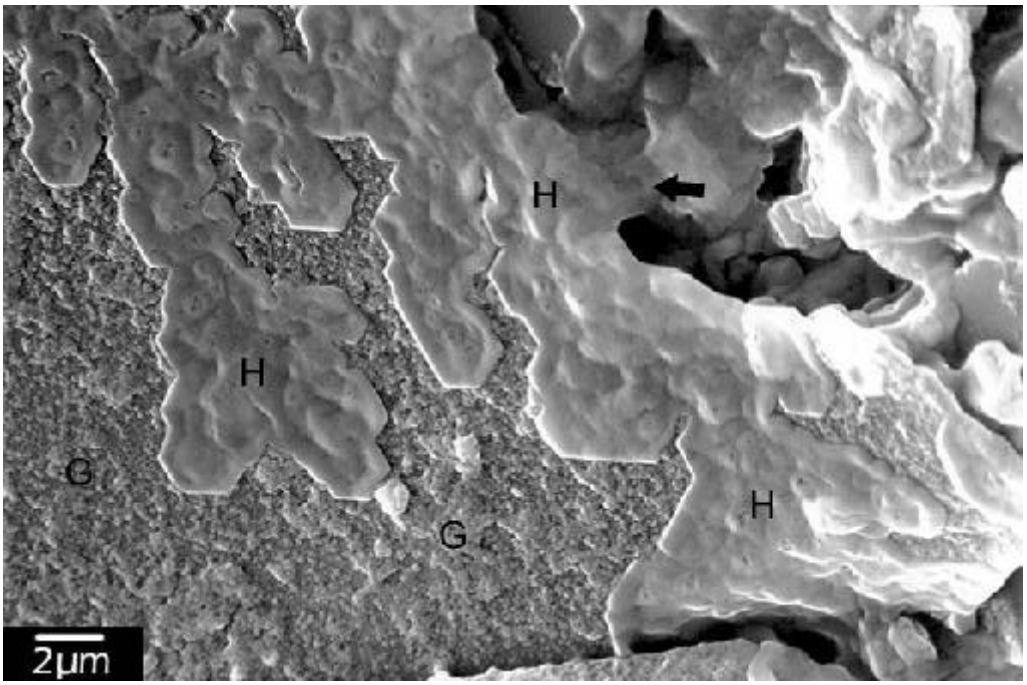

Figure 27: Two types of slime in air-dried reservoir sandstone sample: globular slime (G) and sheet-like hexagonal slime (H). The sheet-like hexagonal layer forms a meniscus over a fracture (arrow).

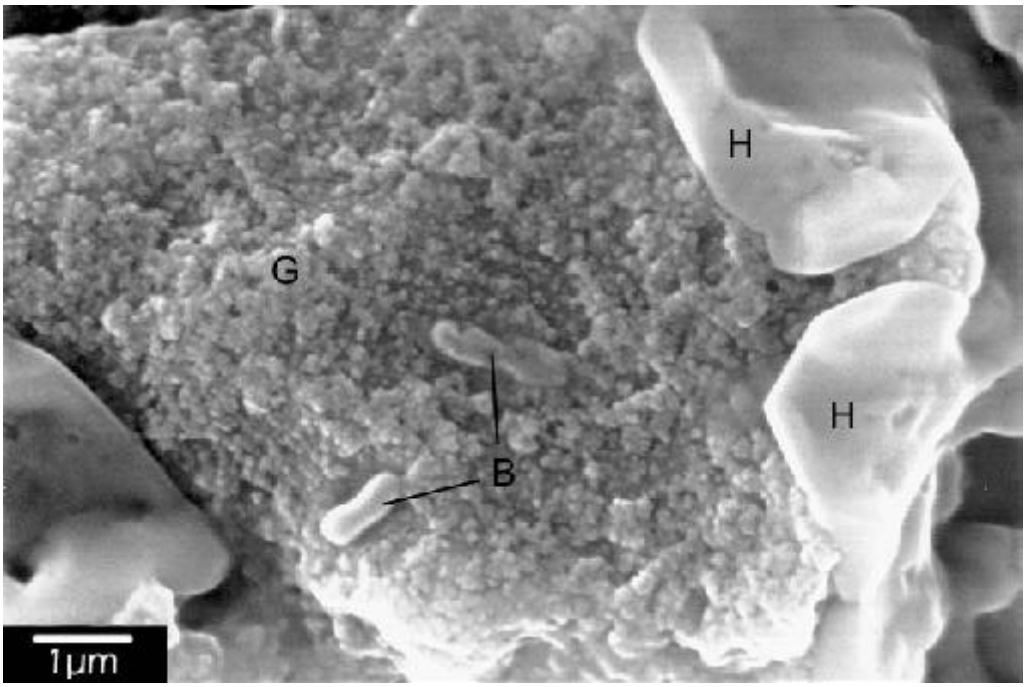

Figure 28: Air-dried reservoir bacteria (B) and two types of slime: globular (G) and hexagonal (H). The bacteria are distorted sausage shapes on the surface of the globular slime.

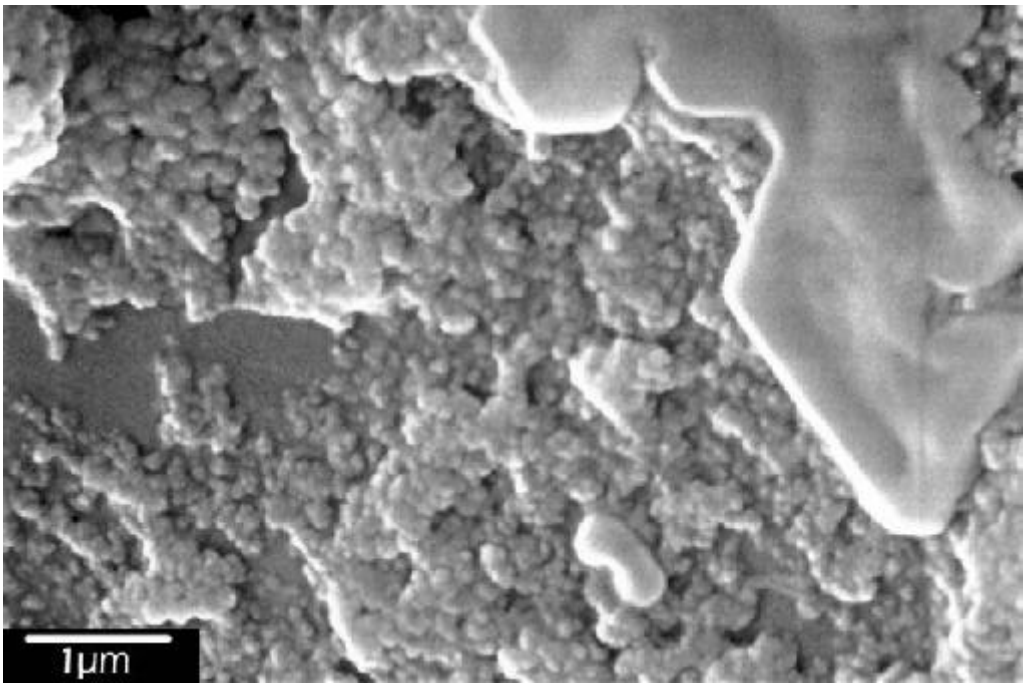

Figure 29: High-magnification photo of two types of slime in reservoir sandstones. The small spheroids that make up the globular slime layer are about 100 nm in diameter.

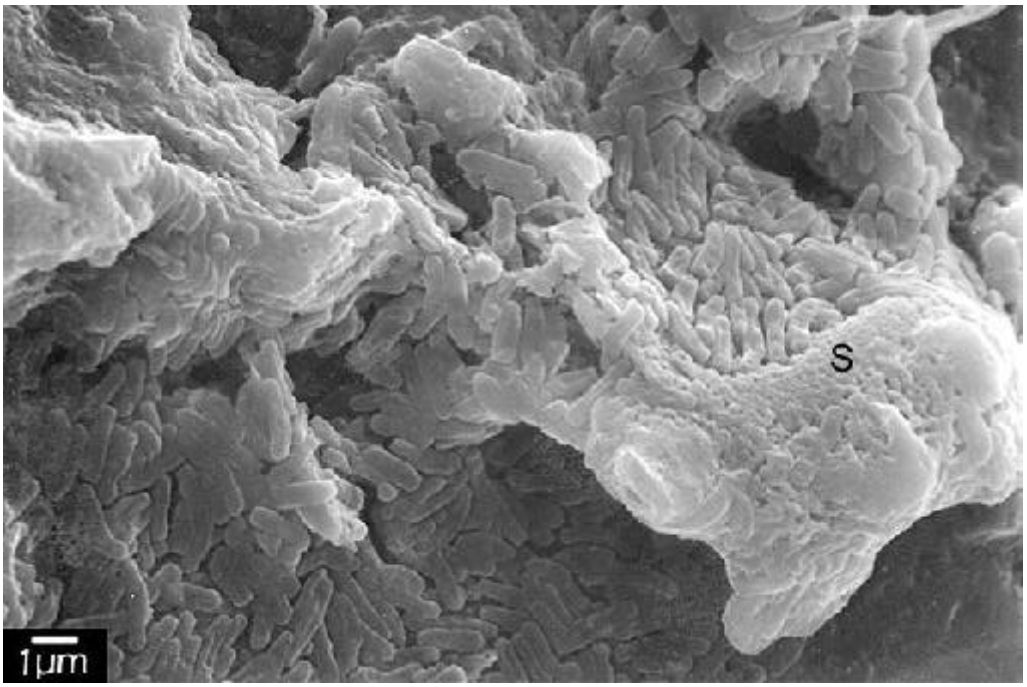

Figure 30: A rare colony of slightly flattened, air-dried, reservoir bacteria and an irregular layer of slime (S) preserved by air drying. The "slime layer" may at least partially be made of distorted bacterial bodies.

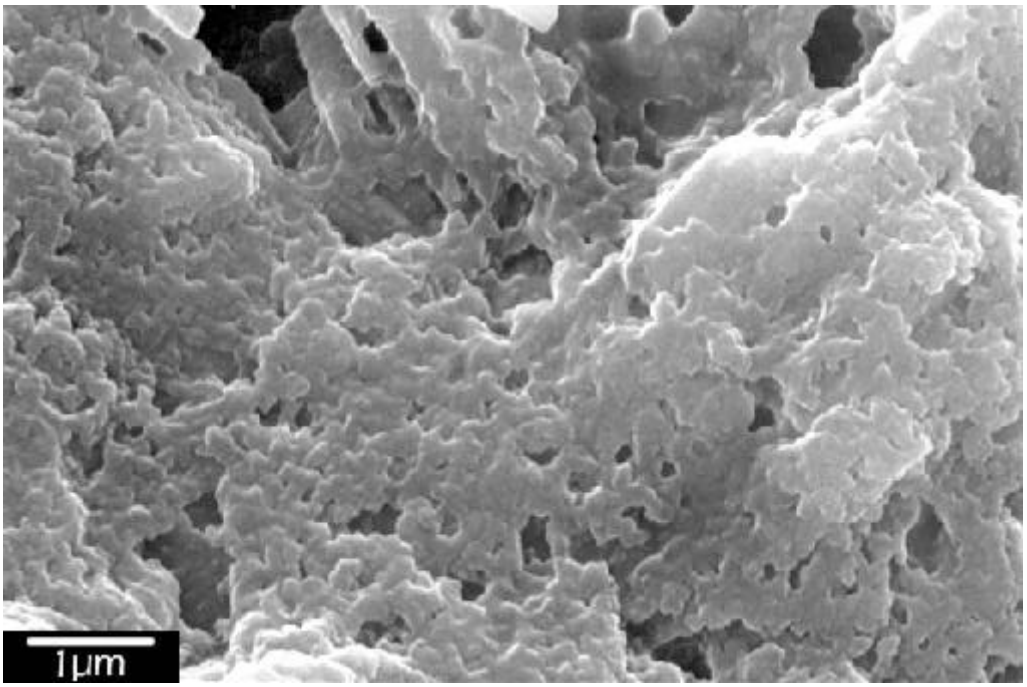

Figure 31: Thick, irregular layer of slime in reservoir sandstone preserved in 10% glutaraldehyde. This layer is slightly more coherent than in air-dried samples (Fig. 30), but is still very lumpy.

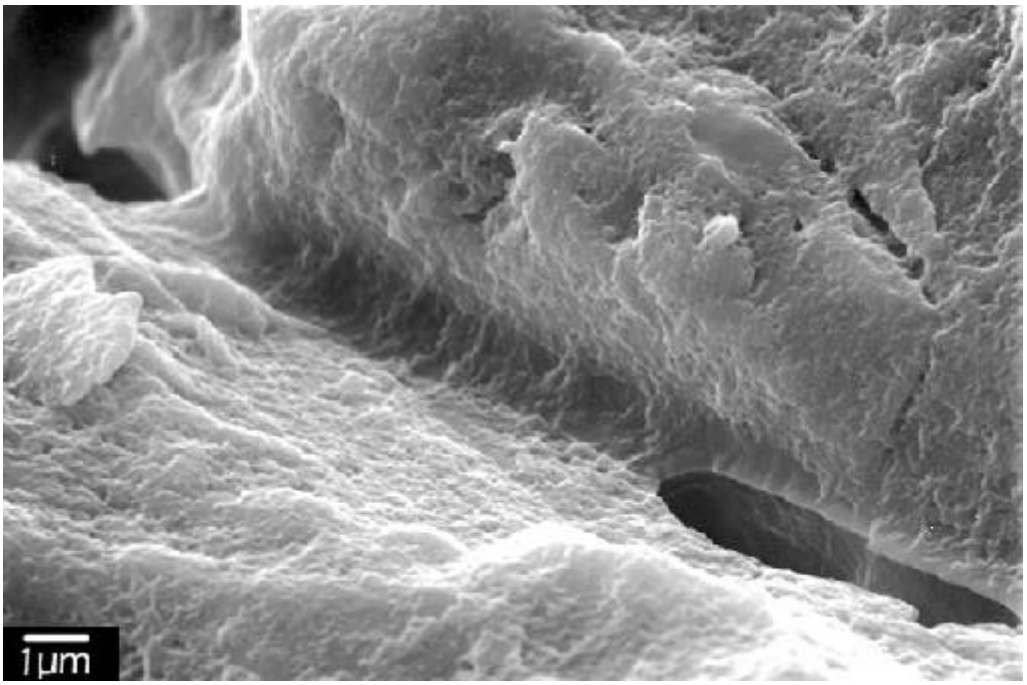

Figure 32: A meniscus of slime in reservoir sandstone preserved in 10% glutaraldehyde. The slime is stretching across a narrow pore space, occluding the porosity of this sandstone.

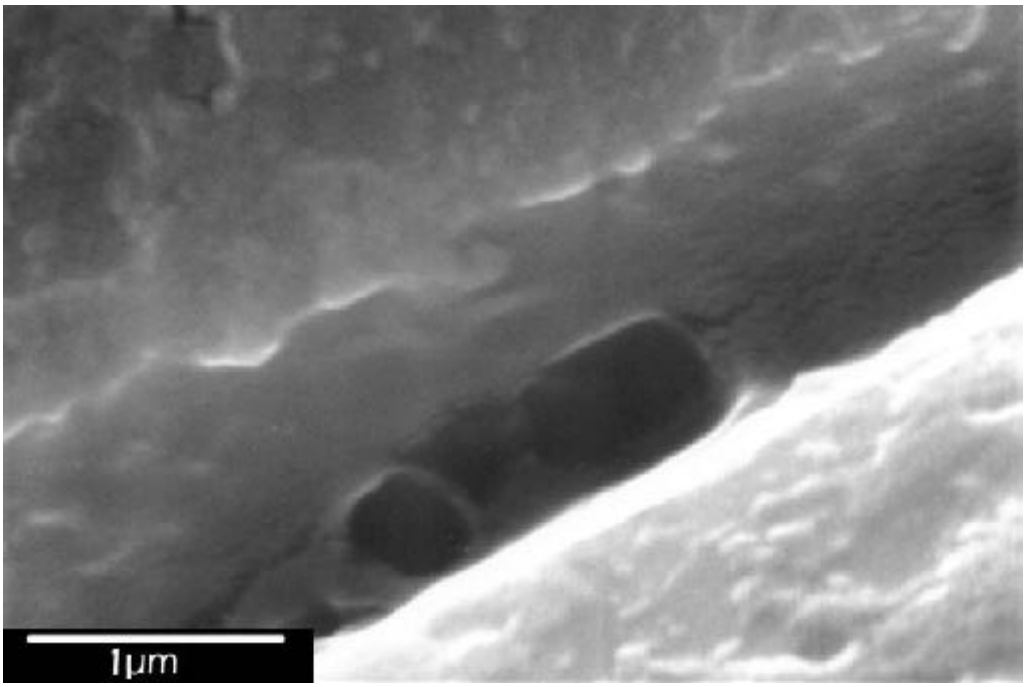

Figure 33: A meniscus of slime in reservoir sandstone preserved with 10% glutaraldehyde. The meniscus has begun to crack.

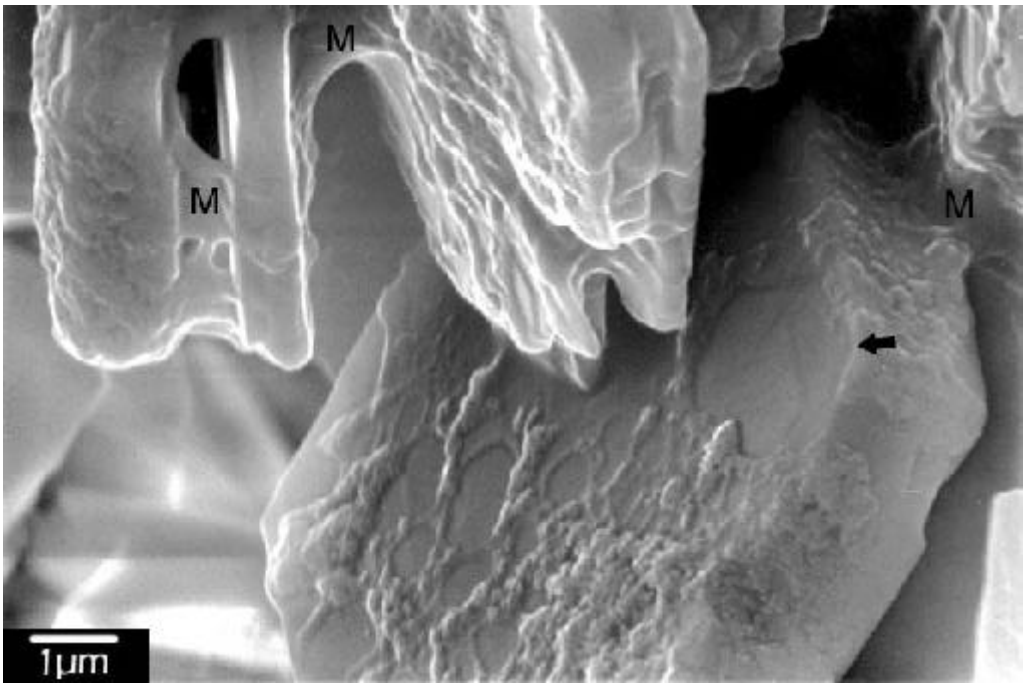

Figure 34: Glutaraldehyde-preserved slime layer and menisci of slime (M) on kaolinite crystallites in a reservoir sandstone. The slime is showing faint signs of a hexagonal outline on the larger surface (arrow).

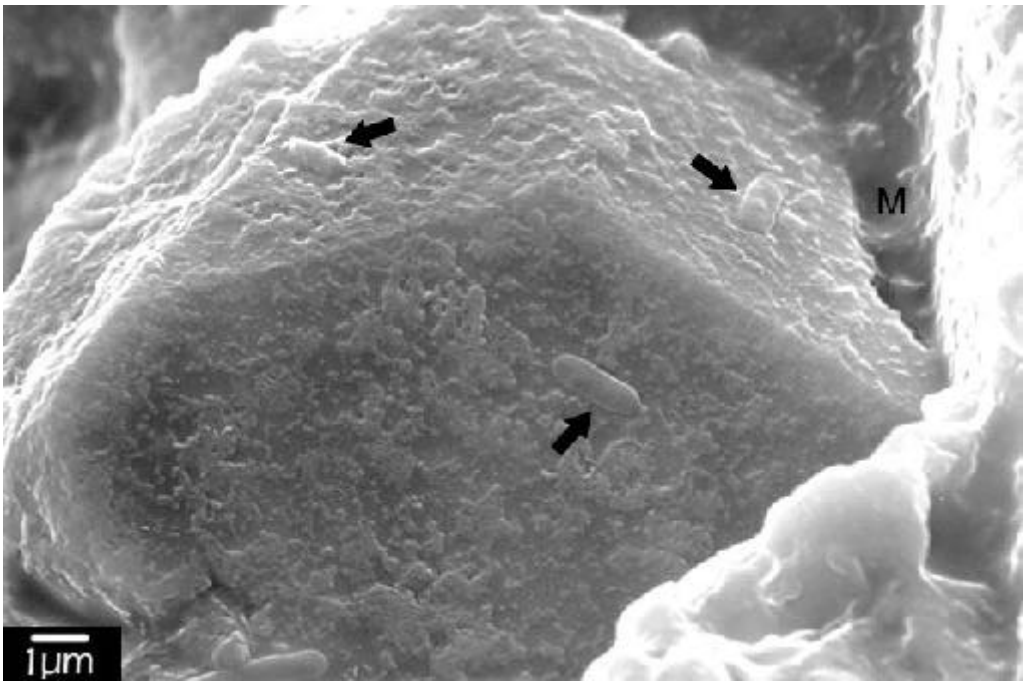

Figure 35: Flattened bacteria (B) and irregular slime layer covering a quartz overgrowth in a 10% glutaraldehyde sample. The slime layer forms a meniscus (M) in the upper right corner of the photo which spans the pore space between this grain and the next one.

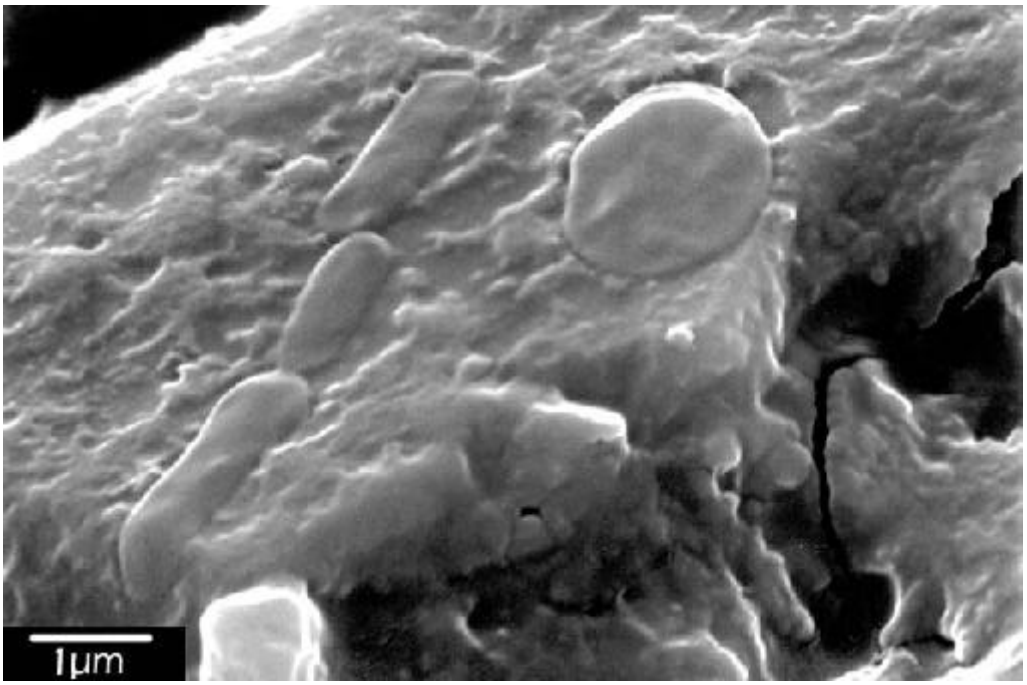

Figure 36: Flattened reservoir bacteria and slime layer preserved with 10% glutaraldehyde fixation. The spheroid-shaped bacteria are rare. The slime layer has started to separate on the right side of the photo.

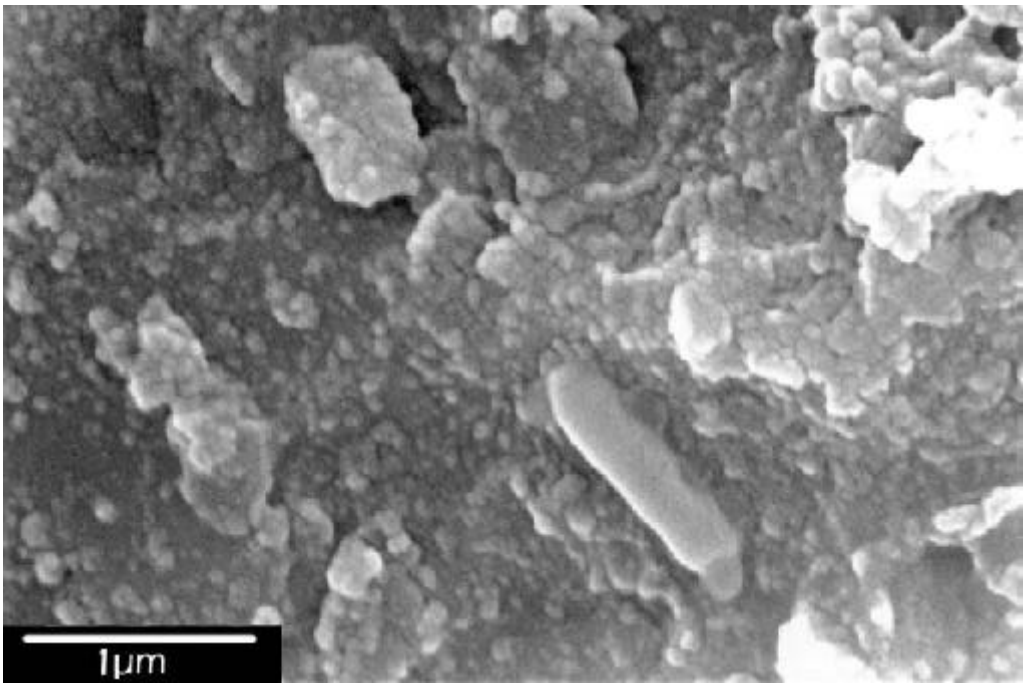

Figure 37: Reservoir bacterium and slime preserved with ethanol/hexamethyldisilazane. Slime preserved with this method is chunkier than glutaraldehyde-preserved slime of this type.

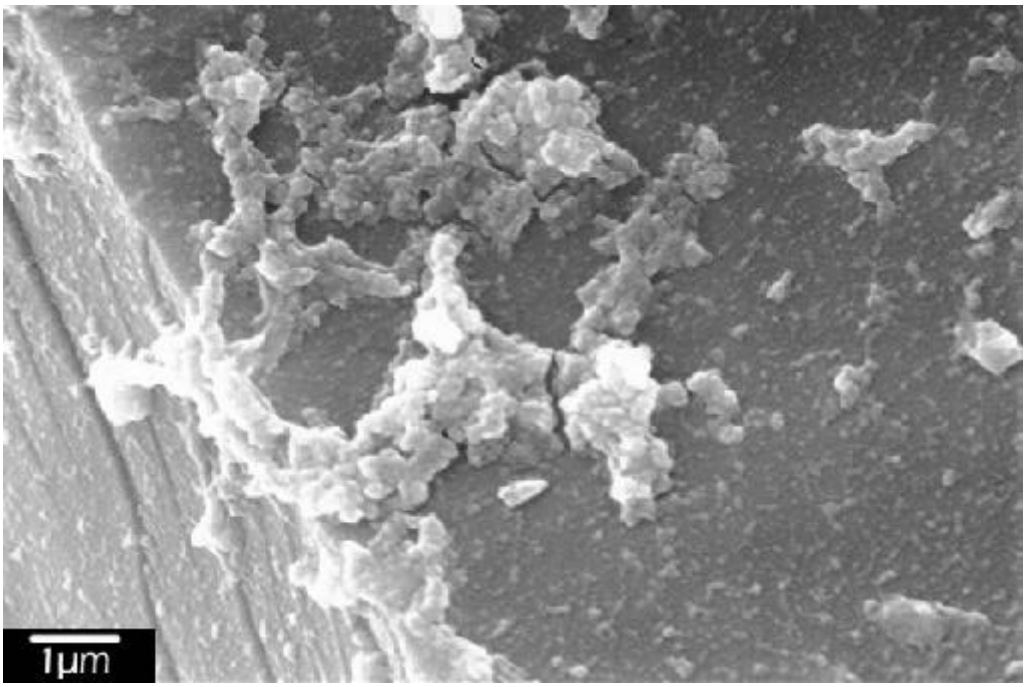

Figure 38: Slime on the surface of a quartz overgrowth in a reservoir sandstone preserved with ethanol/hexamethyldisilazane. A thin layer of detritus covers all grains preserved with this method. Occasional patches of thicker, chunkier slime are scattered over the surface.

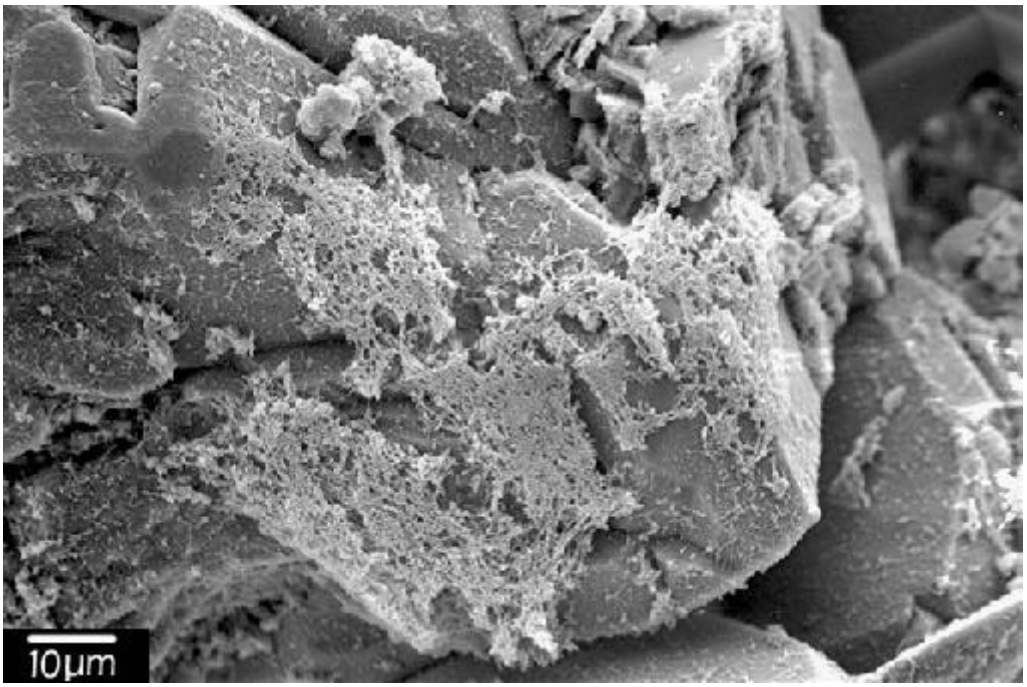

Figure 39: Mats of slime in reservoir sandstone preserved with ethanol/critical point drying. The mats are composed of weblike networks of slime strands.

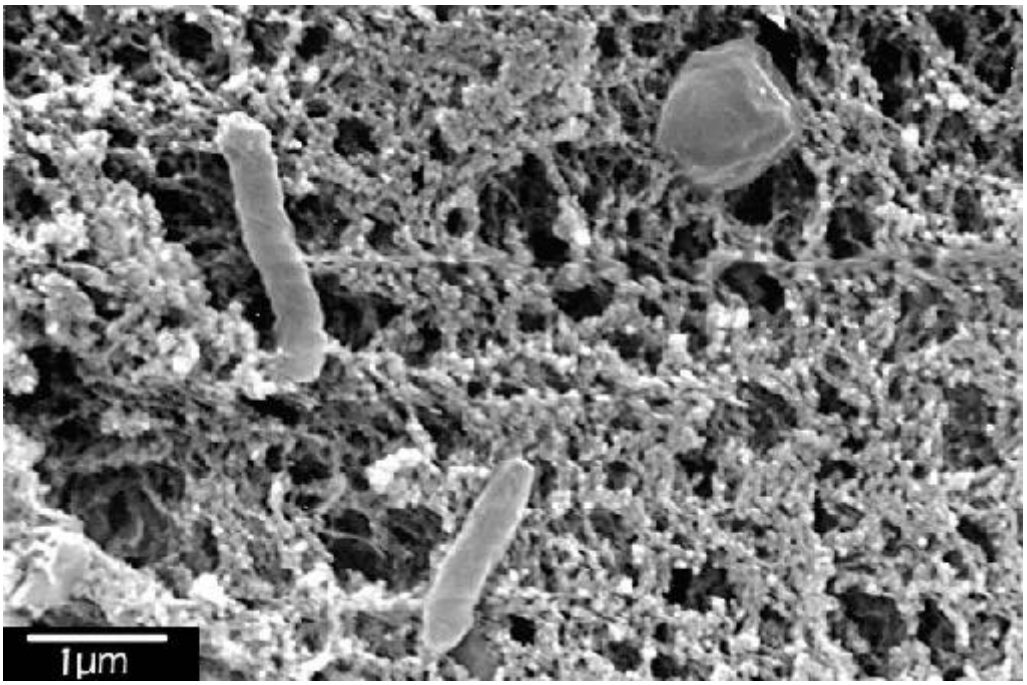

Figure 40: High-magnification photo of reservoir bacteria and slime web from Fig. 39. The web incorporates spheroid shapes about 100 nm in diameter. The volume of the bacteria is preserved but their shapes and surfaces are slightly irregular.

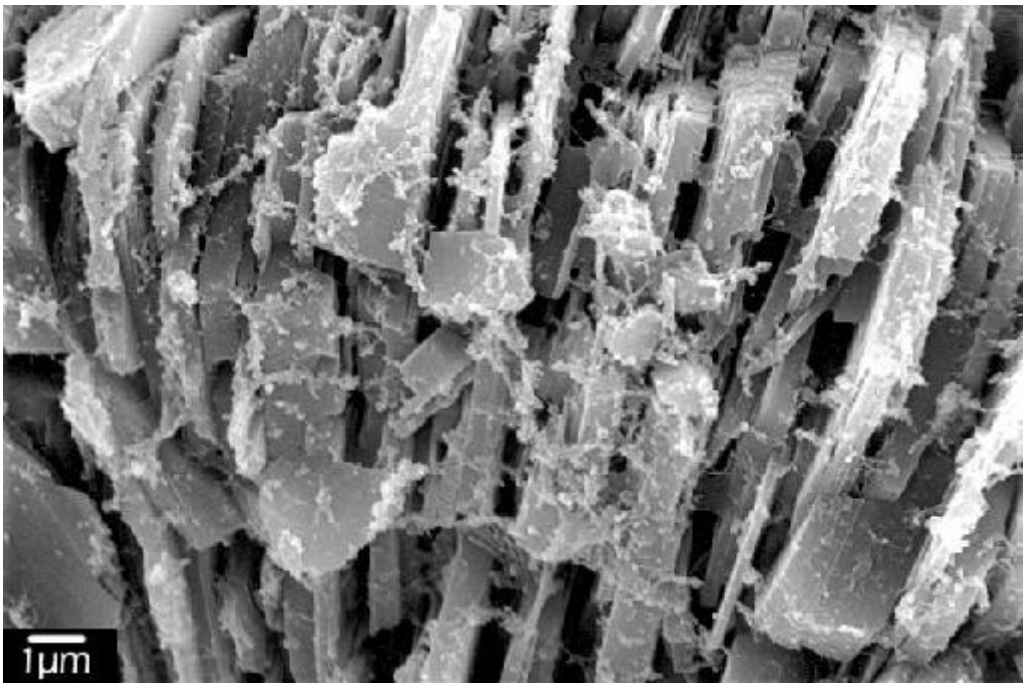

Figure 41: Web of slime over kaolinite crystallites in a reservoir sandstone. Nanno-scale balls are attached to the strands of slime that make up the webs.

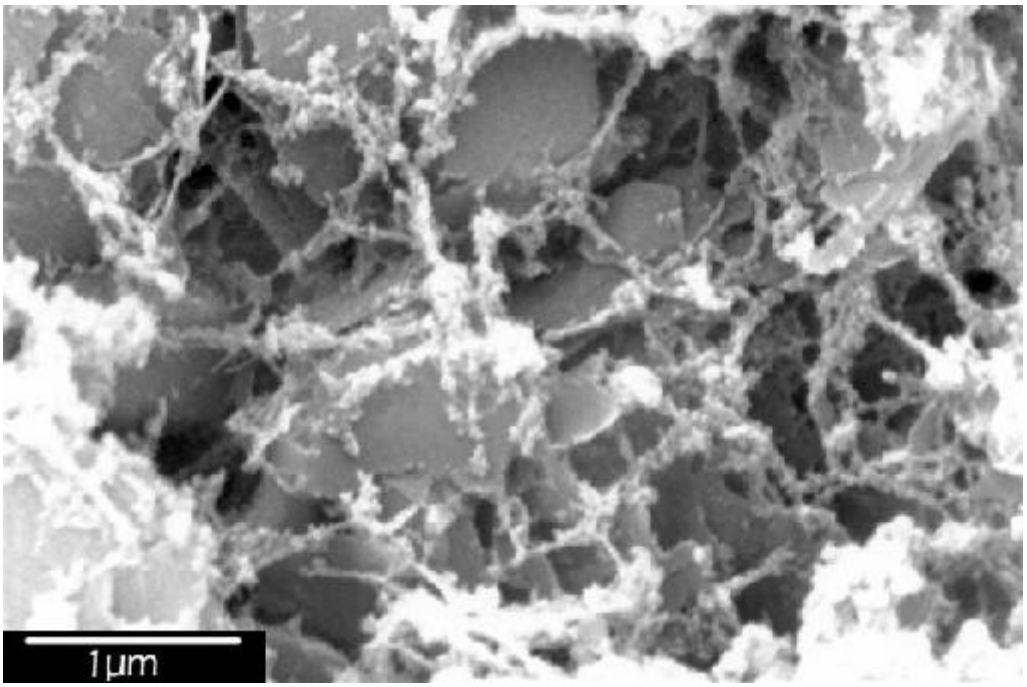

Figure 42: High-magnification photo of slime web in reservoir sandstone preserved with ethanol/critical point drying.

EXPERIMENT I: OCCURRENCE OF SLIME AND BACTERIA IN FULLY PLUGGED CORES

In cores that had been completely plugged over a duration of approximately 3-4 weeks in microbial enhanced oil recovery experiments, the slime occurs as irregular or smooth, confluent sheets coating the surfaces of the grains and the insides of pore spaces (Figs. 43-46). Thick menisci of slime span pore spaces (Figs. 44 and 45). Strands and webs of slime occur in both glutaraldehyde-fixed samples and ethanol-dehydrated samples, spanning pore spaces and incorporating bacteria (Figs. 47-50). Bacteria occur individually (Fig. 47) and only rarely in colonies (Figs. 48 and 50).

EXPERIMENT II: GROWTH OF BACTERIA AND SLIME LAYER IN TIMED FEEDING EXPERIMENTS

Week 1. Two distinct sizes of rod-shaped bacteria were observed within the first week of the experiment: full-sized forms about 2 µm in length associated with small forms less than 1 µm in length (Figs. 51-55). Small (<1µm) spheroid-shaped bacteria-like forms are associated with the rod-shaped ones. Large (>1µm) spheroid-shaped bacteria are rare (Figs. 36 and 40). The small spheroids occur in both glutaraldehyde-fixed and ethanol-dehydrated samples. Some of the full-sized, rod-shaped bacteria occur in joined pairs (Fig. 51). It should be noted that bacteria in unfed control samples were extremely rare, and no small forms were observed.

Some of the bacteria have finger-like, branching strands of slime that serve as holdfasts connecting them to the substrate (Figs. 54-56). One bacterium was observed

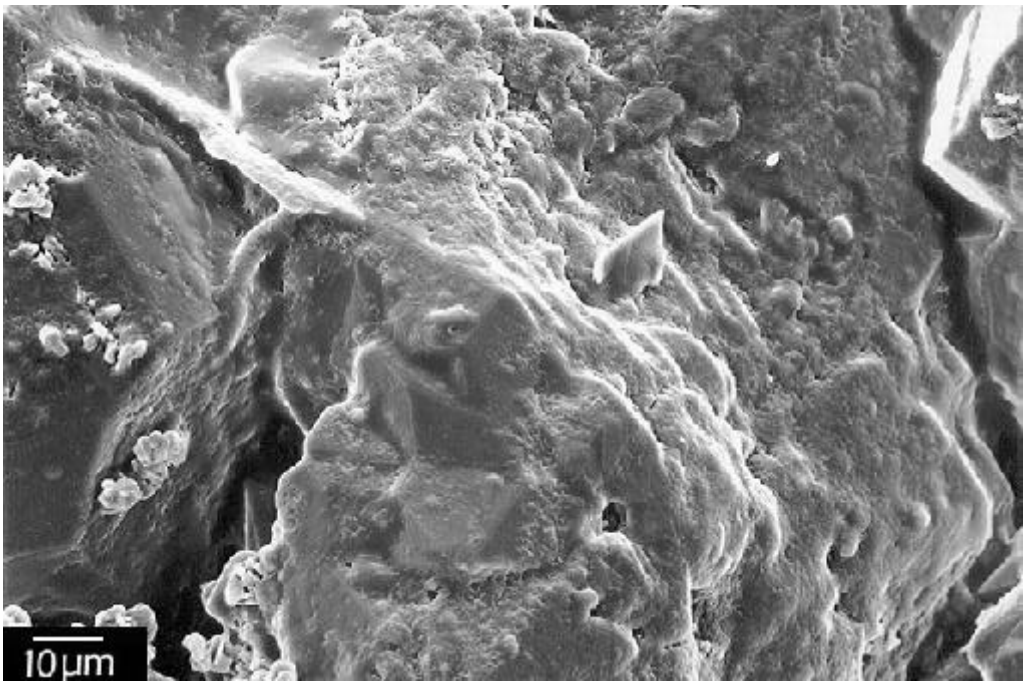

Figure 43: Thick slime layer coating the surface of quartz overgrowths in a fully plugged North Blowhorn Creek sandstone. (Preserved in 10% glutaraldehyde.)

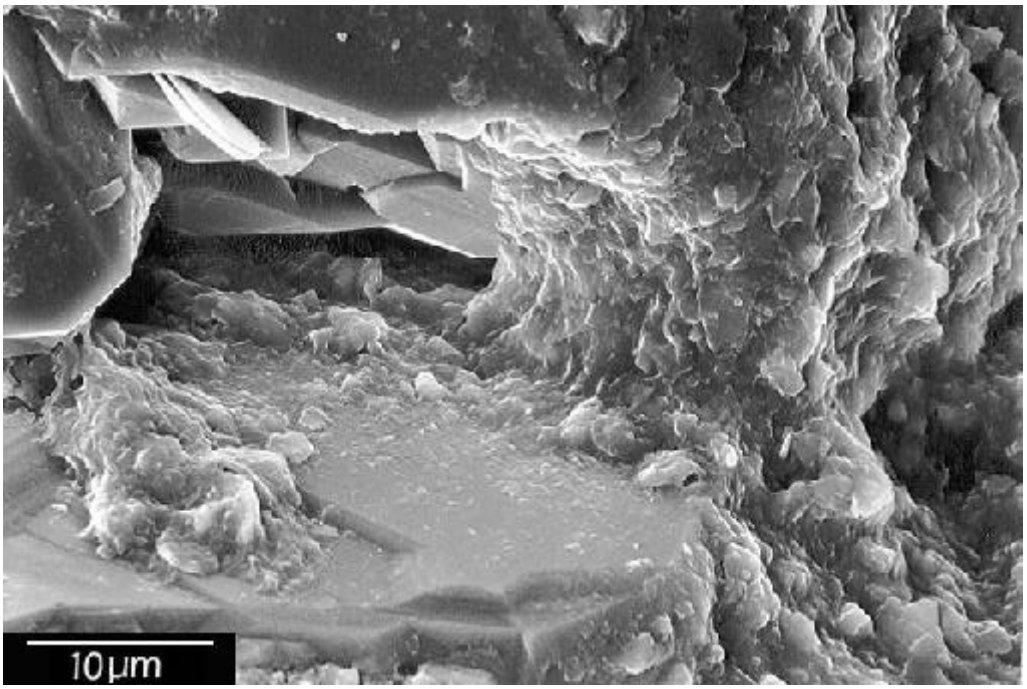

Figure 44: Thick meniscus of slime spanning pore throat in a fully plugged North Blowhorn Creek sandstone. (Preserved in 10% glutaraldehyde.)

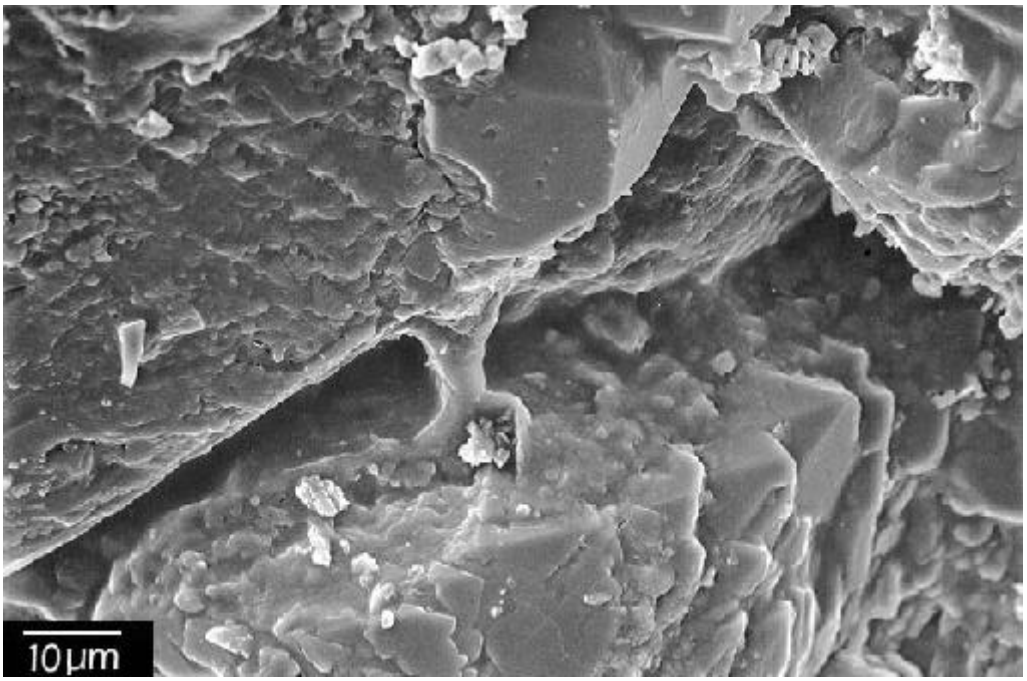

Figure 45: Meniscus and layer of slime within a pore space of a North Blowhorn Creek sandstone. (Preserved in 10% glutaraldehyde.)

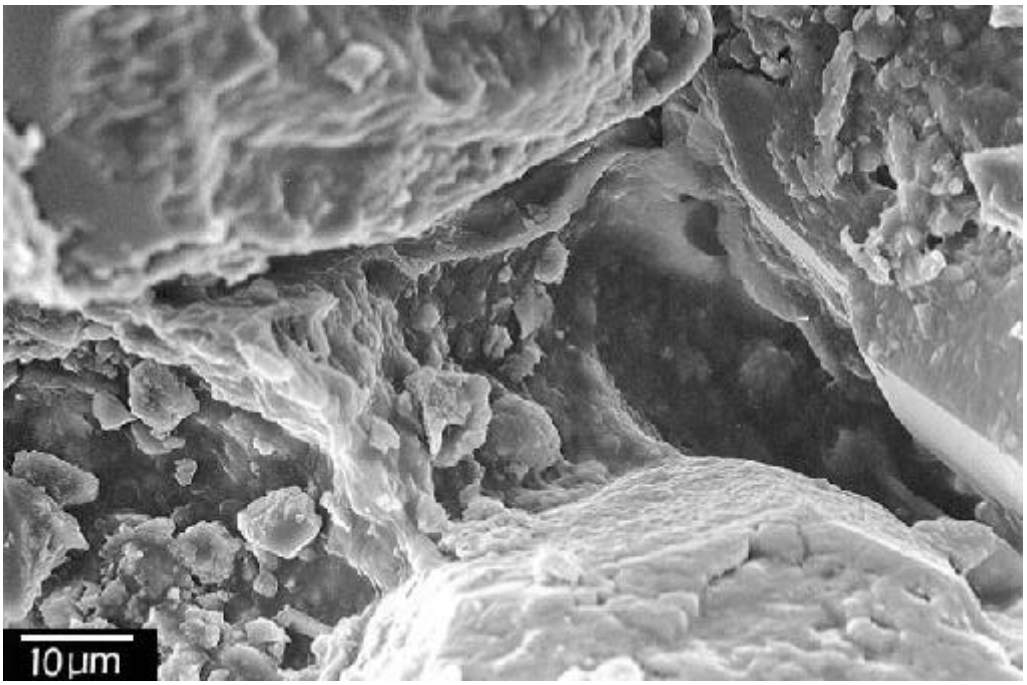

Figure 46: Pore-lining slime layer in a North Blowhorn Creek sandstone. (Preserved in 10% glutaraldehyde.)

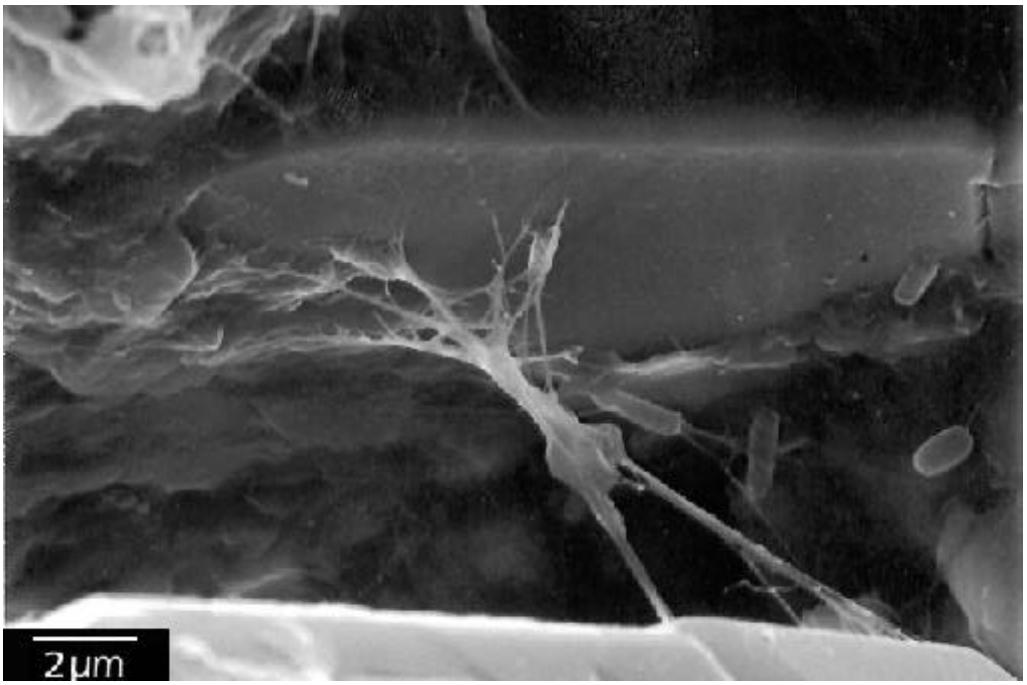

Figure 47: Web of slime in pore space of North Blowhorn Creek sandstone. Individual bacteria are on surfaces nearby and incorporated into the web itself. (Preserved with ethanol/hexamethyldisilazane.)

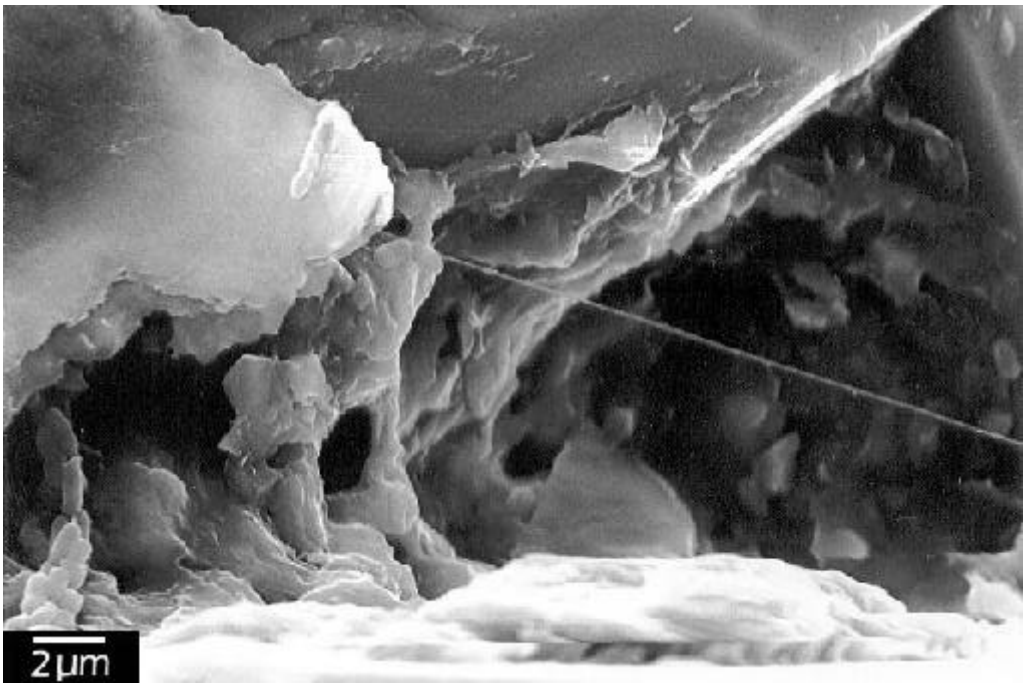

Figure 48: Strand of slime in North Blowhorn Creek sandstone. A colony of bacteria is visible in the lower left corner. (Preserved with ethanol/hexamethyldisilazane.)

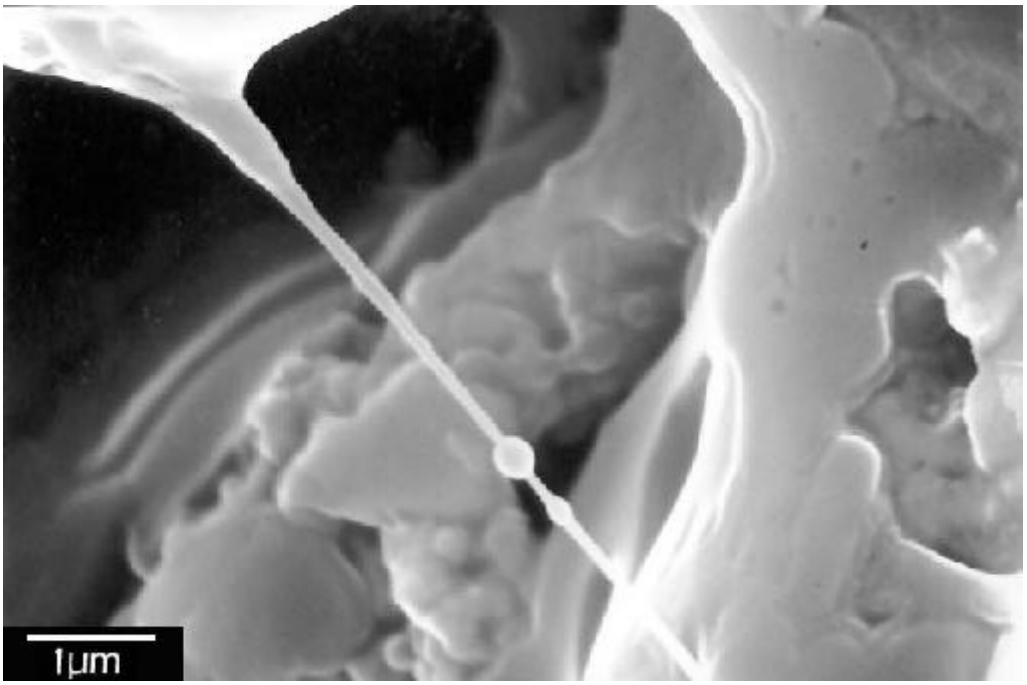

Figure 49: Strand of slime in fully plugged North Blowhorn Creek sandstone. (Preserved with 10% glutaraldehyde.)

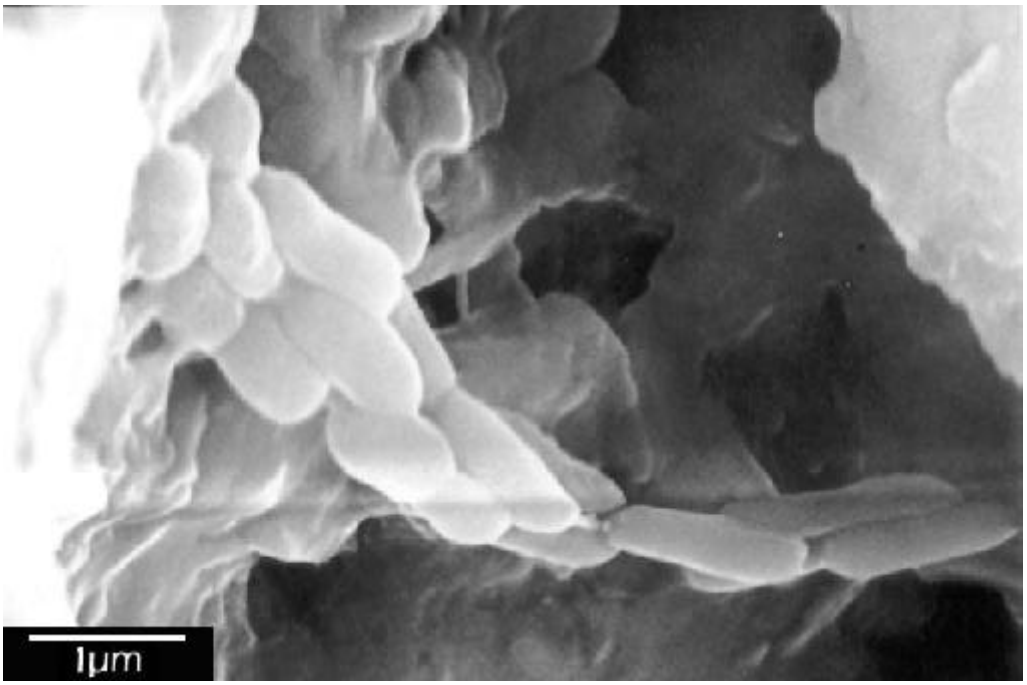

Figure 50: Rare colony of bacteria in fully plugged North Blowhorn Creek sandstone. A layer of slime covers the substrate beneath the bacteria.

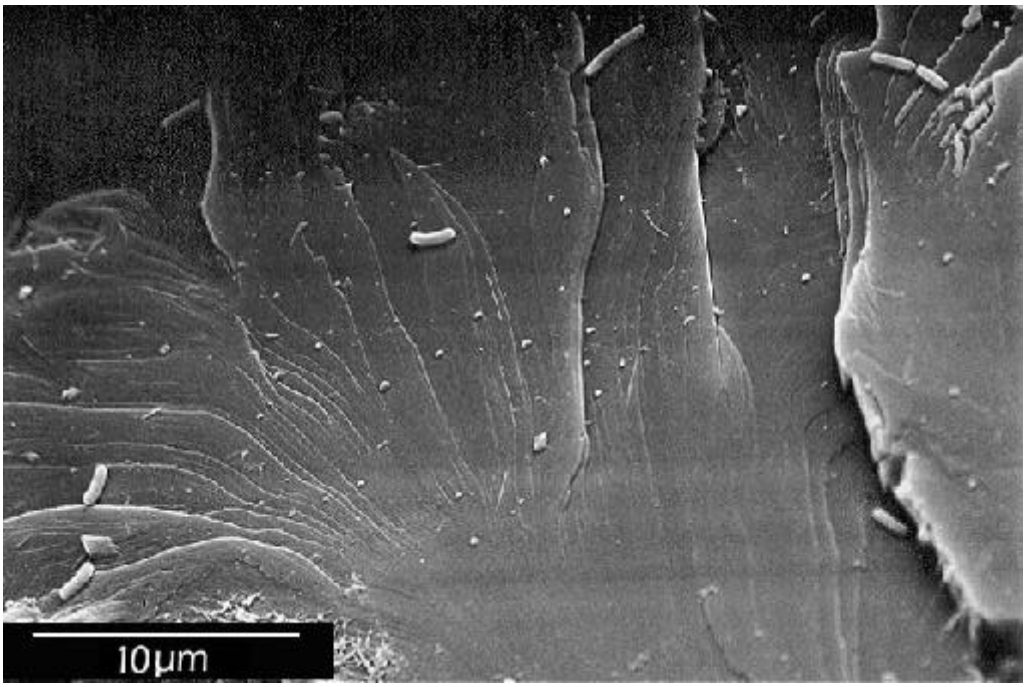

Figure 51: Two distinct sizes of bacteria during first week of growth experiment. Full-sized, rod-shaped bacteria are present as individuals and in pairs. Smaller bacteria are either rod-shaped or spheroid in shape.

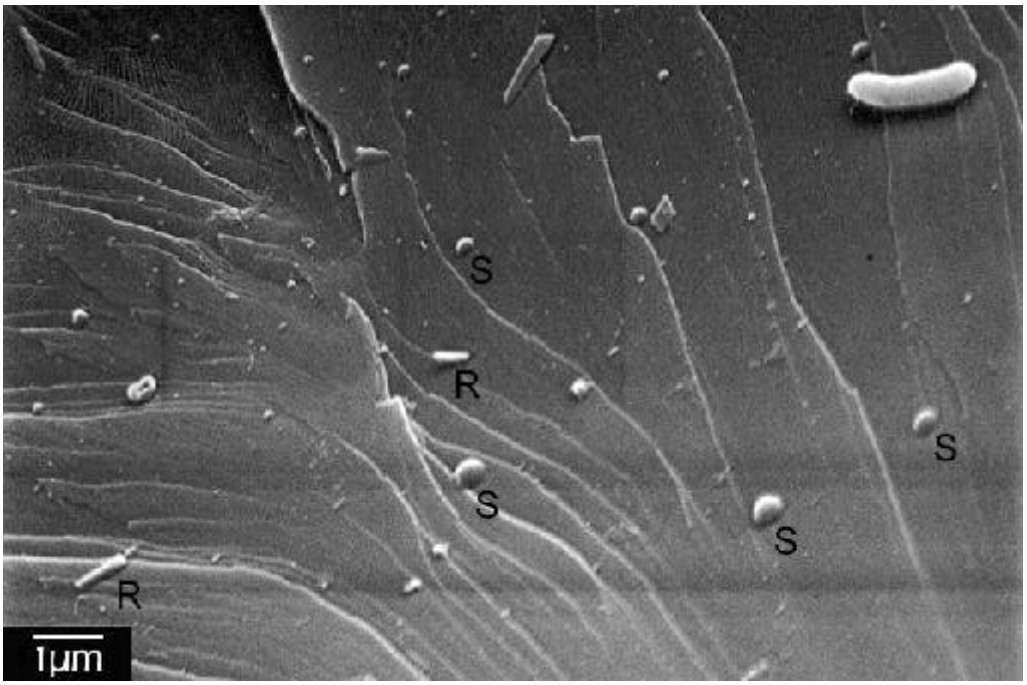

Figure 52: Full-sized, rod-shaped bacterium and smaller bacteria in both rod-shaped (R) and spheroid (S) shapes. Full-sized spheroid-shaped bacteria are present in North Blowhorn Creek sandstones during previous experiments (Figs. 40 and 36) but were rare in the timed experiment. (Preserved with ethanol/hexamethyldisilazane.)

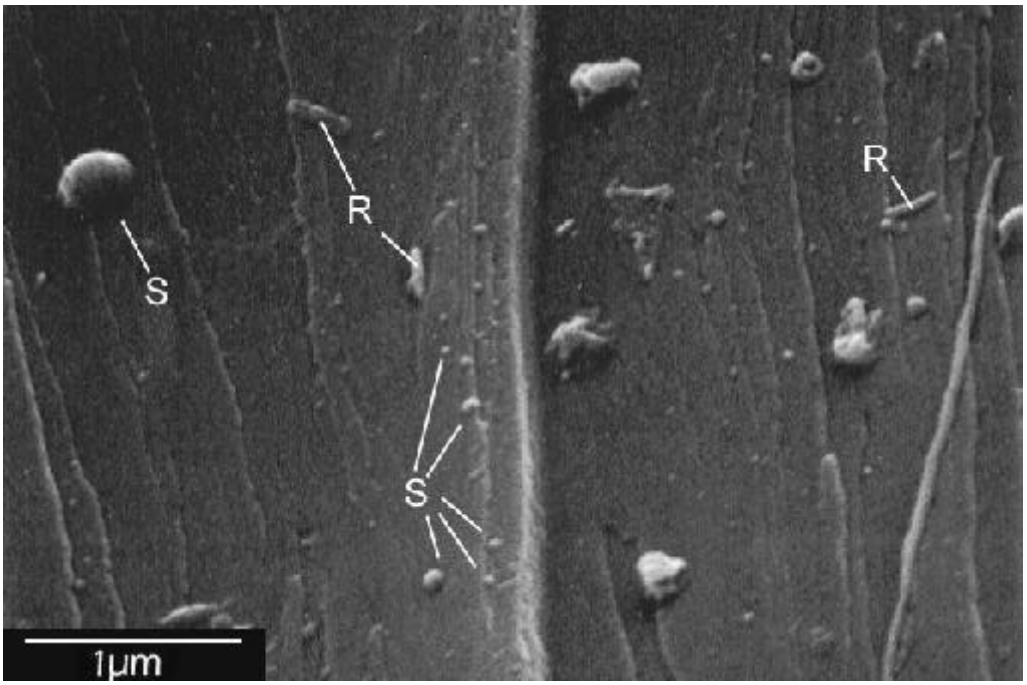

Figure 53: Small bacteria-like forms in first week of timed experiments. Several different sizes of spheroidal shapes (S) are present. Rod-shaped bacteria of varied size (R) are also present. (Preserved in ethanol/hexamethyldisilazane.)

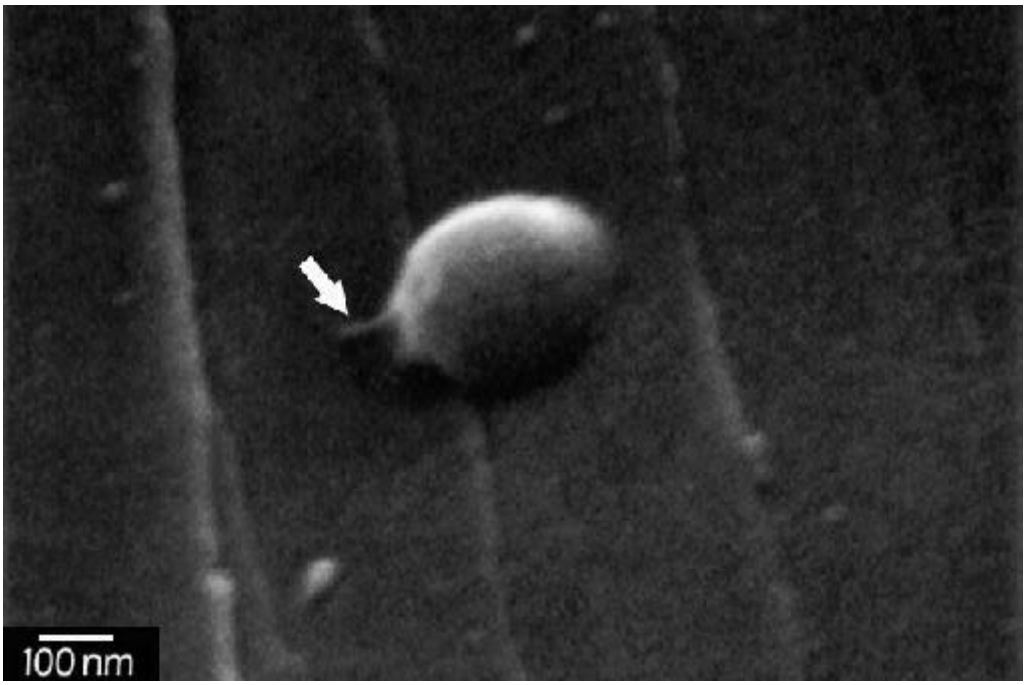

Figure 54: Small bacterium with holdfast (arrow) during first week of timed experiments. (Preserved with ethanol/hexamethyldisilazane.)

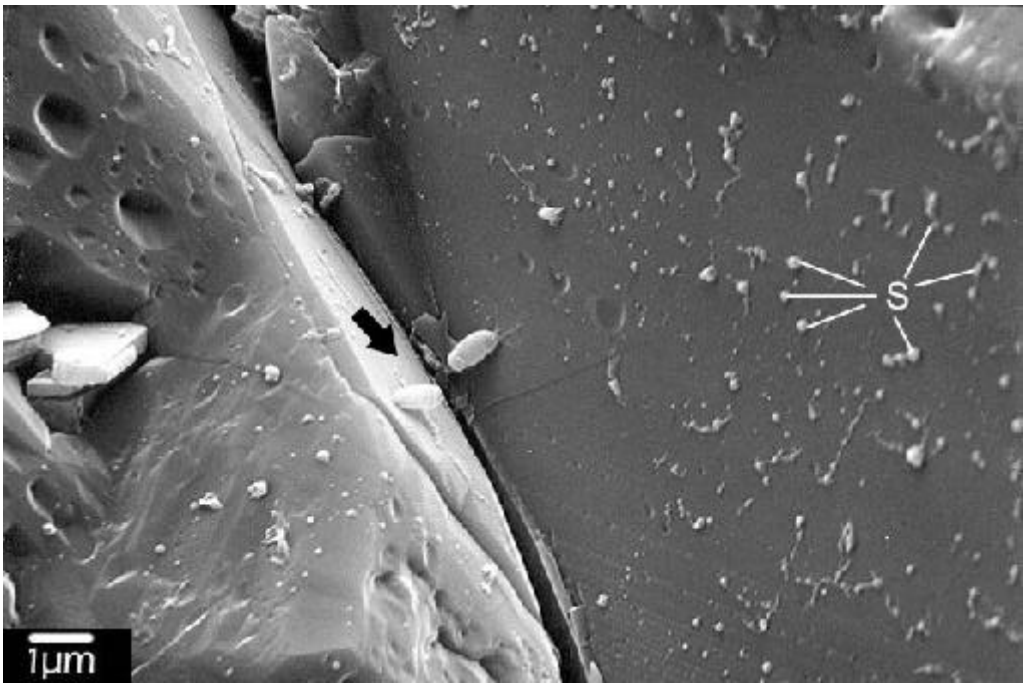

Figure 55: Full-sized, rod-shaped bacteria with holdfasts (arrow) on quartz overgrowths during first week of timed experiments. Small spheroid structures (S) are scattered across the surface of the overgrowth. (Preserved in ethanol/hexamethyldisilazane.)

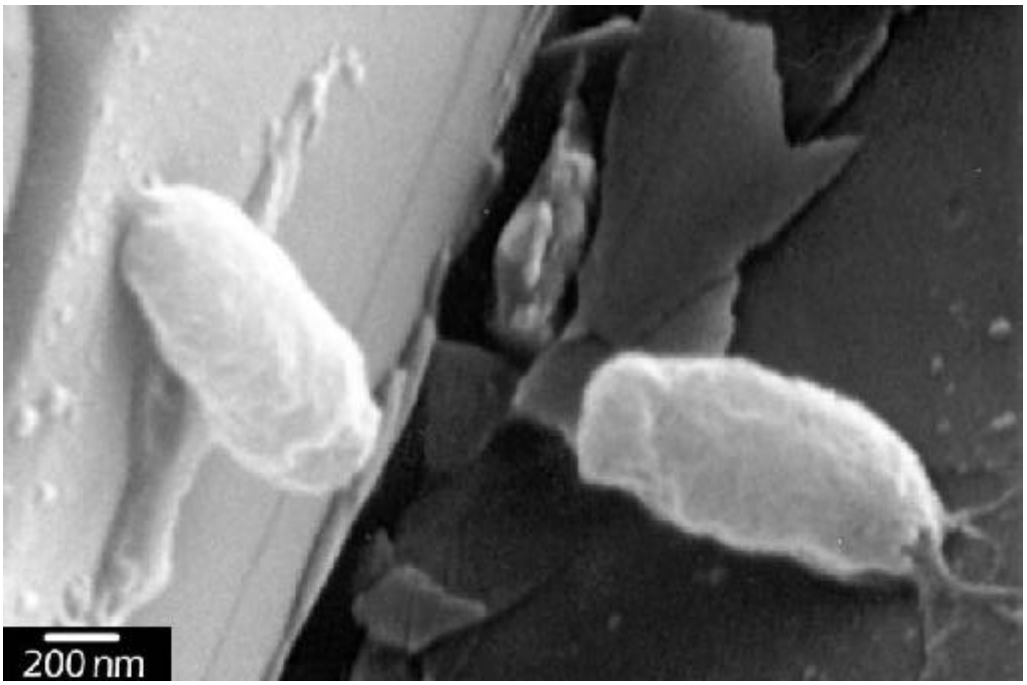

Figure 56: High magnification photo of full-sized, rod-shaped bacteria with exopolysaccharide holdfasts from Fig. 55.

with the thin halo of a sheathlike exopolysaccharide capsule (Fig. 57). Although a thick, continuous sheet of slime is not present, the surface of the quartz grains is easily burned by the electron beam (Fig. 58), implying that the surface of the quartz overgrowths is covered with a thin coat of organic material. A small amount of exopolysaccharide slime occurs in the first week of growth in the form of ropy masses and globular masses scattered across the surface of the grains in both glutaraldehyde-fixed and ethanol-dehydrated samples (Figs. 59 and 60). The slime also occurs as thin sheets of limited areal extent in glutaraldehyde-fixed samples (Figs. 61 and 62). Some thin sheets of slime have needle-like protrusions from their edges (Fig. 62).

Week 2. Small forms of rod-shaped bacteria were less common in samples taken during the second week of growth (Fig. 63). Spheroid-shaped small structures are abundant (Fig. 63-67). Slime is present again in ropy masses as well as globular masses (Figs. 63-66). Slime growing in thin sheets also occurs, stretching between quartz grains, and sometimes with an hexagonal outline (Fig. 67). Most thin sheets overlie small spherical structures (Fig. 67). Thin sheets of slime are curled in samples which have been dehydrated with ethanol/hexamethyldisilazane (Fig. 68).

Week 3. Small, rod-shaped bacteria and spherical structures still occur in the third week of the timed experiments (Fig. 71), but full-sized rods are the most common forms of bacteria during this week (Figs. 69 and 70). The slime at this point in the experiment appears to be massive, confluent, and thick (Fig. 72). Some pores appear to be completely filled with slime

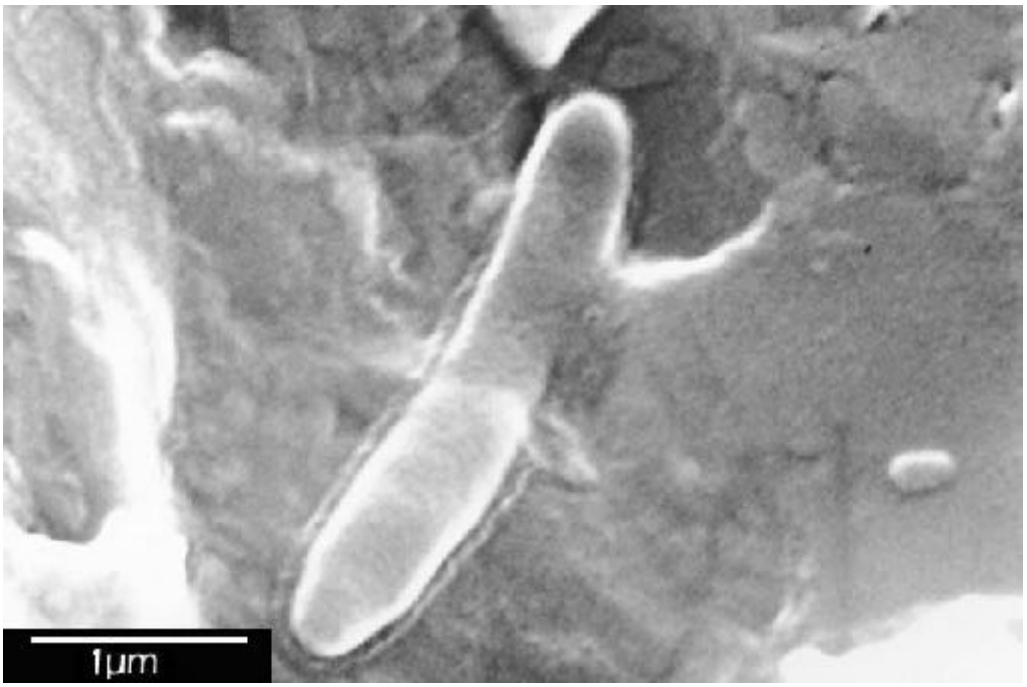

Figure 57: A bacterium in the first week of timed experiments covered with a thin exopolysaccharide sheath. The sheath appears as a faint halo around the bacterium itself. (Preserved with 10% glutaraldehyde)

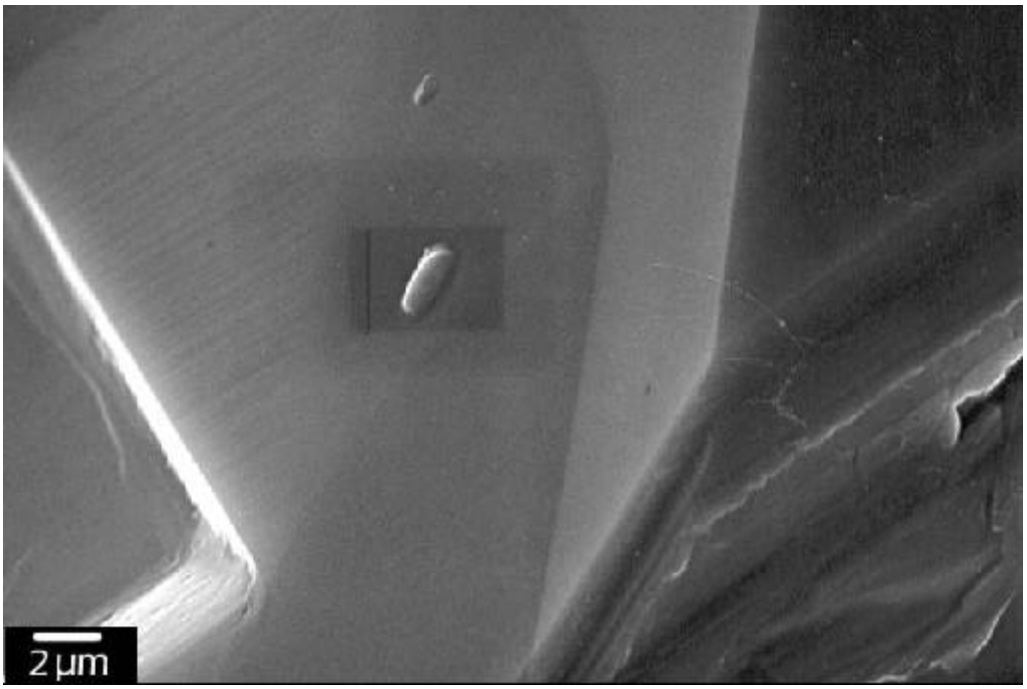

Figure 58: A flattened bacterium on the surface of a quartz overgrowth during the first week of the timed experiments. The dark rectangle around the bacterium is a burn mark produced by the electron beam. (Preserved with 10% glutaraldehyde)

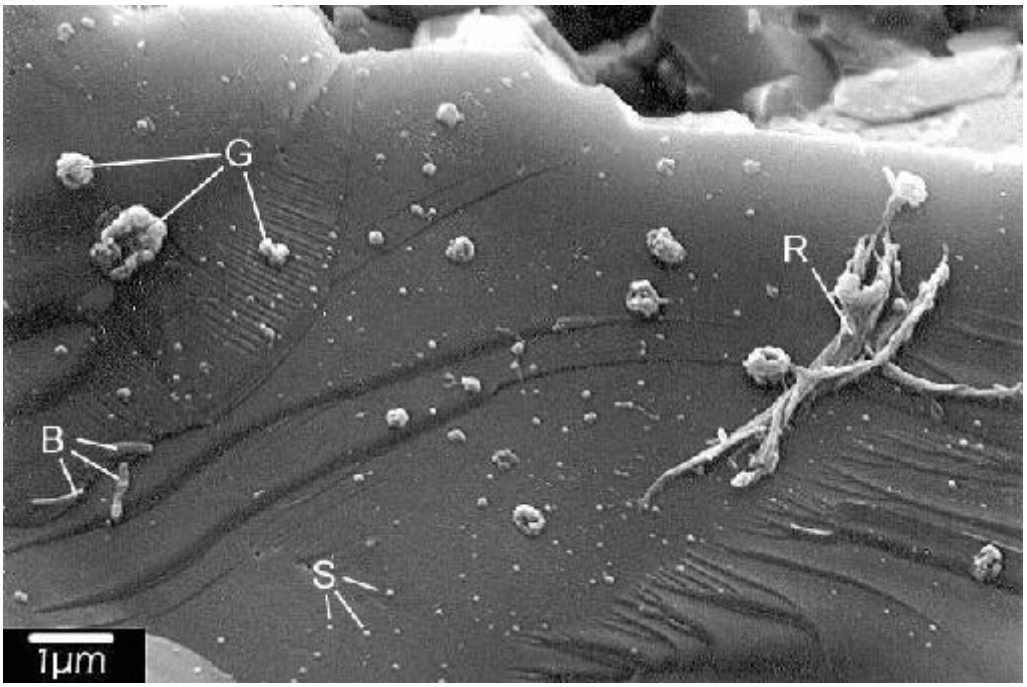

Figure 59: Ropy slime masses (R) and small globular masses (G) of slime in the first week of timed experiments. Small, rod-shaped bacteria (B) and spheroidal structures (S) are also present. (Preserved with standard dehydration.)

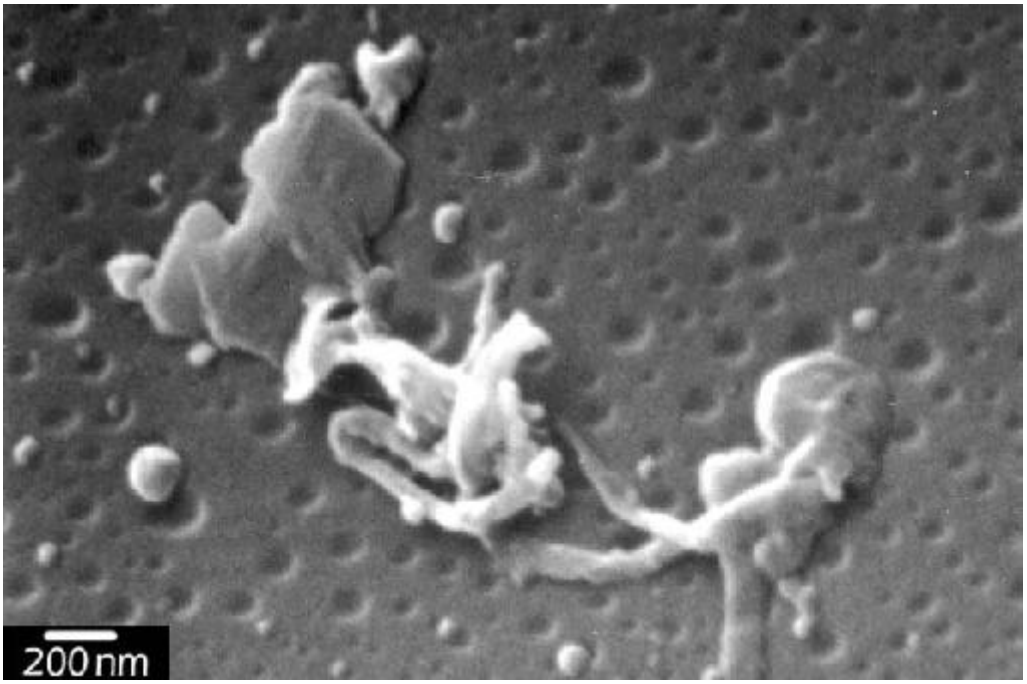

Figure 60: Ropy slime mass in first week of timed experiments. (Preserved with standard dehydration.)

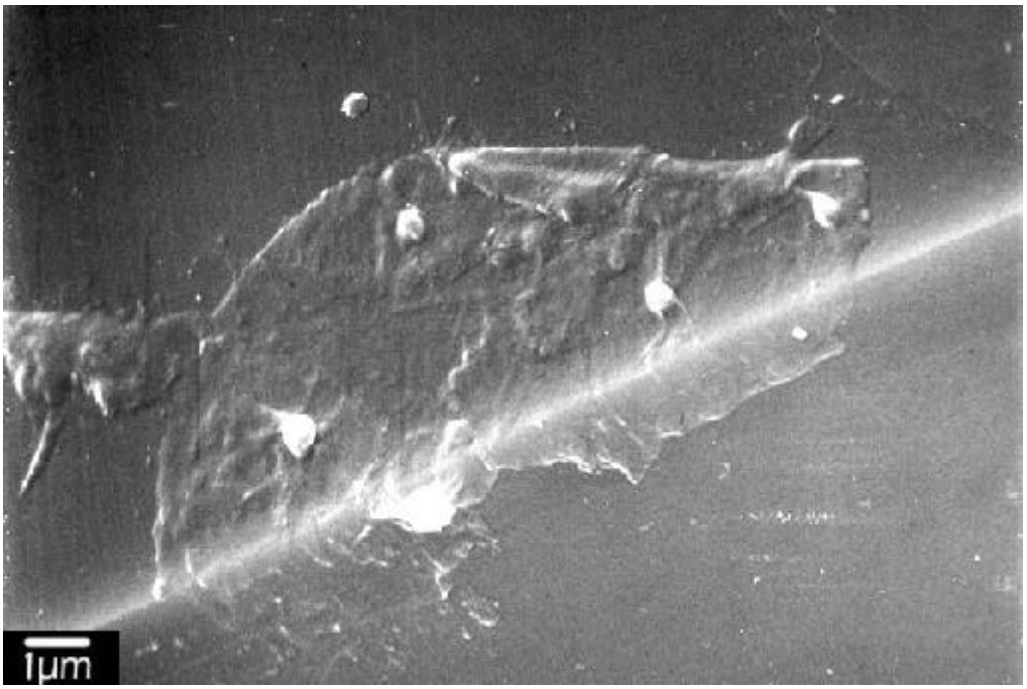

Figure 61: Thin slime sheet draped over the edge of a quartz overgrowth in first week of timed experiments. Small, bacteria-like spheroid shapes are underneath the slime layer. (Preserved with 10% glutaraldehyde.)

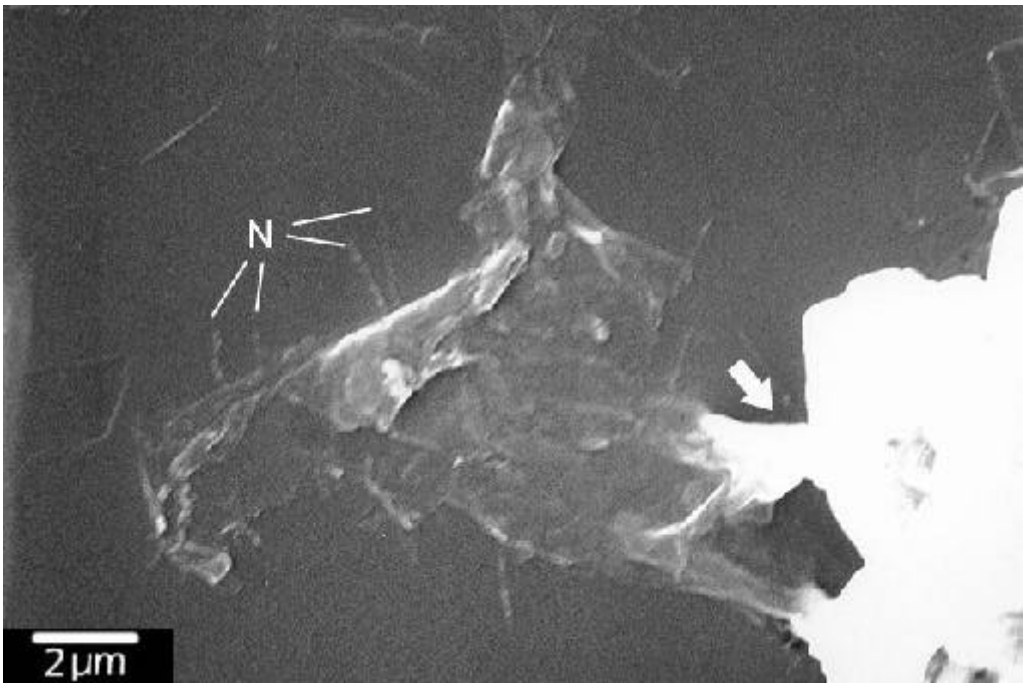

Figure 62: Thin slime sheet draped across the surface of a quartz overgrowth. The slime sheet is attached to the grain at lower right (arrow), and incorporates some needle-like shapes (N) along its margin. (Preserved with 10% glutaraldehyde.)

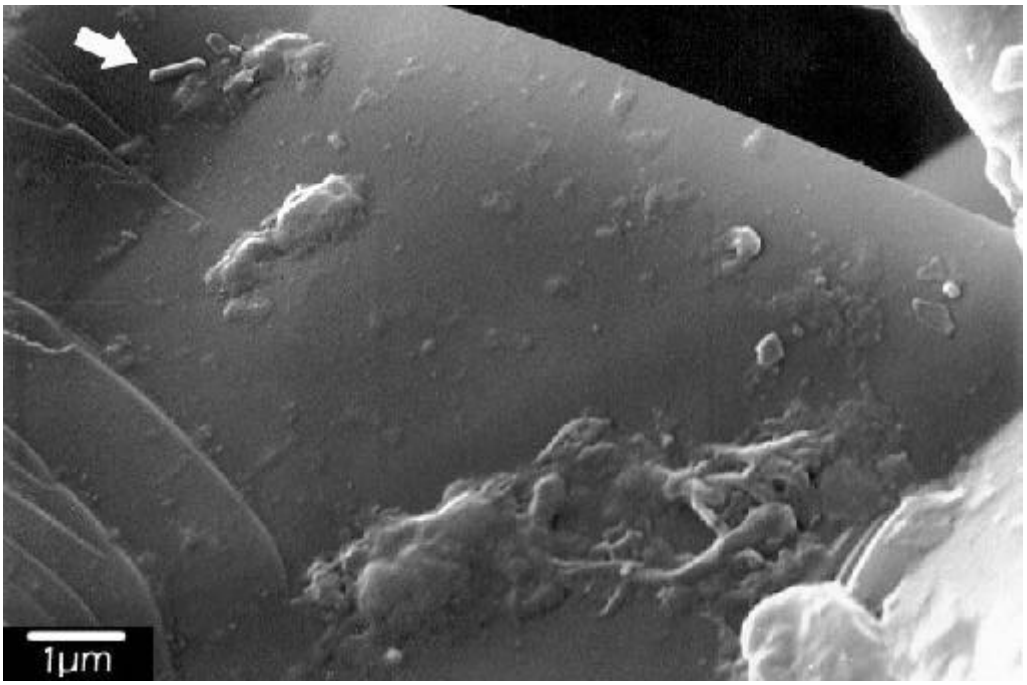

Figure 63: Ropy masses of slime and a small, rod-shaped bacterium (arrow) on the surface of a quartz overgrowth during the second week of the timed experiments. (Preserved in 10% glutaraldehyde.)

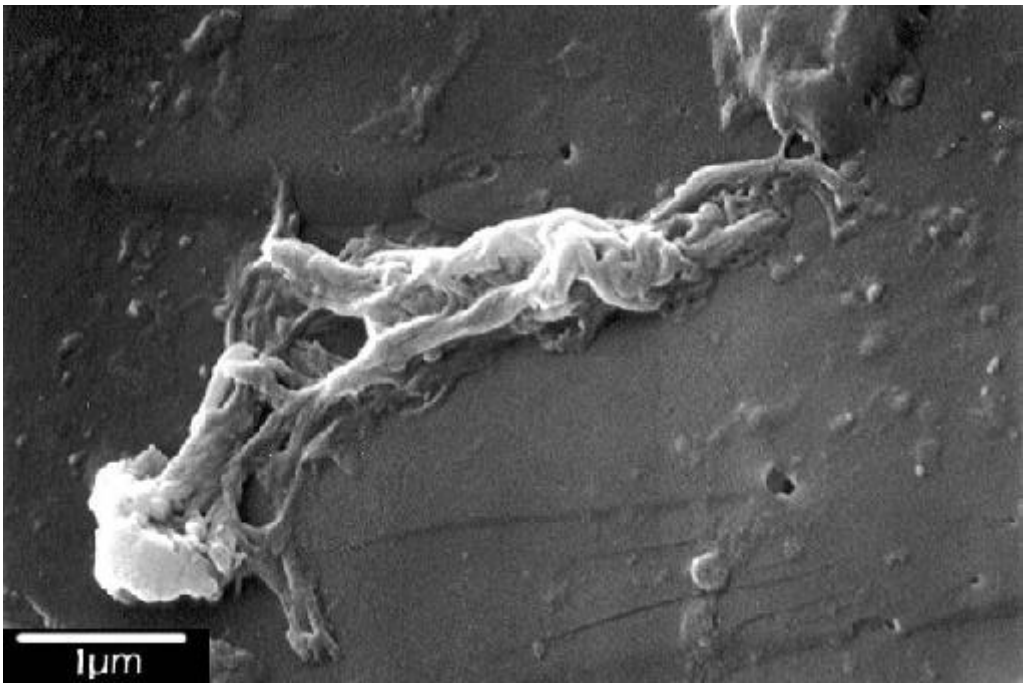

Figure 64: Ropy slime mass on a quartz overgrowth during the second week of the timed experiments. (Preserved in 10% glutaraldehyde.)

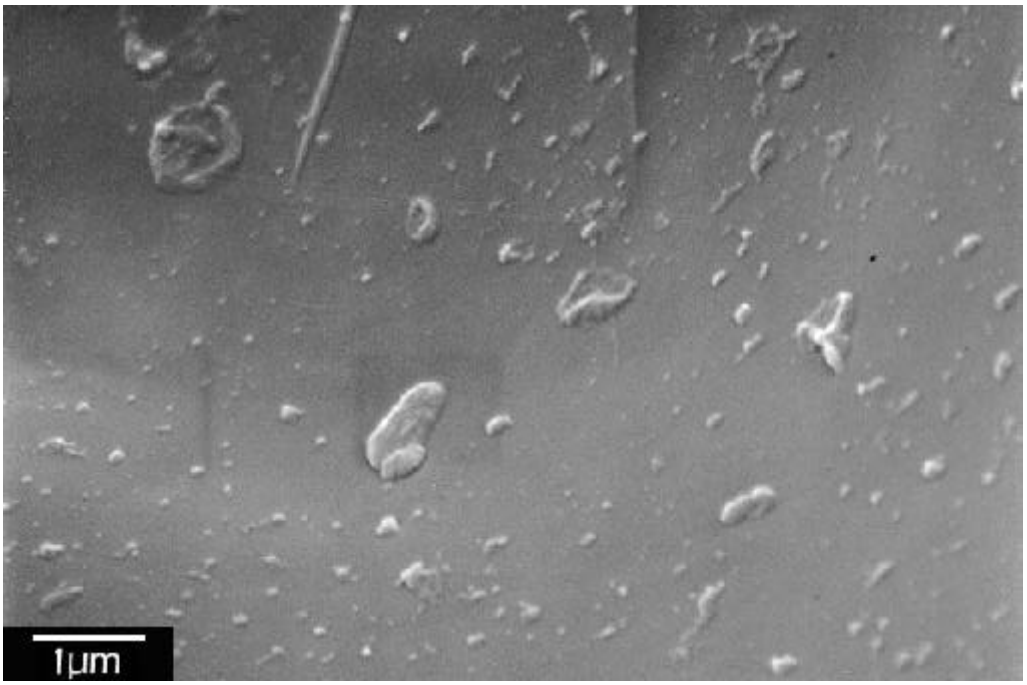

Figure 65: Globular masses of slime scattered over the surface of a quartz overgrowth during the second week of the timed growth experiment. The dark rectangle in the center of the photo is a burn mark caused by the electron beam. (Preserved in ethanol/hexamethyldisilazane.)

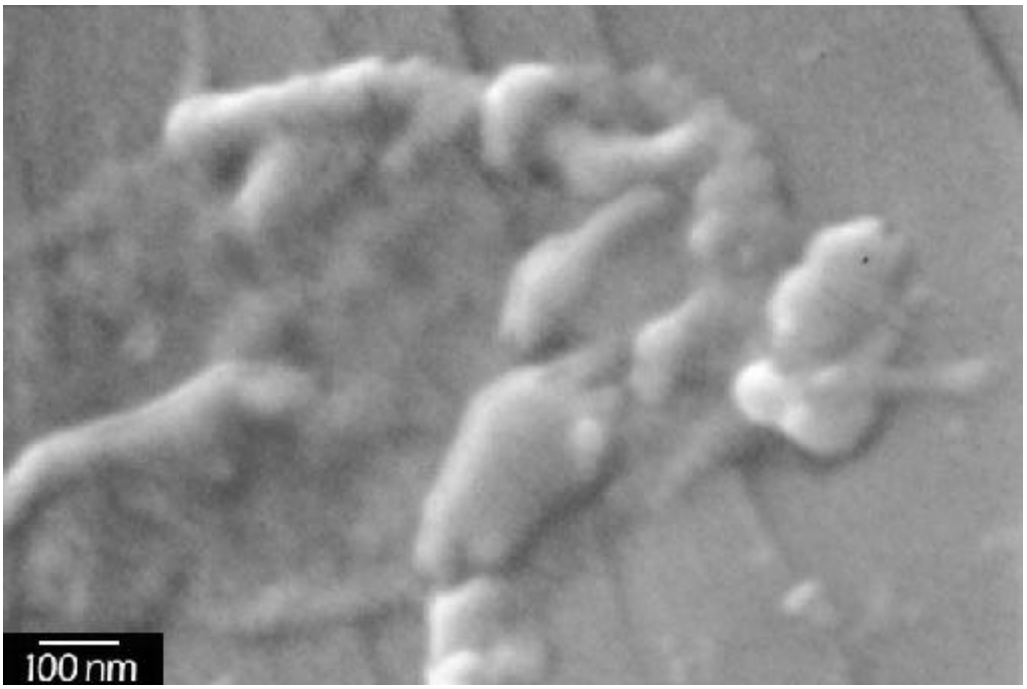

Figure 66: High-magnification photo of a globular mass of slime during the second week of the timed experiments. (Preserved with ethanol/ hexamethyldisilazane.)

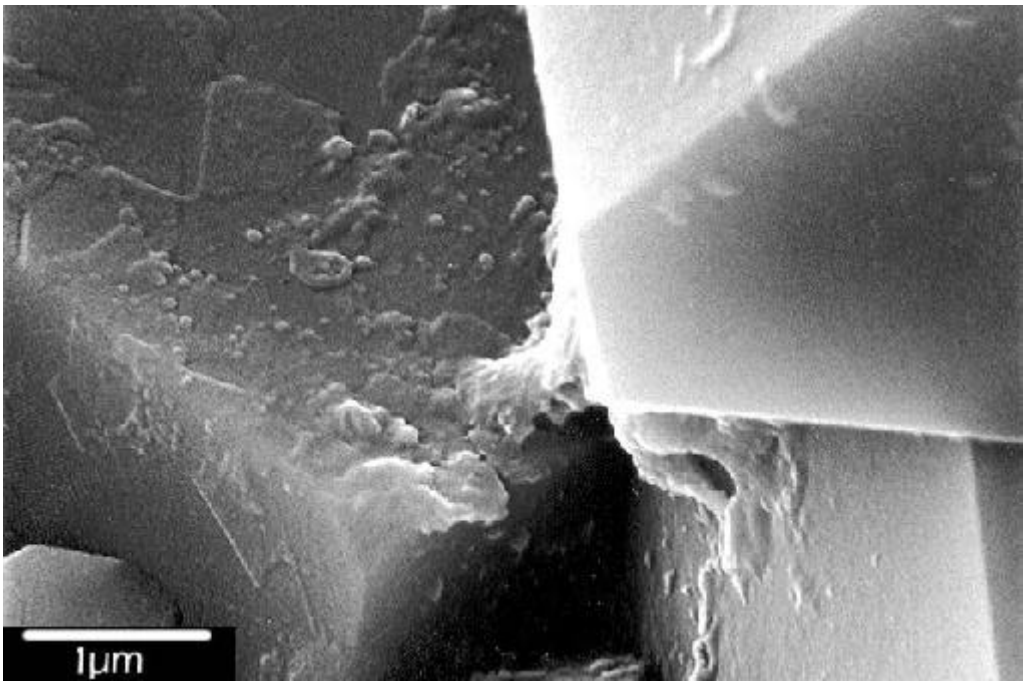

Figure 67: Thin slime layer stretching between two quartz overgrowths in the second week of the timed experiments. The slime layer is covering numerous spheroid shapes and has a hexagonal outline. (Preserved in 10% glutaraldehyde.)

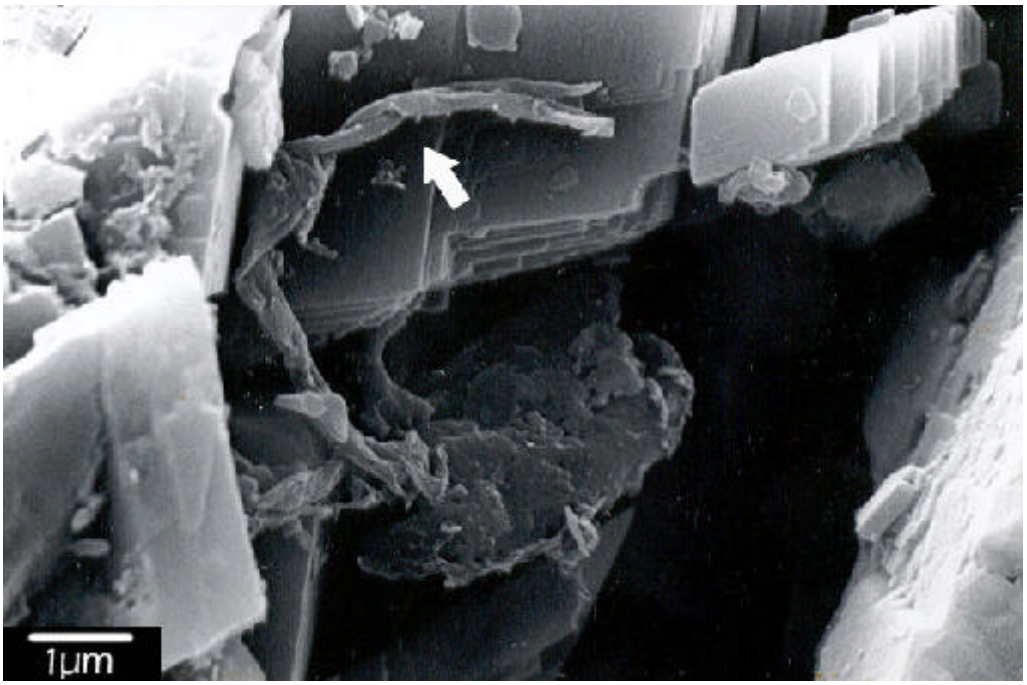

Figure 68: Curled slime sheet (arrow) in a reservoir sandstone during the second week of timed growth experiments. (Preserved in ethanol/hexamethyldisilazane.)

Figure 69: Full-sized bacteria in the third week of the timed experiments. The bacteria are surrounded by a halo, and possibly a thin layer, of slime. (Preserved with 10% glutaraldehyde.)

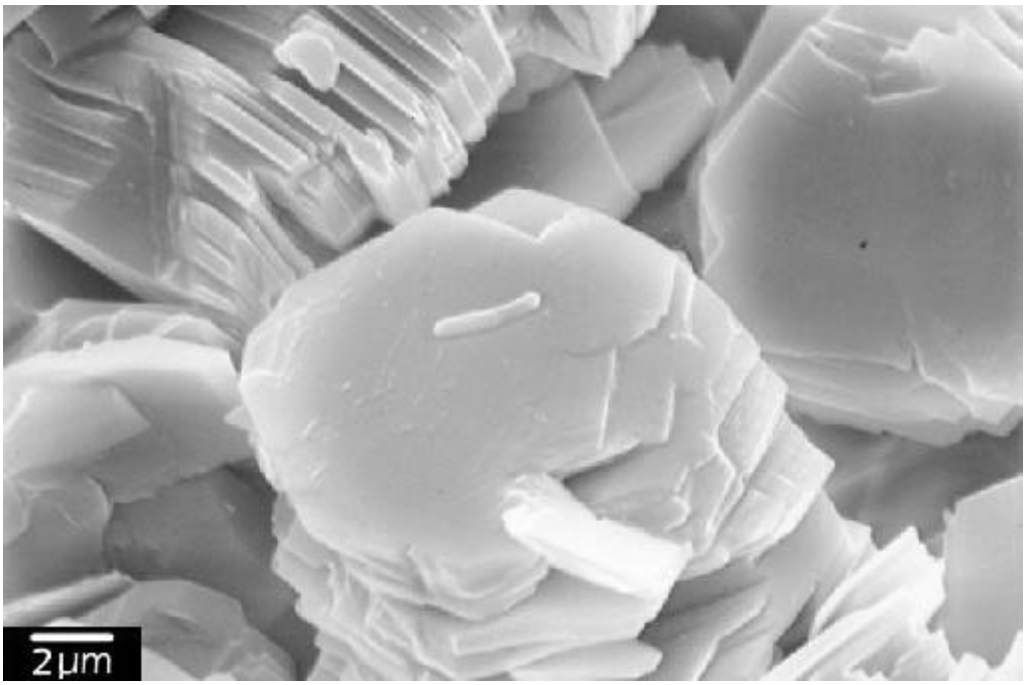

Figure 70: Full-sized, rod-shaped bacterium in the third week of the timed experiments. The rod-shaped bacteria tended to be sparsely distributed across the surfaces of crystals. (Preserved with ethanol/hexamethyldisilazane.)

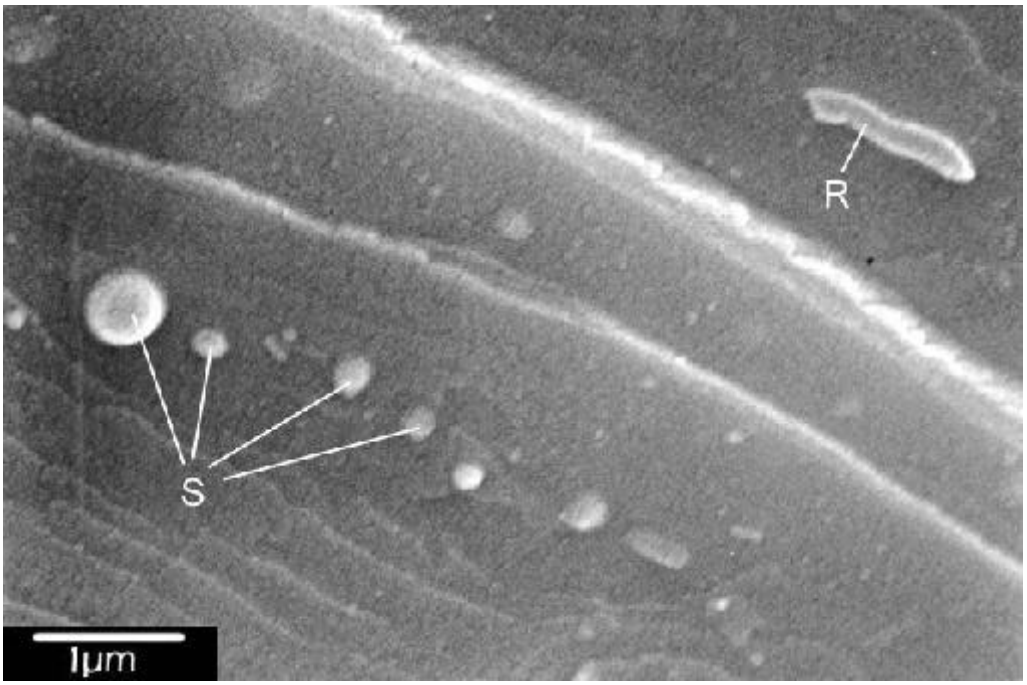

Figure 71: Small forms of rod-shaped (R) and spheroid-shaped (S) bacteria during the third week of the timed experiments. These forms are rare in the third week and absent in the fourth week. (Preserved with ethanol/hexamethyldisilazane.)

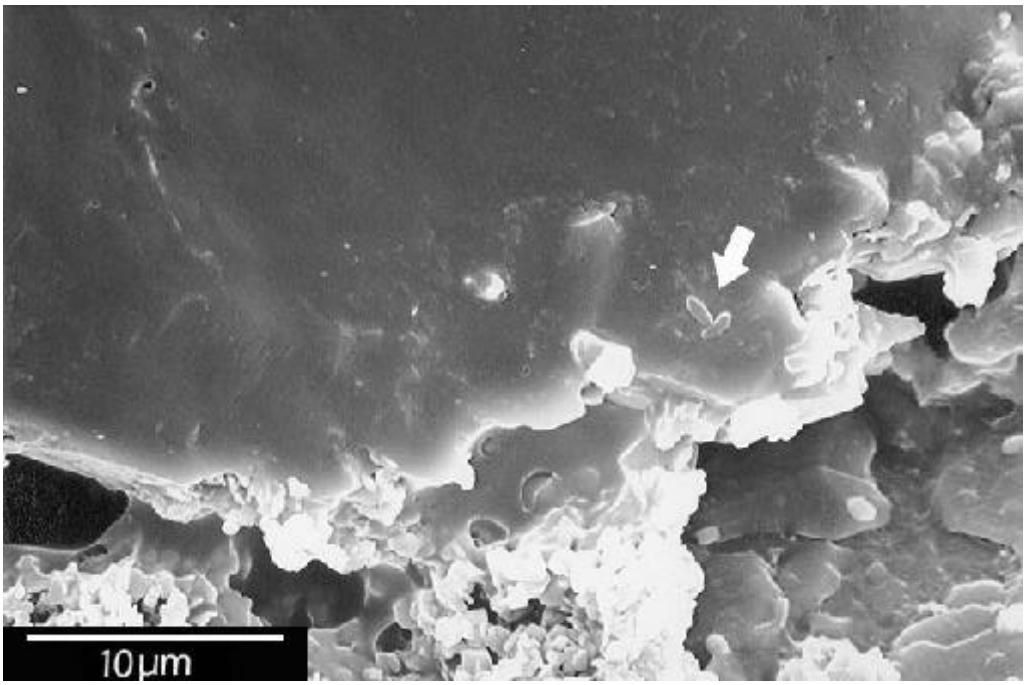

Figure 72: Thick, continuous slime sheet in the third week of timed experiment. Two rod-shaped bacteria are visible at the edge of the slime sheet (arrow). This sheet is thicker than any other slime sheets observed during our experiments. (Preserved with 10% glutaraldehyde.)

(Figs. 73 and 74). The surface of some slime plugs is marked with pits not seen in other slime layers (Figs. 73 and 74).

Week 4. Although some pore-filling masses were present during the fourth week, the most prevalent slime texture during the fourth week consisted of large balls about 10 µm in diameter (Figs. 75-80). The balls are roughly polyhedral to spheroidal and are easily deformed (swelling, cracking) under the electron beam, indicating their organic nature (Figs. 76-78 and 80). Some can be seen attached to the substrate (Fig. 76). At least one was observed in conjunction with a colony of rod-shaped bacteria (Figs. 77-79). During the fourth week, slime also occurs rarely in thin sheets and ropy masses (Figs. 81 and 82).

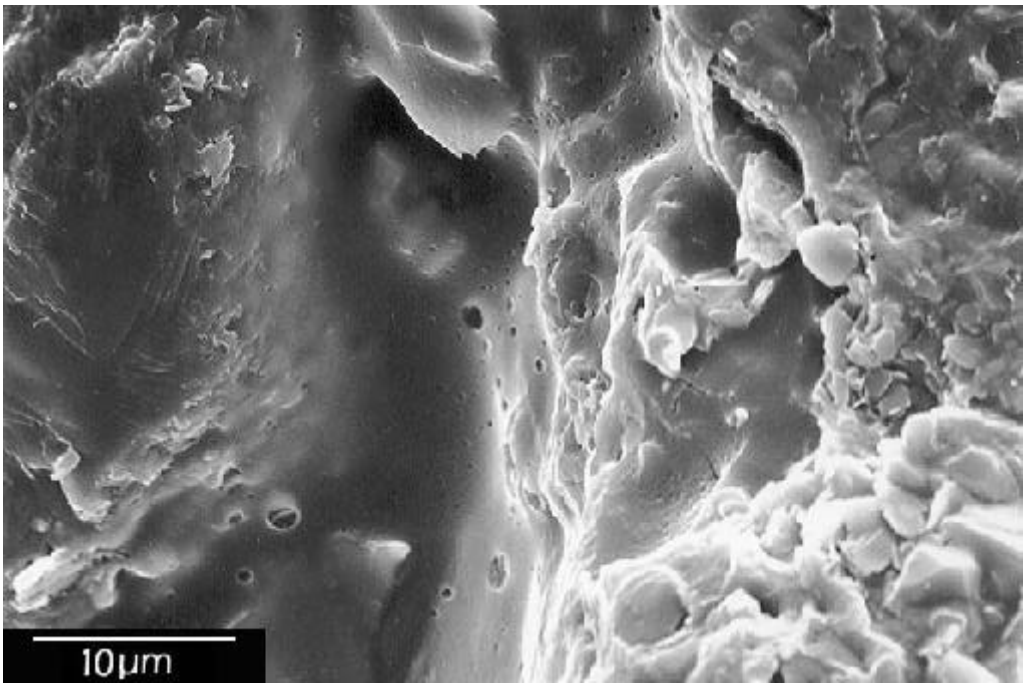

Figure 73: Pore-filling mass of slime in the third week of the timed experiments. The pore is indicated with a dashed line. This texture was rare in the fourth week. (Preserved with 10% glutaraldehyde.)

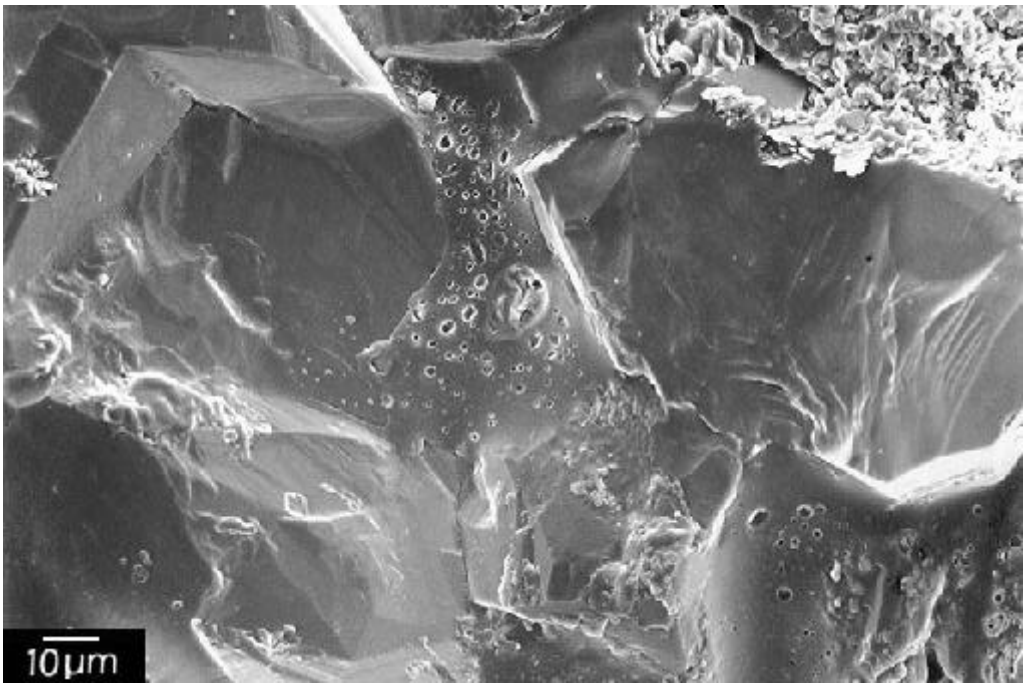

Figure 74: Pore-filling mass of slime in the third week of the timed experiments. Pore is indicated with dashed line. The surface of the slime mass is marked with pits. (Preserved with 10% glutaraldehyde.)

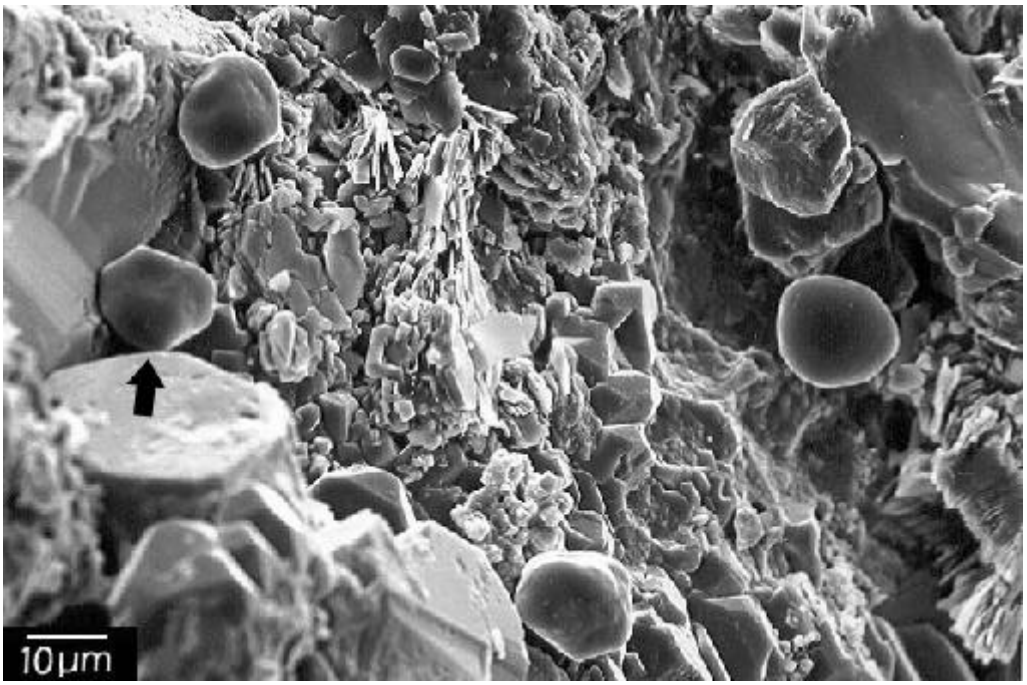

Figure 75: Large (10µm) balls of slime in the fourth week of the timed experiments. The balls are sub-polyhedral to spheroidal in shape and are attached to surfaces of grains. Arrow indicates location of Fig. 76. (Preserved with 10% glutaraldehyde.)

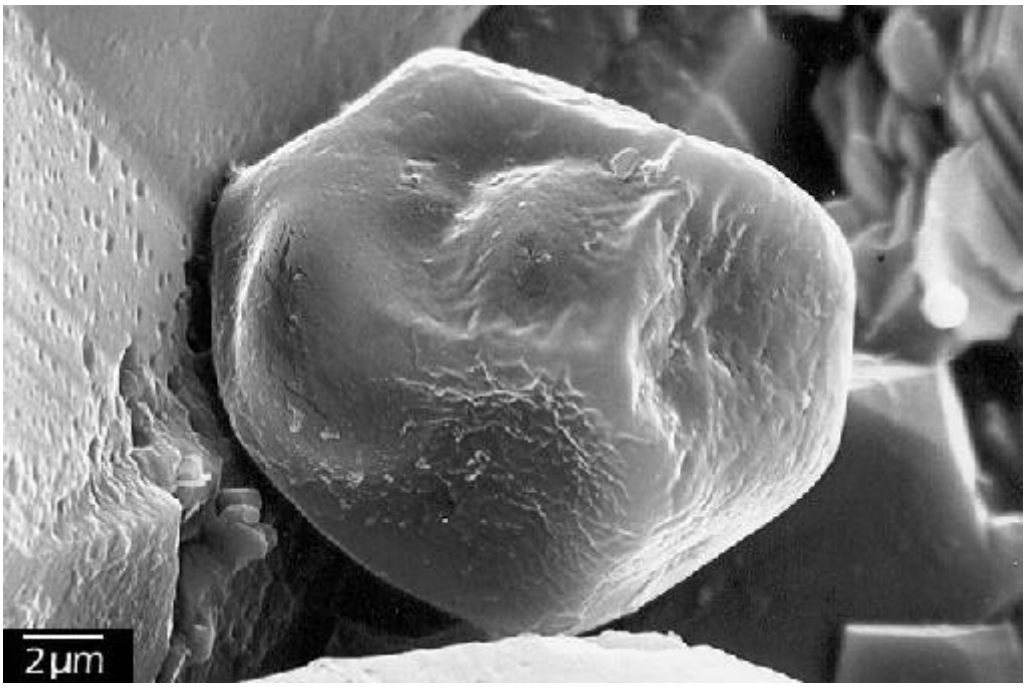

Figure 76: Higher magnification photo of a large ball of slime from Fig. 75. The slime is attached to the quartz overgrowth at its upper left margin. Buckling and wrinkling of the surface is caused by extended exposure to the electron beam. (Preserved with 10% glutaraldehyde.)

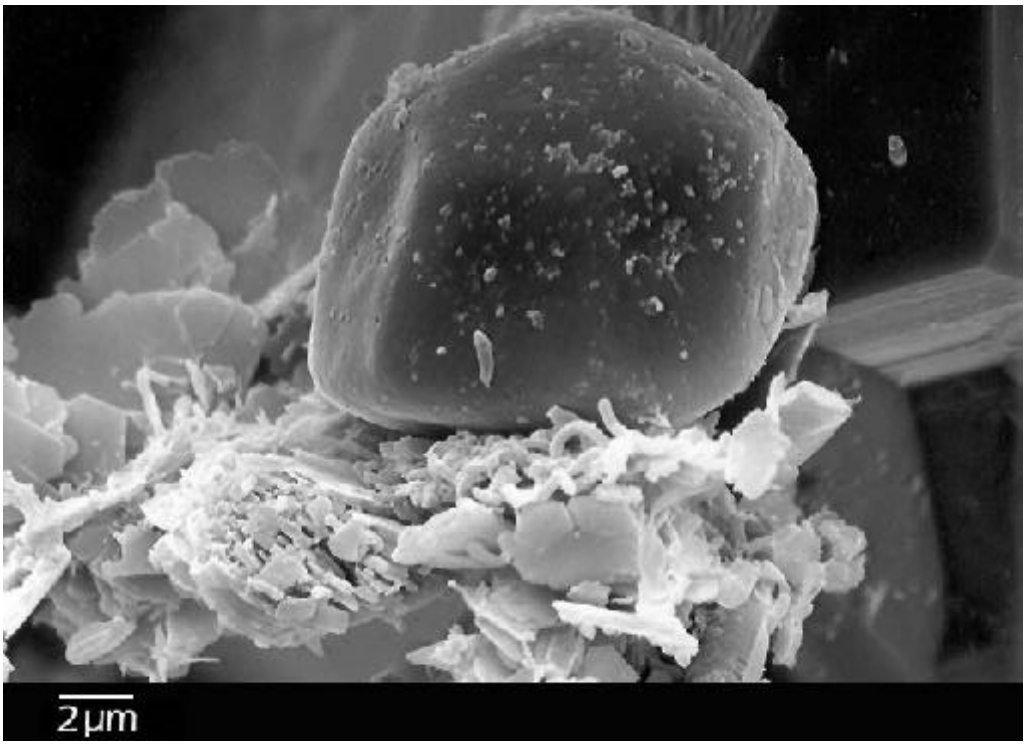

Figure 77: Large ball of slime and colony of rod-shaped bacteria during fourth week of growth. (Preserved with ethanol/hexamethyldisilazane.)

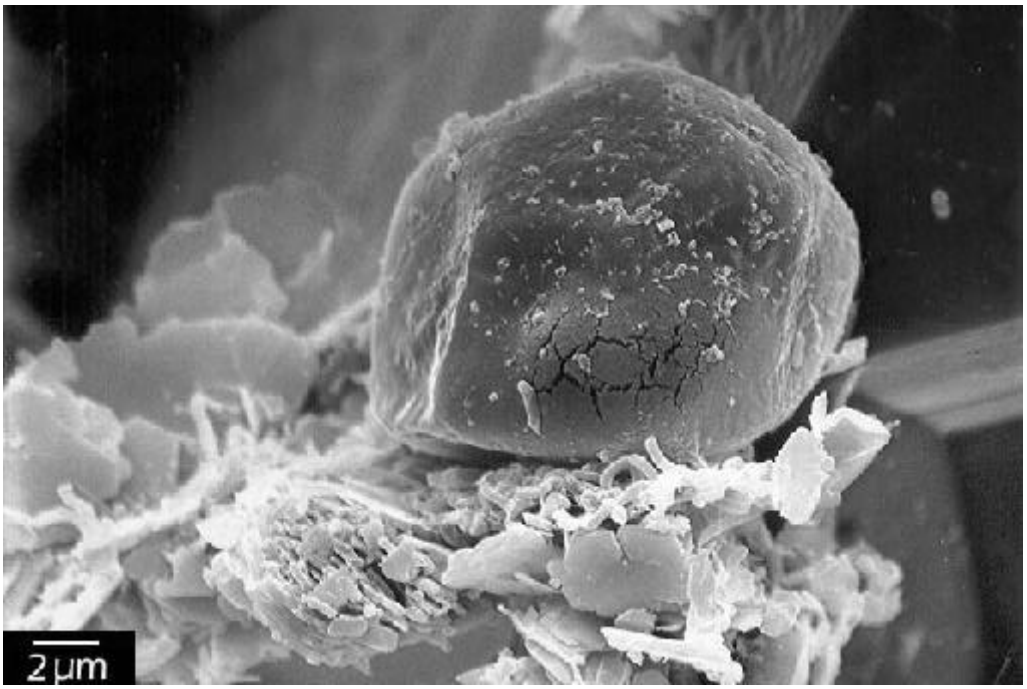

Figure 78: Large ball of slime from Fig. 73. The surface of the ball has been burned with the electron beam, causing swelling and cracking. (Preserved with ethanol/hexamethyldisilazane.)

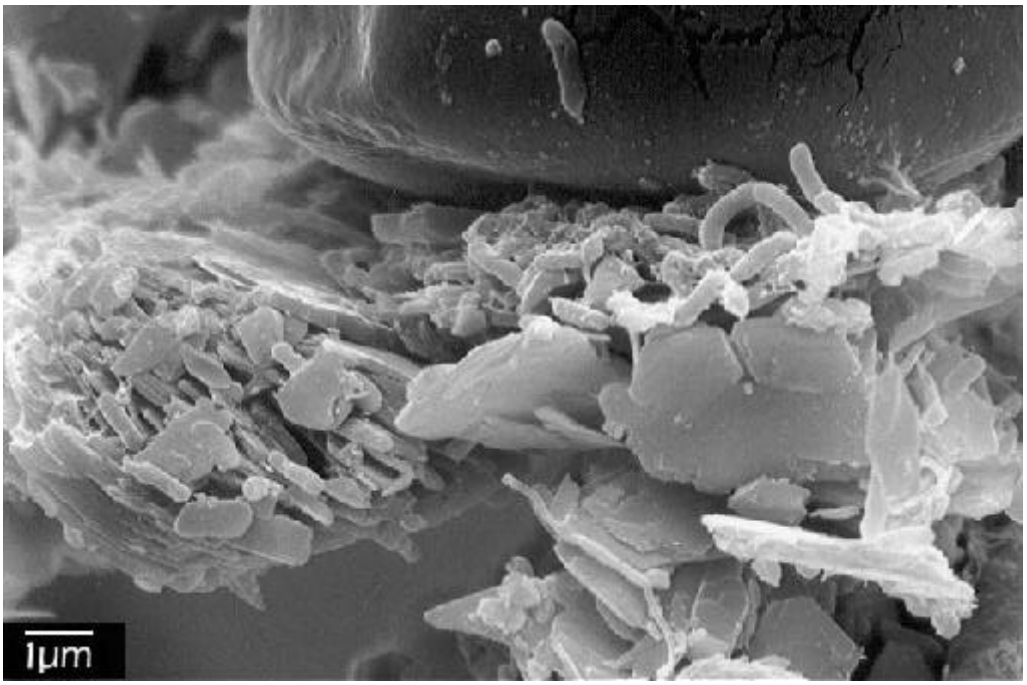

Figure 79: Higher magnification photo of colony of bacteria at the base of the ball of slime from Figs. 73 & 74. Colonies of bacteria were rare during the timed experiments. (Preserved with ethanol/hexamethyldisilazane.)

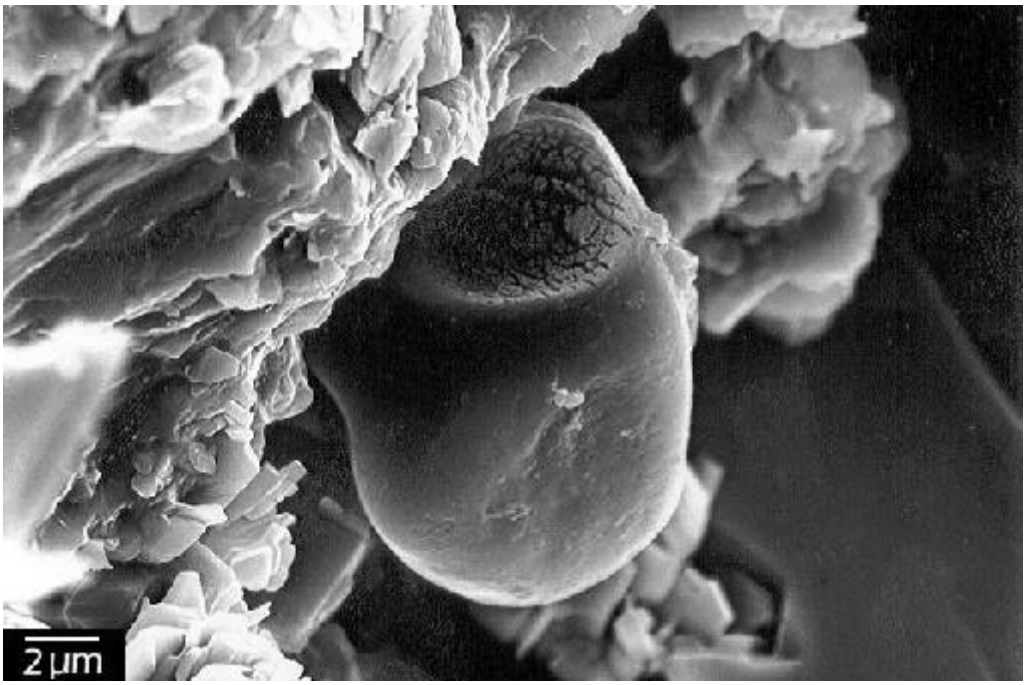

Figure 80: Large ball of slime during the fourth week of timed experiments. The top part of this ball has been deformed with the electron beam. (Preserved with 10% glutaraldehyde.)

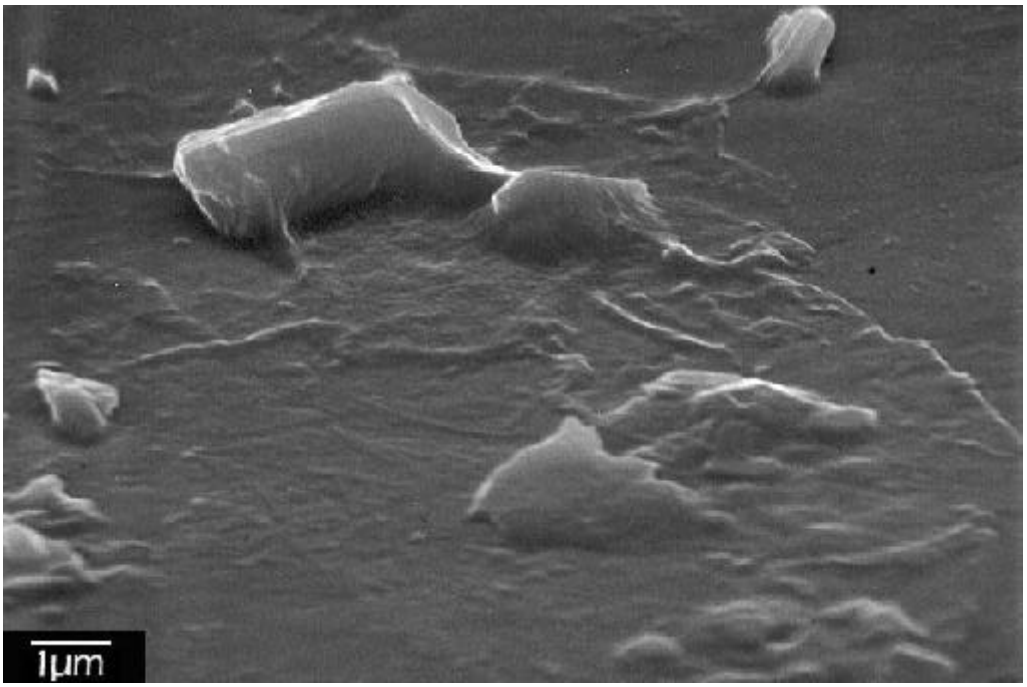

Figure 81: Thin sheet of slime on the surface of a quartz overgrowth during the fourth week of the timed experiments. (Preserved in ethanol/hexamethyldisilazane.)

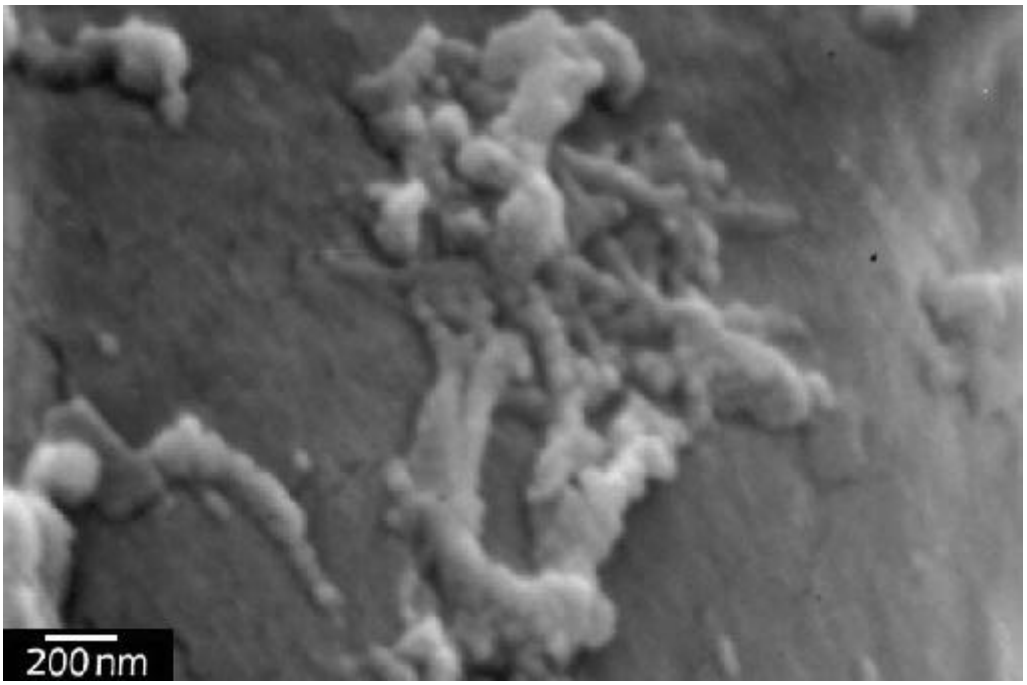

Figure 82: High-magnification photo of a ropy mass of slime during the fourth week of the timed experiments. (Preserved with ethanol/hexamethyldisilazane.)

CHAPTER V

DISCUSSION AND CONCLUSIONS

PRESERVATION OF BACTERIA AND SLIME LAYER

Fixation and dehydration of organic matter for scanning electron microscopy is known to cause artifacts such as shrinkage, collapse of structures, and cracking (Postek and others, 1980). Although the effects of dehydration are well documented for bacteria, the dehydration process of the exopolysaccharide slime layer that they produce has not been extensively studied.

In the preservation experiments in this study, air drying and 10% glutaraldehyde fixation preserved the slime layer as a relatively continuous sheet. However, the slime layer in some samples preserved with these techniques is slightly cracked (Figs. 1, 8 and 33), indicating that at least some shrinkage has occurred. Both air drying and glutaraldehyde fixation failed to preserve the full volume of the bacteria, resulting in collapsed, flattened bacterial forms (Figs. 2, 7, 30 and 36). Ethanol dehydration with hexamethyldisilazane, ethanol dehydration with critical point drying, and ethanol/acetone dehydration with critical point drying all preserved the bacterial bodies with more volume and surface detail than air drying methods but resulted in a highly fragmented slime layer consisting mainly of plates, strands, and balls of slime (Figs. 11-14, 18-20 and 22-26).

Both preservation techniques which most severely distorted the bacterial shapes (air drying and 10% glutaraldehyde preservation) involved the direct evaporation of water from the sample. This implies that the escape of water from within the bacteria is responsible for the distortion of the bacteria. The high surface tensions associated with the air/water interface are responsible for much of the distortion that occurs (Postek and others, 1980). This deformation is mitigated by the ethanol dehydration process, in which the water in the organic material is gradually replaced by ethanol. Ethanol, having a much lower surface tension than water, causes less distortion as it evaporates. Hexamethyldisilazane replacement (Oshel, 1997) and critical point drying (Anderson, 1951) are two other methods by which the air/water interface, and even the air/ethanol interface is avoided, resulting in less distortion of bacteria. The techniques that incorporate ethanol dehydration, while preserving the bacteria in a more or less intact form result in extensive modification of the slime layer. The distortion and fragmentation evident in these samples may be induced by the solubility of some polysaccharides in ethanol, as well as the length and frequent liquid changes of the dehydration processes.

The textures of slime in preserved Scanning electron microscope samples include continuous sheets, plates, strands, balls and are all considered to be the result of some modification of the original slime layer.

Sheets. Although sheets represent the least distorted morphology of slime in these rocks, it is possible that dehydration has caused shrinkage of the slime layer, changing a pore-filling mass

of slime into a sheet that drapes across the grains and pore spaces, forming menisci as it shrinks and stretches (Fig. 83). The amount of water in the slime layer makes it improbable that these dehydration techniques would preserve the layer without at least some loss of volume.

Plates. The plates of slime observed in some ethanol dehydrated samples may represent a moderate stage of deformation, in which the slime sheet is segmented and slightly curled, but not yet completely destroyed. These plates are strikingly similar in texture to clays seen in subsurface reservoirs (Figs. 84 and 85).

Strands and Balls. These are interpreted to be textures associated with the highest level of deformation. They may simply be caused by the most severe fragmentation of the slime layer, which is pulled apart into fragments so small that surface tensions dictate their shape, turning them into spheroid shapes. Alternatively, these structures, both balls and strings, may exist as resistant components within a heterogenous slime layer that are revealed when less resistant material is stripped away during ethanol dehydration (Fig. 86). In this case, they are not entirely artifacts of preservation and may be considered parts of the biofilm structure.

The textures seen during the preservation experiment on reservoir bacteria and slime indicate that these structures are actually present within a heterogenous biofilm before preservation. Nanno-scale balls were seen in the air-dried and critical point dried sample, as well as in an unpreserved sample run as an adjunct to the slime morphology esperiment (Fig. 83). These structures were not obvious in glutaraldehyde-preserved samples and

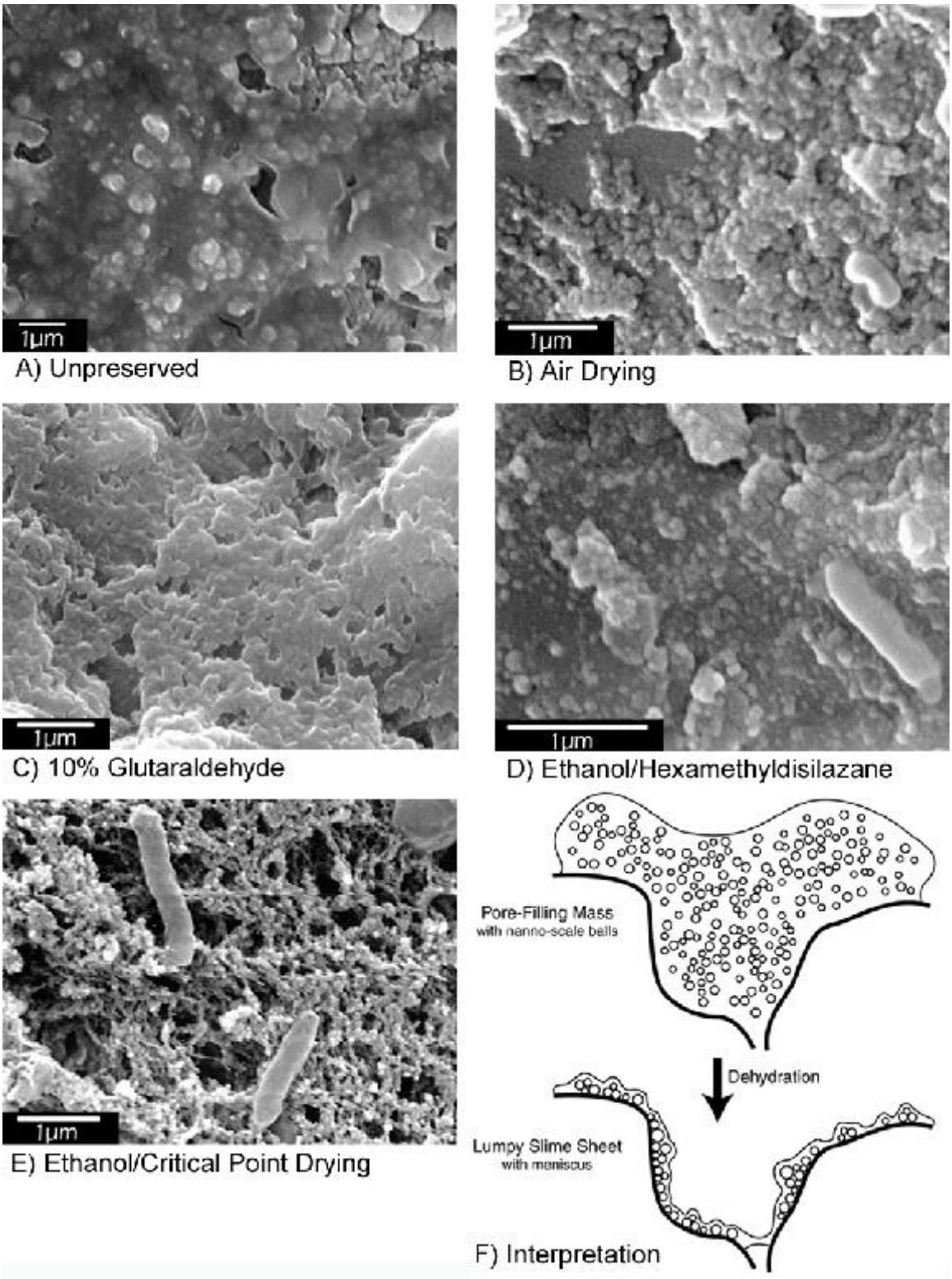

Figure 83: Comparison of nanno-scale spheroidal structures in slime layer with different preservation techniques and interpretation of the effects of dehydration on slime texture.

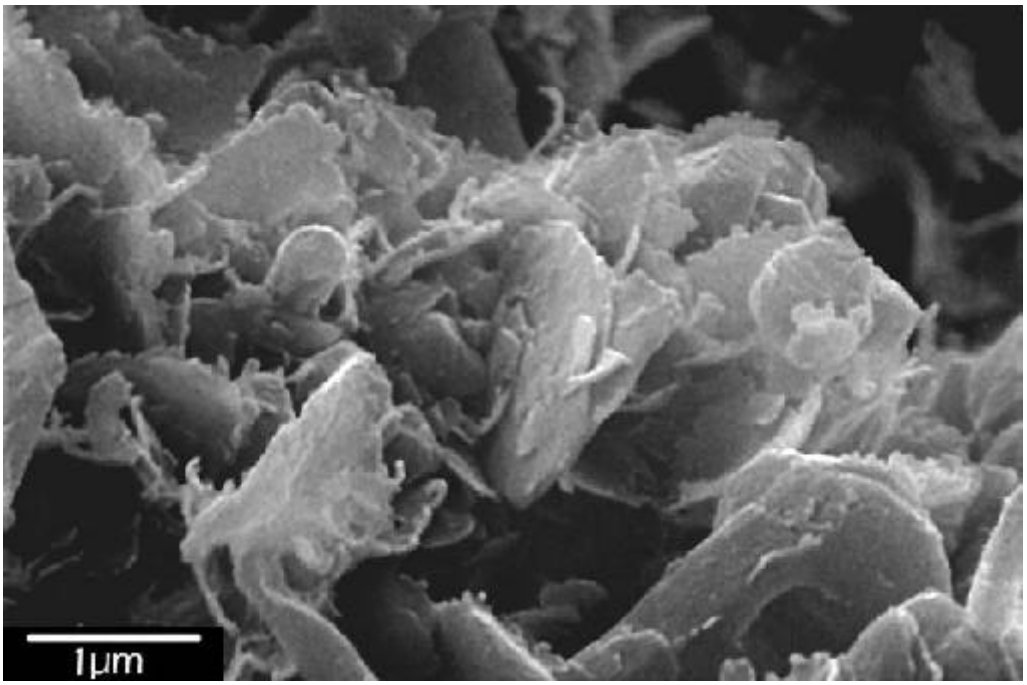

Figure 84: Platy slime with fingers along the edges of the plates. Preserved with ethanol/critical point drying.

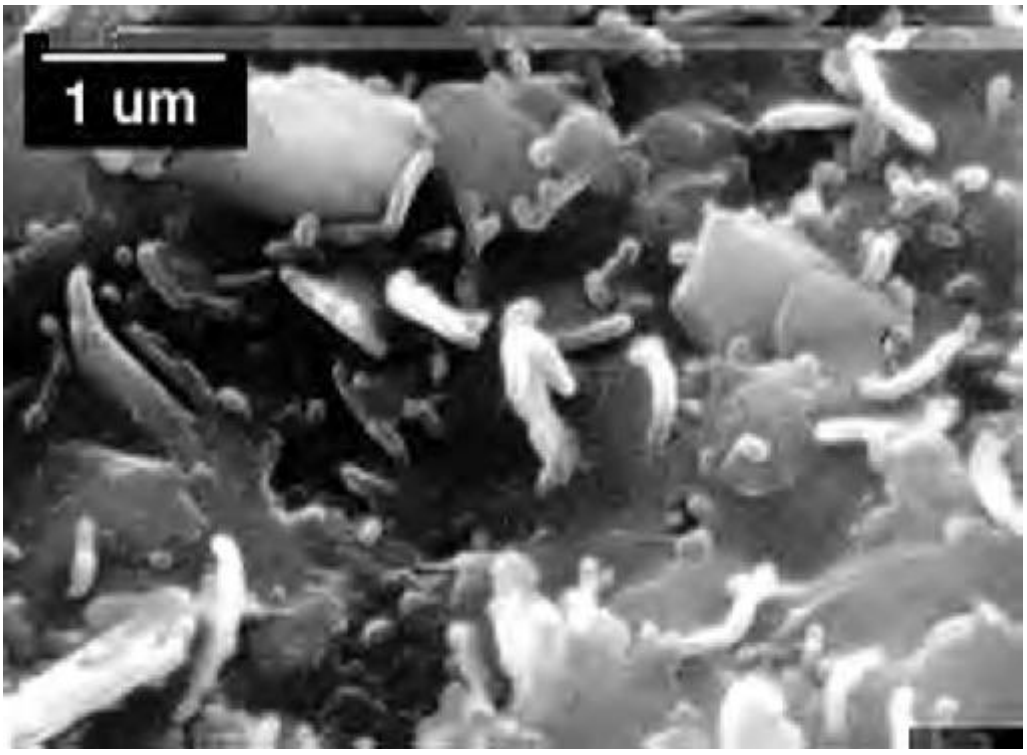

Figure 85: Clays from subsurface oil reservoir in Texas.

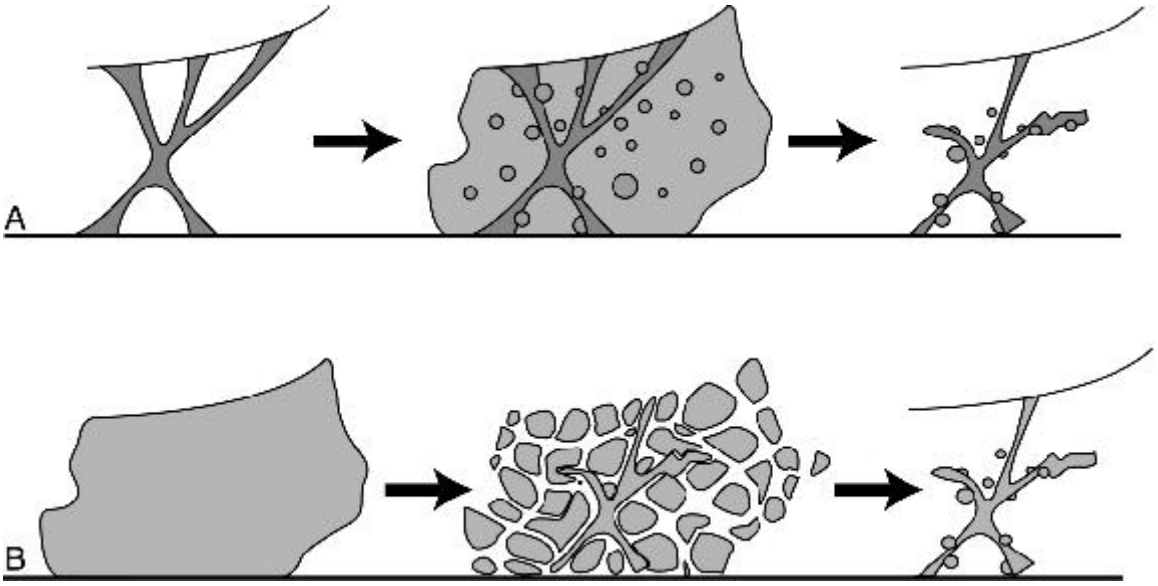

Figure 86: Two alternative explanations for the formation of balls and strands from dehydration of the slime layer. A: Formation of a slime layer around resistant structures (webs and balls) that are left behind when the less dense material is stripped away; B: Fragmentation of an homogenous slime layer into strands and pieces which take on ball shapes.

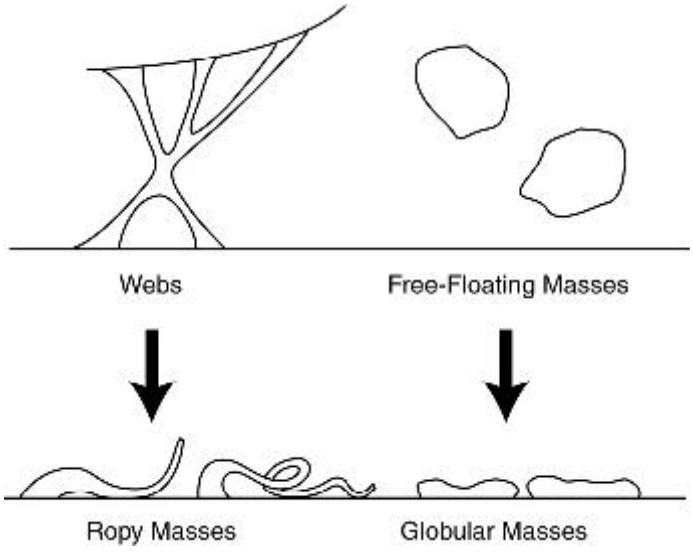

Figure 87: Possible genesis of ropy masses and globular masses. Since very few globular slime masses are associated with bacterial bodies, it is possible that at least some are free-floating in pore water before the rock is opened and the pores drained.

ethanol/hexamethyldisilazane samples, but could be present beneath the still-intact surface of the slime layer of the glutaraldehyde-preserved sample and may be responsible for the chunky texture of the ethanol-dehydrated sample (Fig. 83).

The role that these structures play in the operation of the biofilm is not known. Nanno-scale structures such as these have been interpreted as "nannobacteria" (Figs. 88 and 89), but they cannot be positively identified as bacteria with scanning electron microscopy by surface texture alone. Indeed, debate continues over the existence of nannobacteria in general (Kirkland and others, 1999, and references therein).

Preservation of Different Slime Layers. It was observed during the course of this study that slime layers produced by different types of bacteria and slime layers of different ages responded differently to dehydration. The thicker slime layer produced by the reservoir bacteria during preservation experiments was more likely to separate into chunks of slime when dehydrated than to curl into sheets or strings, as the slime layer produced by the rod-shaped bacteria did. During the experiments, it was noted that young, thin sheets of slime tended to curl when dehydrated in ethanol (Figs. 67 and 68), whereas the older, thicker slime layer grown during preservation experiments tended to separate into chunks.

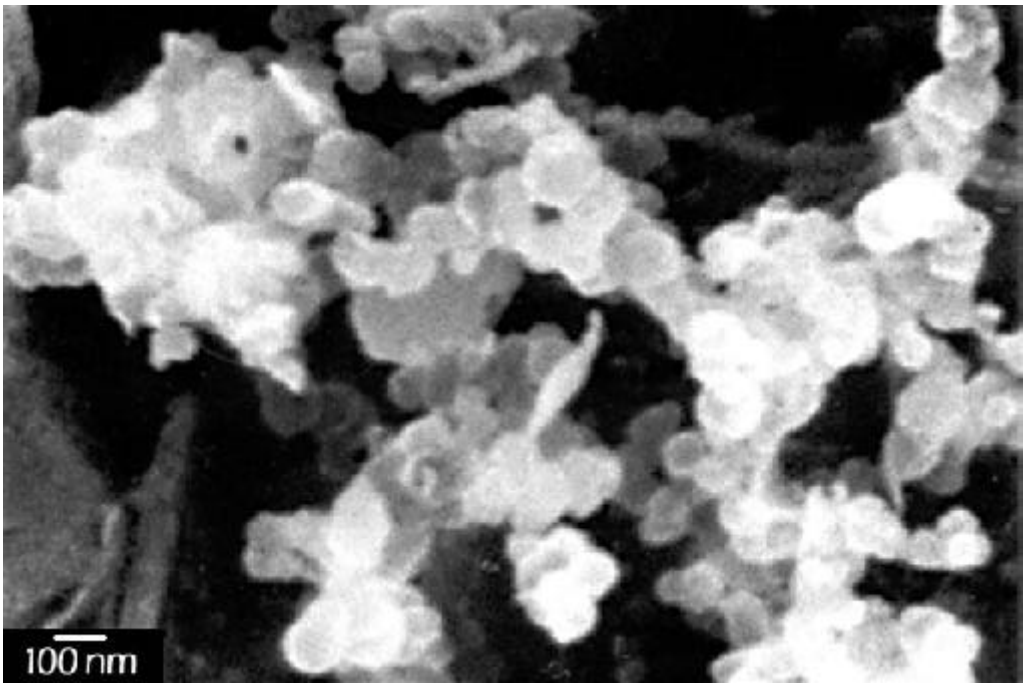

Figure 88: “Grape cluster” slime texture composed of nanno-scale spheroids in preservation experiments on rod-shaped bacteria. (Preserved with ethanol/ acetone/critical point drying.)

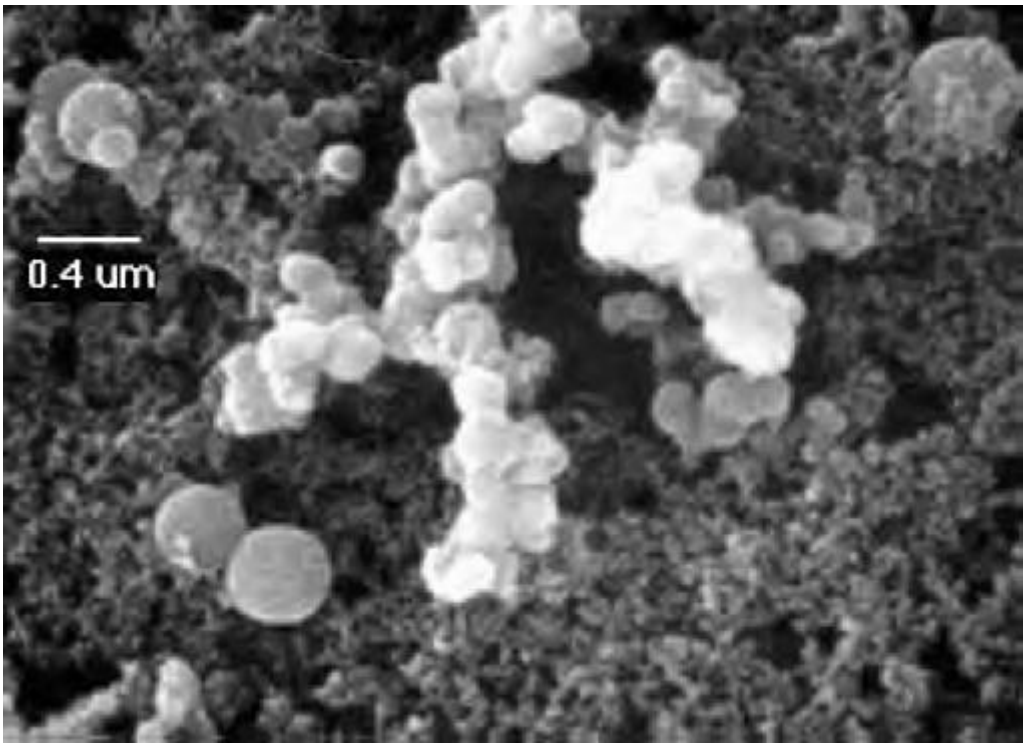

Figure 89: “Grape cluster” texture in filtrate from Austin city drinking water.

SLIME LAYER AS PLUGGING AGENT

In the examinations of fully-plugged cores, the dominant organic species present was an irregular, confluent slime sheet that spanned pore throats and lined pore spaces (Figs. 43-46). It is likely that the actual plugging mechanism is a pore-filling mass of slime that collapses into a sheet during dehydration (Fig. 83). While the importance of exopolysaccharide production as plugging mechanism in microbial enhanced oil recovery experiments has been noted (Mitchell and Nevo, 1964; Bayeve, 1992; Lappan and Fogler, 1995), this is the first direct observation of the process in action.

NANNOBACTERIA AND ULTRAMICROBACTERIA

Small rod-shaped and spherical forms of bacteria less than 1 micron in diameter were observed in the first three weeks of the timed growth experiments (Figs. 51-55 and 71). They occur in conjunction with normal-sized, rod-shaped bacteria, some of which occur in joined pairs, which are interpreted to be reproducing bacteria. The small forms have not been observed in pairs.

These structures cannot be identified as bacteria on the basis of surface texture alone. This research shows that nm-scale balls may be formed by dehydration of the slime sheet. Previous research shows that dissolution of calcite produces these textures (Kirkland and others, 1999), as does a thick layer of gold coat on Scanning electron microscope samples. The likelihood of creating a rod-shaped artifact is lower, however, and these structures are considered to be bacteria in this study.

Two separate terms have been defined for small (<1µm) bacteria. Ultramicrobacteria are dwarf forms of full-sized bacteria which form in response to starvation (Torrella and Morita, 1981; Casida, 1965). They do not reproduce or produce a slime layer in dwarf form. When fed with a low-nutrient broth, these ultramicrobacteria grow to full size and begin to multiply. Nannobacteria, in contrast, are distinguished from bacteria, defined by their size (25-300nm) and their occurrence, usually in chains or clusters, within soils and rocks (Folk, 1993). The absence of dividing small forms and the fact that the small forms are not seen after two weeks of feeding suggests that these are in fact growing into full-sized bacteria and may therefore be called ultramicrobacteria.

DEVELOPMENT OF SLIME LAYER OVER TIME

A clear progression of slime morphologies was not evident in the growth experiments. Several morphologies existed at the same time in different areas of the samples. Morphologies of exopolysaccharides observed in this experiment included sheaths over bacteria, holdfasts, ropy masses, globular masses, thin sheets, large balls, and confluent sheets and masses (Figs. 54, 56, 57, 59-69 and 72-82).

Early exopolysaccharides. The early forms of exopolysaccharide include a capsule over the bacterial body and holdfasts. Exopolysaccharides have been demonstrated to be part of the attachment process of individual bacteria, as seems to be the case here. These

exopolysaccharides, which cover the bacterial body itself, have been distinguished from the slime layer, which is involved in the growth of colonies (Whitfield, 1988).

Early slime forms. Small globular masses, ropy masses, and thin sheets all occur in the first through third weeks of slime growth. These are interpreted to be early forms of the slime layer. These ropy masses may actually be webs that collapsed against the grain surface when the rock was broken apart and the pore spaces drained (Fig. 87). Weblike forms appear in fully plugged cores in both ethanol-dehydrated and glutaraldehyde-preserved samples, so it is unlikely that these particular forms are dehydration artifacts. It is possible that these webs represent an early stage in the growth of the slime as seen in Paulsen and others (1997), the morphology of which is preserved in more resistant structures within the slime layer, revealed when the less resistant material is stripped away (Fig. 86). No intact webs were seen in the timed experiment, however, so the relationship between intact slime layer and the weblike forms seen in fully plugged samples is not known. In addition, the assumption that all slime pieces were attached to the substrate before dehydration is unwarranted. Free-floating pieces of slime might collapse against the surface of the rock during dehydration (Fig. 87), which would explain the rarity of visible bacteria in association with these small globular masses.

Hexagonal outline. The growth of slime in a hexagonal outline is seen in several samples. It is not known why this happens. Either the slime growth is governed by charge sites on the crystals, or the polysaccharide molecules form a self-organizing, sub-crystalline lattice.

Large balls. The large (10um) balls occur rarely in the first week but are very common in the fourth week of growth. They are easily distorted by the electron beam. Burning by the electron beam is a characteristic exclusive to organic materials, so these balls are organic in nature. Their actual genesis is not clear, although at least one occurs in conjunction with a colony of bacteria.

Although a linear progression from one morphology to another is not clearly seen in these experiments, the general order of events seems to begin with the growth of non-reproducing ultramicrobacteria into full-sized bacteria. The bacteria then begin to reproduce and produce a slime layer in the form of ropy masses, globular masses, and thin sheets. The slime layer thickens over time, eventually filling the pore spaces completely and sometimes taking the form of large (10µm) balls.

CHAPTER VI

SUMMARY

Microbial enhanced oil recovery is one of the most economical and effective methods for extending the life of production wells in declining reservoirs. The purpose of this study was to characterize the bacteria and their byproducts in sandstones used in microbial enhanced oil recovery experiments. This research showed that preservation techniques for scanning electron microscopy can create artifacts by dehydration of the slime layer, that plugging in microbial enhanced oil recovery experiments is caused largely by the exopolysaccharide slime layer produced by the bacteria, and that the slime layer takes on several distinct morphologies during different phases of its development.

No preservation technique for scanning electron microscopy preserved both the bacteria and the slime layer. Air drying and 10% glutaraldehyde fixation preserved the slime layer intact with some shrinking but caused distortion and flattening of the bacteria. Techniques which involved ethanol dehydration preserved the textures of the bacteria but caused extensive fragmentation and shrinkage of the slime layer.

In sandstones which had been plugged during microbial enhanced oil recovery experiments, bacteria are present but sparsely distributed. An irregular, confluent slime sheet cover grains

and coats the inside of pore spaces. Other slime textures are present, such as webs.

The general progression of textures seen during the growth of the slime layer over time seems to be: ultramicrobacteria growing into full-sized bacteria and then creating a capsule of slime, the growth of blobs or small sheets of slime, the growth of webs, and finally a thicker, pore-filling mass of slime in conjunction with large balls of slime in some areas.

The preservation experiments were a necessary part of ensuring that the observations made during this study accurately reflected the condition of the organic material within these rocks. In most biologic studies, the exopolysaccharide slime produced by the bacteria is usually intentionally washed off during preparation of scanning electron microscope samples. Few enough Scanning electron microscope studies have been done on the function of this slime layer that no preservation protocols have been developed specifically for preserving the slime. As a result, workers unfamiliar with the preservation techniques used may misidentify dehydration artifacts as primary structures of the biofilm.

The identification of slime as the major plugging agent in microbial enhanced oil recovery operations has been done indirectly, but direct observations of the extent to which slime can fill the pore spaces of the reservoir rock and the volume of slime produced have not been previously made. Because of the lack of knowledge of the morphology of biofilms in porous media, some of the textures observed in this study were completely unanticipated. Whether these morphologies are an exclusive response to growth within the porous medium or whether they are present in surficial biofilms as well remains to be seen. Knowledge of the plugging mechanism can improve the predictability of microbial enhanced oil recovery operations, as

well as giving biologists a tool with which they may engineer different types of plugs by altering the nutrient mix given to the bacteria.

REFERENCES CITED

Allison, D. G., and Sutherland, I. W., 1987, The role of exopolysaccharides in adhesion of freshwater bacteria: Journal of General Microbiology, v. 133, p. 1319-1327.

Anderson, T. F., 1951, Techniques for the preservation of three-dimensional structure in preparing specimens for the electron microscope: Transactions of the New York Academy of Sciences, v. p.130-134.

Azadpour, A., Brown, L. R., and Vadie, A. A., 1996. Examination of thirteen petroliferous formations for hydrocarbon-utilizing sulfate-reducing microorganisms: Journal of Industrial Microbiology, v. 17, p. 128-136.

Bayer, M. E., Carlemalm, E., and Kellenberger, E., 1985, Capsule of *Escheria coli K29*: Ultrastructural preservation and immunoelectron microscopy: Journal of Bacteriology, v. 162, no. 3, p. 985-991.

Bennett, P. C., Hiebert, F. K., and Rogers, J. R., 2000, Microbial control of mineral-groundwater equilibria: Macroscale to microscale: Hydrogeology Journal, v. 8, p. 47-62.

Brown, L. R., 1982, Method for increasing oil recovery, U. S. Patent No. 4,475,590.

Brown, L. R., and Vadie, A. A., 2000, Slowing production decline and extending the economic life of an oil field: New MEOR technology: Society of Petroleum Engineers, 2000 SPE/DOE Improved Oil Recovery Symposium, Tulsa, OK.

Brown, L. R., Pittman, C. U., Jr., Lynch, F. L., and Vadie, A. A., 2002, Augmenting a microbial selective plugging technique with polymer flooding to increase the efficiency of oil recovery – a search for synergy: Fifth semi-annual progress report, DOE Award Number DE-AC26-99BC15210.

Carr, J. H., Anderson, R. L., and Favero, M. S., 1996, Comparison of chemical dehydration and critical point drying for the stabilization and visualization of aging biofilm present on interior surfaces of PVC distribution pipe: Journal of Applied Bacteriology, v. 80, p. 225-232.

Casida, L. E., Jr., 1965, Abundant Microorganism in Soil: Applied Microbiology, v. 13, p. 327-334.

Christensen, B. E., and Characklis, W. J., 1990, Physical and Chemical Properties of Biofilms, *In* Characklis, W. G., Kevin, C., and Marshall, K. C., Biofilms: New York, Wiley, p. 93-130.

Clark, J. B., Munnecke, D. M., and Jenneman, G. E., 1981, *In situ* microbial enhancement of oil production: Developments in Industrial Microbiology, v. 22, p. 695-701.

Costerton, J. W., Lewandowski, Z., DeBeer, D., Caldwell, D., Korber, D., and James, G., 1994, Biofilms, the customized microniche: Journal of Bacteriology, v. 176, no. 8, p. 2137-2142.

Crawford, P. B., 1961, Possible bacterial correction of stratification problems: Producers Monthly, v. 25, p. 10-11.

Cusack, F., Lappin-Scott, H. M., Costerton, J. W., 1987, Bacteria can plug waterflood injection wells: Oil and Gas Journal, Nov. 9, p. 59-64.

Davey, M. E., Gavertz, D., Wood., W. A., Clark, J. B., and Jenneman, G. E., 1998, Microbial selective plugging of sandstone through stimulation of indigenous bacteria in a hypersaline reservoir: Geomicrobiology, v. 15, p. 335-352.

Davis, J. B., and Updegraff, D. M., 1954, Microbiology in the petroleum industry: Bacteriological Reviews, v. 18, p. 215-238.

Department of Energy, 2002, Oil & Gas Reservoir Life Extension.
Internet on-line. <http://www.fe.doe.gov/oil_gas/life_extension/>.
[1 April 2002].

Fletcher, M., and Floodgate, G. D., 1973, An electron-microscopic demonstration of an acidic polysaccharide involved in the adhesion of a marine bacterium to solid surfaces: Journal of General Microbiology, v. 74, p. 325-334.

Folk, R. L., 1993, SEM imaging of bacteria and nannobacteria in carbonate sediments and rocks: Journal of Sedimentary Petrology, v. 63, pp. 990-999.

Folk, R. L., and Lynch, F. L., 1997, The possible role of nannobacteria (dwarf bacteria) in clay mineral diagenesis and the importance of careful sample preparation in high magnification SEM study: Journal of Sedimentary Research, v. 67, p. 583-589.

Jack, T. R., Shaw, N., Wardlaw, N., Costerton, J. W., 1989, Microbial plugging in enhanced oil recovery: Developments in Petroleum Science, v. 31, p. 125-150.

Jenneman, G. E., Knapp, R. M., McInerney, M. J., Menzie, D. E., and Revus, D. E., 1984, Experimental studies of in-situ microbial enhanced oil recovery: Society of Petroleum Engineers Journal, February, p. 33-37.

Jenneman, G. E., Moffitt, P. D., and Young, G. R., 1996, Application of a microbial selective-plugging process at the North Burbank Unit: Prepilot tests: SPE Production & Facilities, Feb. 1996, p. 11-17.

Kalish, P. J., Stewart, J. A., Rogers, W. F., and Bennett, E. O., 1964, The effect of bacteria on sandstone permeability: Journal of Petroleum Technology, July, p. 805-813

Kirkland, B. L., Lynch, F. L., Rahnis, M. A., Folk, R. L., Molineaux, I. J., and McLean, R. J. C., 1999, Alternative origins for nannobacteria-like objects in calcite: Geology, v. 27, p. 347-350.

Lappan, R. E., and Fogler, H. S., 1995, Reduction of porous media permeability from *in situ Leuconostoc mesenteroides* growth and dextran production: Biotechnology and Bioengineering, v. 50, p. 6-15.

Lappin-Scott, H. M., Cusack, F., and Costerton, J. W., 1988, Nutrient resuscitation and growth of starved cells in sandstone cores: a novel approach to enhanced oil recovery: Applied and Environmental Microbiology, v. 54, p. 1373-1382.

Lawrence, J. R., Korber, D. R., Hoyle, B. D., Costerton, J. W., and Caldwell, D. E., 1991, Optical sectioning of microbial biofilms: v. 173, p. 6558-6567.

MacLeod, A. H., Lappin-Scott, H. M., and Costerton, J. W., 1988, Plugging of a model rock system by using starved bacteria: Applied and Environmental Microbiology, v. 54, 1365-1372.

Mitchell, R., and Nevo, Z., 1964, Effect of bacterial polysaccharide accumulation on infiltration of water through sand: Applied Microbiology, v. 12, p. 219-223.

Oshel, P., 1997, HMDS and Specimen drying for SEM: Microscopy Today, May 1997, p. 16.

Paulsen, J. E., Oppen, E., and Bakke, R., 1997, Biofilm morphology in porous media, a study with microscopic and image techniques: Water Science and Technology, v. 36, p. 1-9.

Postek, M. T., Howard, K. S., Johnson, A. H., and McMichael, K. L., 1980, Scanning Electron Microscopy: A Student's Handbook: Ladd Research Industries, 305 p.

Raiders, R. A., McInerney, M. J., Revus, D. E., Torbati, H. M., Knapp, R. M., and Jenneman, G. E., 1986, Selectivity and depth of microbial plugging in Berea sandstone cores: Journal of Industrial Microbiology, v. 1, p. 195-203.

Ransom, B., Bennett, R. H., Baerwald, R., and Shea, K., 1997, TEM study of *in situ* organic matter on continental margins: occurrence and the "monolayer" hypothesis: Marine Geology, v. 138, p. 1-9.

Ravenscroft, N., Walker, S. G., Dutton, G. G. S., Smit, J., 1991, Identification, isolation, and structural studies of extracellular polysaccharides produced by *Caulobacter crescentus*: Journal of Bacteriology, v. 173, p. 5677-5684

Shaw, J. C., Bramhill, B., Wardlaw, N. C., and Costerton, J. W., 1985, Bacterial fouling in a model core system: Applied and Environmental Microbiology, v. 49, p. 693-701.

Torrella, F., and Morita, R. Y., 1981, Microcultural study of bacterial size changes and mocricolony and ultramicrocolony formation by heterotrophic bacteria in seawater: Applied and Environmental Microbiology, v. 41, p. 518-527.

Updegraff, D. M., and Wren, G. B., 1954, The release of oil from petroleum-bearing materials by sulfate-reducing bacteria: Applied Microbiology, v. 2, p. 309-322.

Vandevivere, P., and Bayeve, P., 1992, Effect of extracellular polymers on the saturated hydraulic conductivity of sand columns: Applied and Environmental Microbiology, v. 58, p. 1690-1698.

Whitfield, C., 1988, Bacterial extracellular polysaccharides: Canadian Journal of Microbiology, v. 34, p. 415-420.

Zobell, C. E., 1947, Bacterial release of oil from sedimentary materials: Oil and Gas Journal, Aug. 2, p. 62-65.